Alma Mater Studiorum · Università di Bologna

Scuola di Scienze
Dipartimento di Fisica e Astronomia
Corso di Laurea Magistrale in Fisica

Wavefunctions and correlations of the complex Kitaev model on a finite chain

Relatore:
Prof.ssa Elisa Ercolessi

Correlatore:
Dott. Davide Vodola

Presentata da:
Roberto Rubboli

Anno Accademico 2018/2019

Abstract

In this thesis, we discuss the Kitaev model, a one-dimensional topological superconductor. In the non-trivial phase, it shows two *Majorana edge states* that can be combined, in the thermodynamic limit, into a non-local zero-energy Dirac fermion which can be populated without affecting the energy of the states. In this work, we find the analytical expressions of the Majorana edge states for finite chain length and some extension of the model. In particular, we consider generic boundary conditions and complex-valued parameters. In order to do this, we extend the Lieb-Schultz-Mattis method to the fully complex case. Then we discuss the splitting of the degeneracy of the ground state for finite systems and the emergence of the massive edge states. Finally, we calculate the entanglement entropy of the complex Kitaev model from the correlation functions by proposing an extension of the standard real method to the complex case.

Sommario

In questa tesi viene discusso il modello di Kitaev, un superconduttore topologico unidimensionale. Nella fase non triviale presenta due *Majorana edge states* che possono essere combinati, nel limite termodinamico, in un unico fermione di Dirac a energia nulla che può essere popolato senza influenzare l'energia degli stati. In questo lavoro, vengono trovate le espressioni analitiche degli edge states per lunghezza finita della catena e per alcuni estensioni del modello. In particolare vengono considerati i parametri del modello complessi e le condizioni al contorno generiche. Per fare questo, il metodo di Lieb-Schultz-Mattis viene esteso al caso complesso. Inoltre, vengono discussi lo splitting della degenerazione del ground state per sistemi finiti e la presenza di edge states massivi. Infine, viene calcolata l'entropia di entanglement del modello di Kitaev complesso dalle funzioni di correlazione proponendo una estensione del metodo reale standard al caso complesso.

Contents

Introduction

The field of Topological Matter has grown in the last decades into what is arguably one of the most interesting and stimulating developments in Condensed Matter Physics. New kinds of quantum states which present "interesting" properties like non-dissipative charge transport, fractional excitations, non-abelian statistics of quasi-particles, etc. [6, 18] have been discovered. For a long time, physicists believed that Landau's symmetry breaking theory described all possible phases in materials, and all possible phase transitions [40]. However, in the 1980s, it became clear that Landau symmetry breaking theory did not describe all possible orders. Actually it is back in the 70's that D.Koesterlitz and M.Thouless put on a firm theoretical background the characterization of what now goes under the name of BKT transition. In the following decade, M.Thouless introduced the notion of the *topological order* also in the context of the theory of conductors [23] and D.Haldane in the context of magnetic materials [17] (for their achievements, Koesterlitz, Thouless and Haldane won the Nobel Prize in 2016). Since then, both theoretical and experimental progress has been made in this field starting from the Fractional Quantum Hall (FQH) effect up to the most recent *topological insulators* and *topological superconductors*. The topological order cannot be probed by any linear responses as for the symmetry breaking order; it can be completely characterized by using only topological -hence global- properties, such as non-dissipative edge states, geometric phases, topological invariants and non-local order parameters [38].
Two states are in the same topological phase if they can be adiabatically connected through a path in the parameter space that doesn't cross a gapless phase. In addition, this transformation must be slow (compared to the energy scales of the system) and must preserve the symmetries of the system [4]. This idea of smooth deformations was brought in the context of condensed matter physics from mathematics where topology is the study of the properties of a geometric object which are preserved under continuous deformations, such as stretching and twisting but not tearing.
One of the most important practical applications of topological phases is quantum computation. Implementing a quantum computer is arguably one of the most interesting and stimulating challenges for physics and engineers of our century. One of the main problems in implementing quantum computers is the decoherence of the quantum systems. Topological quantum computation provides an elegant way to construct decoherence-protected states, as one encodes quantum information in a non-local fashion that the environment finds difficult to corrupt [2].

This thesis focuses on the Kitaev model [21], a one-dimensional topological superconductor which should act, at least theoretically, as a reliable quantum memory being intrinsically im-

mune to decoherence. It's the simplest topological superconductor that presents both a trivial and symmetry protected topological phase. The topological phase is characterized by the presence of the Majorana edge states, that is quasi-particle excitations localized at the beginning and at the end of the chain. This model is important because it can be easily solved analytically in the thermodynamic limit [21].
In this work, we will try to extend these results by finding the finite-size corrections. Moreover, we will consider some extension of the model; we will take into account generic boundary conditions and we will discuss the more general case where both the hopping amplitude and superconductive gap are complex parameters.
In fact, in general in quantum many-body systems the superconductive gap arises when the electron-electron interaction is treated in the mean-field approximation. It is related to the expectation value of a pair of creation or annihilation operators (the so-called "anomalous correlators") and it's generally complex. This phase produces observable effects when two superconductors with different phases are placed close to each other as in the Josephson junction which is made of two superconducting electrodes separated by a barrier [39].
Furthermore, the complex-valued hopping takes into account interaction with an external field. Indeed, the action of a magnetic field on the fermions can be treated by considering that they acquire a phase each time they jump from one site to the neighboring one. This is the Ahronov-Bohm effect on a discrete lattice.
The diagonalization of the Hamiltonian requires a general method to include generic boundary conditions. In fact, the Fourier transform is a useful tool only with periodic boundary conditions. We will discuss two different equivalent methods to diagonalize a complex quadratic Hamiltonian with generic boundary conditions. In particular, we will generalize the method introduced by Lieb, Schultz and Mattis [26] to the fully complex case.
Once we diagonalize the model, we will find the analytical expressions of the Majorana edge states and we will discuss their behavior for different values of the model parameters and for generic boundary conditions.
Moreover, we will analyze the correlation functions to detect the critical point and the topological phase in the fully complex case. In fact, we expect, in the topological region, the correlations between the first and the last sites of the chain to be substantially different from zero because of the non-local fermion that couples the edges of the chain.
Furthermore, at the critical point, the correlation function should show a power-law decay instead of an exponential one.
Finally, we will calculate the entanglement entropy. Indeed, the quantum phase transitions are governed by quantum fluctuations at zero temperature [11], and therefore we expect to observe signatures of criticality on the level of entanglement.
In the real case, the entanglement entropy can be computed from the correlation functions by exploiting the standard method discussed in [31]. Here we will try to generalize this method to the full complex case.

The chapters of the thesis are structured as follows:

- In Chapter 1 we review the most important concepts in the field of Topological Matter. In the first part of the chapter, we discuss the notions of Berry phase and Chern Number.

Then we introduce the concepts of single-particle Hamiltonian, boundary states, topological invariants, and bulk-edge correspondence via a concrete system: the SSH model. Moreover, we will provide an overview of the classification problem of topological phases of matter focusing on the systems of non-interacting fermions. Finally, we discuss the Kitaev model emphasizing the equivalence with the XY model.

- In Chapter 2 we present two methods to diagonalize a complex quadratic fermionic model with generic boundary conditions that allow us to solve for the energy spectrum and the eigenstates of the Hamiltonian.

- In Chapter 3 we will solve analytically the LSM equations using the perturbation theory. We will find that the eigenvalue problem admits two possible kinds of solutions: scattering states, which are plane waves in the bulk, and edge states, whose eigenfunctions are located at the edges of the chain. Moreover, we will see that, for generic boundary conditions, the model has a new kind of quasi-particle excitations: the so-called *massive edge states*.

- In Chapter 4 we will take as ansatz for the solutions of the LSM equations a linear combination of plane waves. Then we will find the Majorana edge states for different values of the parameters and generic boundary conditions for both the real and the complex cases. Finally, a numerical analysis of the complex Kitaev model will be performed.

- In Chapter 5 we will evaluate the correlation functions of the Kitaev model for finite chain length and we will study the asymptotic behavior in the thermodynamic limit. Then we will develop a new approach to calculate the reduced density matrix from the correlation function in the fully complex case. Finally, we will discuss the structure of the eigenvalues of the reduced density matrix and the scaling properties of the entanglement entropy.

Chapter 1

Topological phases of matter

Condensed matter physics deals with how the particles, at finite density and low temperatures, can reorganize in the different phases of matter. The main paradigm being used in this field is the Ginzburg-Landau theory, based on the mechanism of *Spontaneous Simmetry Breaking*. It describes physical systems where the dynamic, specifically the Hamiltonian or the equations of motions, has some symmetries but, for particular values of the parameters, the equilibrium state of the model experiences a phase transition to a symmetry-broken ground state. Landau's theory of phase transitions relies on a *local* order parameter that acquires a different expectation value depending on the particular phase of matter. For a long time, physicists believed that the Landau Theory described all possible orders and all possible phase transitions in materials. However, in the past decades, it has become gradually apparent that Landau symmetry-breaking theory may not describe all possible orders. In fact, new kinds of states with the same symmetry but different topological order have been found.
Moreover, Topological insulators, i.e. materials with non-trivial symmetry-protected topological order that behaves as an insulator in its interior but whose surface contains conducting states, have been discovered.
In mathematics, topology is concerned with the properties of a geometric object that are preserved under continuous deformations. For example, 2D surfaces can be classified by the genus, i.e. the number of holes it has. This number remains invariant under continuous deformations. Similarly, in the context of Topological phases of matter, two insulating Hamiltonians are said to be *adiabatically equivalent* if there is an adiabatic deformation connecting them with no closure of the gap that respects the important symmetries of the system (see Section 1.1).
In this chapter we will give an overview of the main concepts of Topological insulators like edge states, bulk topological invariants and bulk-edge correspondence via two concrete Topological systems: the Su-Schieffer-Heeger (SSH) model and the Kitaev model. In the first section we briefly introduce two basic concepts: the Berry phase the Chern number. Then these concepts will be applied to the simple case of a two-level system. In the second section we review the main properties of the SSH model and then, after briefly recalling the quantum entanglement-based view of Topological Phases of Matter, in the third section we mention the classification problem of Topological Insulators of non-interacting fermions. Finally, the main topic of this thesis, the Kitaev model, will be introduced and its equivalence with the XY model will be discussed.

1.1 Berry phase and Chern number

Let's consider a system with Hamiltonian $H(\mathbf{R})$ where $\mathbf{R}$ is a vector in the space of parameters (they can be, for example, the chemical potential, the magnetic field etc...). We are interested in the adiabatic evolution of the system as the parameters $\mathbf{R}(t)$ are varied along a path $\mathcal{C}$ in the parameter space. In general, an Hamiltonian is said to be adiabatically deformed if [4]

1. its parameters are changed slowly (compared to the energy scales of the system) and continuously;
2. the symmetries of the system are maintained;
3. the gap between the ground state and all the other excited states remains open.

At each point of the path $\mathbf{R}(t)$ it is possible to introduce an orthonormal basis $|n(\mathbf{R})\rangle$ of $H(\mathbf{R})$ (the snapshot basis) which satisfies [6]

$$H(\mathbf{R})|n(\mathbf{R})\rangle = E_n(\mathbf{R})|n(\mathbf{R})\rangle \tag{1.1}$$

The previous equation determines the eigenkets up to a phase that can be fixed by making a gauge choice to remove the arbitrariness (the phase can be $\mathbf{R}$-dependent). If the system is initially prepared in the eigenstate $|\psi(0))\rangle = |n(\mathbf{R}(0))\rangle$ and the gap around the state remain finite during throughout the evolution, for the adiabatic theorem [5], it will stay in an instantaneous eigenstate $|n(\mathbf{R}(t))\rangle$ of the instantaneous Hamiltonian. The system during this process will acquire a phase $|\psi(t)\rangle = e^{-i\theta(t)}|n(\mathbf{R}(t))\rangle$ which, as shown below, contains the dynamical factor related to the energy of the instantaneous eigenstates and the so-called *Berry phase*. The time-dependent Scröedinger equation of the system

$$H(\mathbf{R}(t))|\psi(t)\rangle = i\hbar\frac{d}{dt}|\psi(t)\rangle \tag{1.2}$$

implies that [6]

$$\theta(t) = \frac{1}{\hbar}\int_0^t E_n(\mathbf{R}(t'))dt' - i\int_0^t \langle n(\mathbf{R}(t'))|\frac{d}{dt'}|n(\mathbf{R}(t'))\rangle dt' \tag{1.3}$$

The first term is the standard dynamical phase. The second one comes from the fact that the eigenkets change with time and is proportional to the Berry phase which is defined as

$$\gamma_n \equiv i\int_0^t \langle n(\mathbf{R}(t'))|\frac{d}{dt'}|n(\mathbf{R}(t'))\rangle dt' = i\int_{\mathcal{C}}\langle n(\mathbf{R})|\nabla_R|n(\mathbf{R})\rangle d\mathbf{R} \tag{1.4}$$

$$= \int_{\mathcal{C}} d\mathbf{R}\cdot\mathbf{A}_n(\mathbf{R}) \tag{1.5}$$

where

$$\mathbf{A}_n(\mathbf{R}) \equiv i\langle n(\mathbf{R})|\nabla_R|n(\mathbf{R})\rangle \tag{1.6}$$

is the *Berry connection* (or *Berry potential*). Hence, the time evolution of the state is

$$|\psi(t)\rangle = e^{-\frac{i}{\hbar}\int_0^t E_n(\mathbf{R}(t'))dt'}e^{i\gamma_n}(t)|n(\mathbf{R}(t)\rangle \tag{1.7}$$

Under a gauge transformation $|n(\mathbf{R})\rangle \to e^{i\chi(\mathbf{R})}|n(\mathbf{R})\rangle$ the Berry connection transforms as

$$\mathbf{A}_n(\mathbf{R}) \to \mathbf{A}_n(\mathbf{R}) - \nabla_{\mathbf{R}}\chi(\mathbf{R}) \tag{1.8}$$

In general, the Berry phase cannot be canceled by a smart choice of the phase $\chi(\mathbf{R})$. Let's consider for example a closed path $\mathcal{C}$ for which $\mathbf{R}(0) = \mathbf{R}(T)$ where T is the time after which the path has been completed. For such a path $|n(\mathbf{R}(T))\rangle = |n(\mathbf{R}(0))\rangle$ and so if a gauge transformation is performed $e^{i\chi(\mathbf{R}(0))}|n(\mathbf{R}(0))\rangle = e^{i\chi(\mathbf{R}(T))}|n(\mathbf{R}(T))\rangle = e^{i\chi(\mathbf{R}(T))}|n(\mathbf{R}(0))\rangle$ and then $\chi(\mathbf{R}(0)) - \chi(\mathbf{R}(T)) = 2\pi m$ with m an integer. Therefore, in this situation, the Berry phase cannot be canceled unless it's an integer number. The Berry phase can be expressed as a surface integral thanks to the Stokes theorem

$$\gamma_n = \int_{\mathcal{C}} d\mathbf{R} \cdot \mathbf{A}_n(\mathbf{R}) = \int_{\mathcal{F}} d\mathbf{S} \cdot \mathbf{F}_n(\mathbf{R}) \tag{1.9}$$

where $\mathcal{F}$ is a surface whose boundary is $\mathcal{C}$ and if we consider a 3D parameter space

$$\mathbf{F}_n(\mathbf{R}) = \nabla_{\mathbf{R}} \times \mathbf{A}_n(\mathbf{R}) = i\langle \nabla_{\mathbf{R}} n(\mathbf{R})| \times |\nabla_{\mathbf{R}} n(\mathbf{R})\rangle \tag{1.10}$$

is the *Berry curvature*. In the three dimensional space the Berry connection and the Berry curvature can be thought of as the vector potential and the magnetic field of the electromagnetic theory, respectively. As Berry himself showed [7], it's possible to obtain a manifestly gauge independent expression for the Berry phase that shifts the derivative from the states (which gives problems when the numerical diagonalization of the Hamiltonian is performed) to the Hamiltonian. Starting from the completeness relation $\sum_n |n(\mathbf{R})\rangle\langle n(\mathbf{R})| = 1$ which holds at every point of the path $\mathbf{R}$ and taking into account that

$$\langle m(\mathbf{R})|\nabla_{\mathbf{R}} H(\mathbf{R})|n(\mathbf{R})\rangle = \frac{\langle m(\mathbf{R})|\nabla_{\mathbf{R}} H(\mathbf{R})|n(\mathbf{R})\rangle}{E_n(\mathbf{R}) - E_m(\mathbf{R})} \qquad m \neq n \tag{1.11}$$

we obtain that [6]

$$\mathbf{F}_n(\mathbf{R}) = -\mathrm{Im} \sum_{n \neq m} \frac{\langle n(\mathbf{R})|\nabla_{\mathbf{R}} H(\mathbf{R})|m(\mathbf{R})\rangle \times \langle m(\mathbf{R})|\nabla_{\mathbf{R}} H(\mathbf{R})|n(\mathbf{R})\rangle}{(E_m(\mathbf{R}) - E_n(\mathbf{R}))^2} \tag{1.12}$$

Remembering the definition of the Berry curvature (1.10), the previous formula shows that the Berry curvature can be thought as the result of the interaction of the level $|n(\mathbf{R})\rangle$ with the other levels $|m(\mathbf{R})\rangle \neq |n(\mathbf{R})\rangle$ which have been projected out by the adiabatic transformation. The limitation of the formula (1.10) is that it only works if the parameter space is three-dimensional. Nevertheless, no condition has been imposed on the dimensionality of the parameter space when the Berry connection has been defined. A more dimension-agnostic definition is possible by means of differential forms, as discussed in [5]. However this description is out if the scope of this thesis.

Two level systems

In the following we obtain an expression for the Berry phase and the Berry curvature of a two-level system. This system represent, for example, a toy model of an insulator or the dynamic of a spin-$\frac{1}{2}$ system. The generic form of the Hamiltonian is

$$H = \epsilon(\mathbf{R})\mathbb{1}_{2\times 2} + \boldsymbol{d}(\mathbf{R})\cdot\boldsymbol{\sigma} \tag{1.13}$$

where $\boldsymbol{\sigma} = (\sigma_x, \sigma_y, \sigma_z)$ is Pauli vector and $\boldsymbol{d}(\mathbf{R})$ is a three dimensional vector that depends on the parameters $\mathbf{R}$. The system has two eigenstates $|+\mathbf{R}\rangle$ and $|-\mathbf{R}\rangle$ with energies E_+ and E_-, respectively. The energies of the two levels of the system are $E_\pm = \epsilon(\mathbf{R}) \pm |\boldsymbol{d}|$. Then the Berry curvature for the upper level reads

$$\mathbf{F}_+(\mathbf{R}) = -\mathrm{Im}\frac{\langle +\mathbf{R}|\nabla_{\mathbf{R}}H(\mathbf{R})|-\mathbf{R}\rangle \times \langle -\mathbf{R}|\nabla_{\mathbf{R}}H(\mathbf{R})|+\mathbf{R}\rangle}{4|\mathbf{R}|^2} \tag{1.14}$$

The term proportional to the identity matrix can be neglected because it only defines the zero of the energy and doesn't affect the dynamics of the system.
Without loss of generality let's assume that the degeneracy point $\mathbf{R}^*$ (for which $E_+(\mathbf{R}^*) = E_-(\mathbf{R}^*)$) is in $\mathbf{R}^* = 0$ and that close to this point (the region that will be considered) $\boldsymbol{d}(\mathbf{R}) = \mathbf{R}$. Then the Hamiltonian becomes $H = \mathbf{R}\cdot\boldsymbol{\sigma}$ and $E_+ = |\mathbf{R}|$ and $E_- = -|\mathbf{R}|$. Moreover, in this particular case $\nabla_{\mathbf{R}}H = \boldsymbol{\sigma}$. In order to simplify the calculations, let's align the z-axis along $\mathbf{R}$. Then, if we set $|+\mathbf{R}\rangle \equiv |+\rangle$ and $|-\mathbf{R}\rangle \equiv |-\rangle$

$$\sigma_z|\pm\rangle = \pm|\pm\rangle \qquad \sigma_x|\pm\rangle = |\mp\rangle \qquad \sigma_y|\pm\rangle = \pm i|\mp\rangle \tag{1.15}$$

Then $F_{+x}(\mathbf{R}) = F_{+y}(\mathbf{R}) = 0$ because $\langle\pm|\sigma_z|\mp\rangle = 0$. The only non-vanishing component is

$$F_{+z}(\mathbf{R}) = -\mathrm{Im}\frac{\langle+|\sigma_x|-\rangle\langle-|\sigma_y|+\rangle - \langle+|\sigma_y|-\rangle\langle-|\sigma_+|+\rangle}{4R^2} = -\frac{1}{2R^2} \tag{1.16}$$

where $R \equiv |\mathbf{R}|$. If the z-axis is not aligned with $\mathbf{R}$, the rotational invariance implies that

$$\boldsymbol{F}_+(\mathbf{R}) = -\frac{\mathbf{R}}{2R^3} \tag{1.17}$$

This is the field generated by a monopole (in $\mathbf{R}$ parameter space) of strength $-1/2$ which is located at $\mathbf{R} = 0$. The Berry phase is

$$\gamma_+(\mathcal{C}) = -\int_{\mathcal{F}} d\mathbf{S}\cdot\frac{\mathbf{R}}{2R^3} = -\frac{1}{2}\Omega(\mathcal{C}) \tag{1.18}$$

Here $\Omega(\mathcal{C})$ is the solid angle that $\mathcal{C}$ subtends at the degeneracy point. Therefore, the degeneracy points act as sources of the Berry curvature. Then the integral of the Berry curvature over a closed manifold is equal to 2π times the number of the degeneracy points contained inside. In general, the Berry curvature integrated over a 2-D surface, usually the Brillouin zone (BZ), is an integer

$$n = \frac{1}{2\pi}\int_{BZ} d\mathbf{S}\cdot\boldsymbol{F}(\mathbf{k}) \tag{1.19}$$

This integer is called the *Chern number*. The previous formula relates local properties (Berry curvature) to local properties (Chern number).

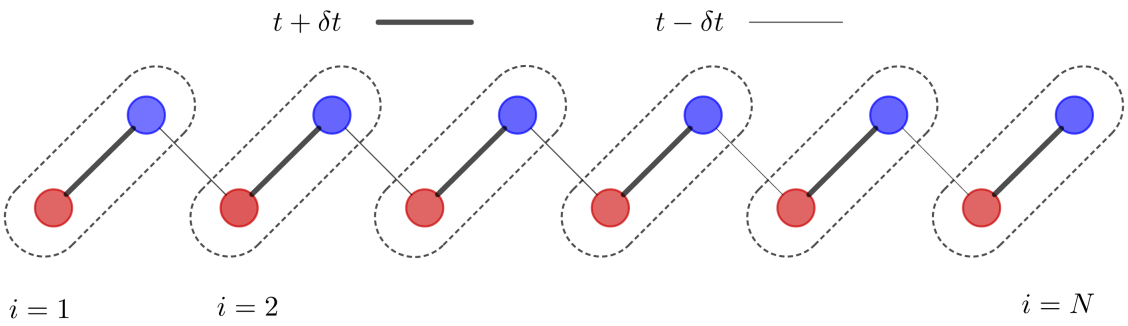

Figure 1.1: Picture of the SSH model. Every elementary cell consists of two sites A (red circles) and B(blue circles). The hopping amplitudes are staggered. There is no hopping between sites of the same sublattice.

1.2 Su-Schrieffer-Heeger Model

In this chapter, we introduce the basic concepts of topological insulators. In particular, the chiral symmetry, the topological invariants, and the bulk-edge correspondence will be discussed through the analysis of the SSH model first developed by Su, Schrieffer and Heeger [34].
The SSH model is an example of a Topological band insulator that belongs to the symmetry class BDI [5](see also Section 1.3). It was first introduced as a model of the trans-polyacetylene. Polyacetylene is the simplest linear conjugated polymer. It consists of weakly coupled chains of CH units forming a quasi-one-dimensional lattice. Three of the four valence electrons for a particular carbon atom in the chain are used in bonding with the nearest carbon atoms and the hydrogen atom. The fourth electron creates a double bond between a pair of carbon atoms. The alternating single and double bonds (these are σ and σ plus Π bonds, respectively) will be considered for simplicity in one dimension. The extra electron, that is responsible for forming the Π bond, will be treated in a tight-binding approximation. The Hamiltonian with OBCs reads (see Fig. 1.1) [20, 4]

$$H = -(t+\delta t)\sum_{i=1}^{N}[c^{\dagger}_{A,i}c_{B,i} + \text{h.c.}] - (t-\delta t)\sum_{m=1}^{N-1}[c^{\dagger}_{A,i+1}c_{B,i} + \text{h.c}] \tag{1.20}$$

For simplicity, let's take $t > 0$ and $|\delta t| \leq t$. The staggered hopping amplitudes $(t+\delta t)$ and $(t-\delta t)$ refer to the single bonds and the double bonds. Here a unit cell with two atoms, labeled A and B has been defined.
Moreover spinless electrons (even though the real SSH model includes spin) have been considered. The SSH model has a bulk and a boundary. The bulk is the long central part of the chain; the boundaries are the two ends, or edges, of the chain. The bulk properties can be studied by

assuming periodic boundary conditions. In this case

$$H = -\sum_{i=1}^{N}[(t+\delta t)c_{A,i}^{\dagger}c_{B,i} + (t-\delta t)c_{A,i+1}^{\dagger}c_{B,i}] + \text{h.c} \tag{1.21}$$

with $c_{i+N} = c_i$. Let's define

$$c_{a,j} = \frac{1}{\sqrt{N}}\sum_{k} e^{ikj}c_{a,k} \tag{1.22}$$

where $a = \{A, B\}$ and $k = 2\pi q/N$, $q = 0, ..., N-1$. The Hamiltonian in Fourier space becomes

$$H = \sum_{k} c_{a,k}^{\dagger}H_{ab}(k)c_{b,k} = \sum_{k}(c_{A,k}^{\dagger}, c_{B,k}^{\dagger})H(k)\begin{pmatrix} c_{A,k} \\ c_{B,k}\end{pmatrix} \tag{1.23}$$

where the Block Hamiltonian $H(k)$ can be written as

$$H(k) = \boldsymbol{d}(k)\cdot\boldsymbol{\sigma}, \qquad \boldsymbol{d}(k) = \begin{pmatrix} -(t+\delta t) - (t-\delta t)\cos k \\ -(t-\delta t)\sin k \\ 0 \end{pmatrix} \tag{1.24}$$

The Hamiltonian $H(k)$ is a two-band Hamiltonian (see equation (1.13)). Then the eigenvalues are

$$E_{\pm}(k) = \pm|\boldsymbol{d}(k)| = \pm\sqrt{2(t^2+\delta t^2) + 2(t^2-\delta t^2)\cos k} \tag{1.25}$$

In the half-filling situation, where all negative energy eigenstates of the Hamiltonian are occupied, the energy gap Δ separating the lower filled band from the upper empty band is $\Delta = 4|\delta t|$ ($\delta > 0$). Therefore without the staggering, i.e. $\delta = 0$, the gap closes and the model behaves like a conductor (see Fig. 1.2). The polymer polyacetylene, at half-filling, undergoes a Peierls instability to a dimerized state. The Peierls' theorem states that if the energy-savings due to the new band gaps outweighs the elastic energy cost of rearranging the ions, the lattice distortion becomes energetically favorable. A detailed analysis of this process necessitates a model where the positions of the atoms are also dynamical. Nevertheless, the energy-saving due to the new band gaps can be understood by analyzing the effects of a slight staggering on the dispersion relation. As the gap due to the staggering of the hopping amplitudes opens, the energy the of occupied states is lowered, while unoccupied states move to higher energies. Thus, the staggering, if the elastic force between the ions is weak, is energetically favored.

1.2.1 Fully dimerized limit

The SSH model becomes particularly simple in the fully dimerized cases $\delta t = t$ and $\delta t = -t$ (with open boundary conditions). In these two limits the eigenstates are even and odd linear combinations of the two sites forming a dimer.

1. $\delta t = t$. The Hamiltonian becomes

$$H = -2t\sum_{i=1}^{N}[c_{A,i}^{\dagger}c_{B,i} + \text{h.c}] \tag{1.26}$$

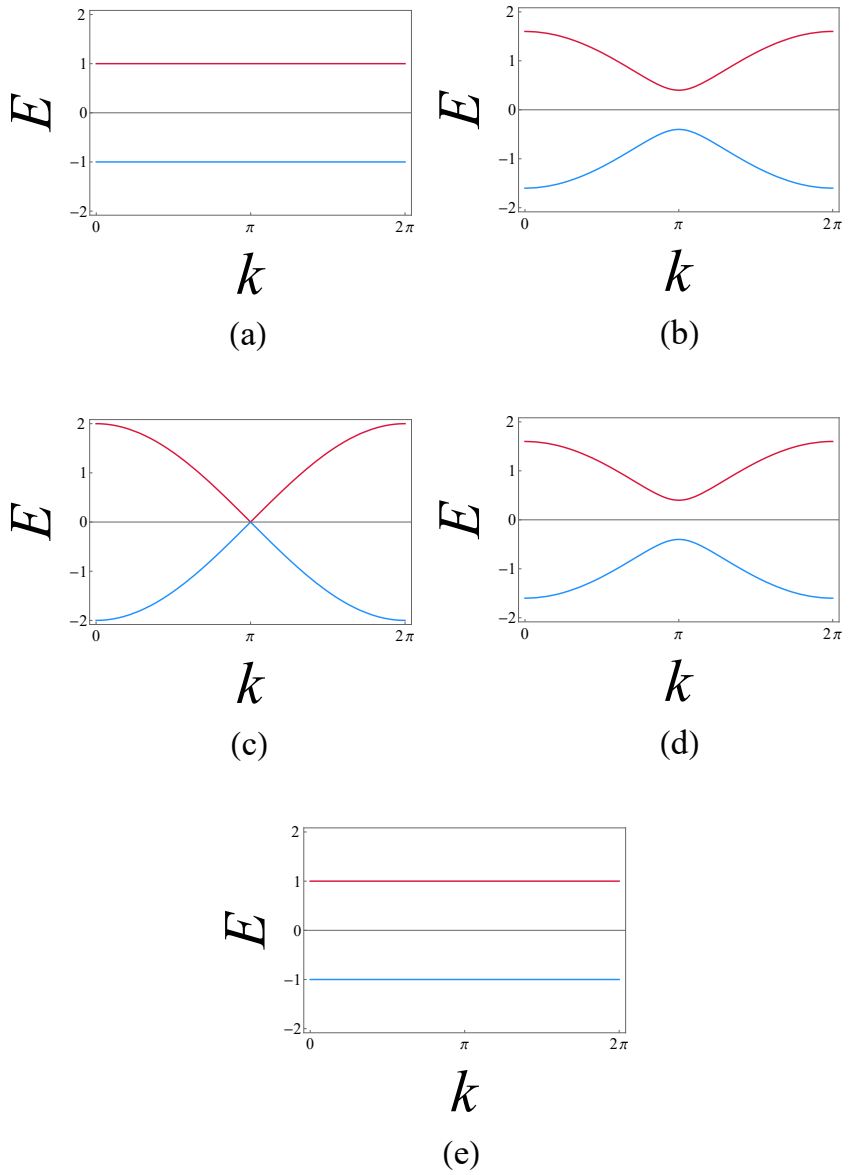

Figure 1.2: Dispersion relations of the SSH model (1.25) for different values of the hopping amplitudes: (a) $(t+\delta t) = 1$, $(t-\delta t) = 0$; (b) $(t+\delta t) = 1$, $(t-\delta t) = 0.6$; (c) $(t+\delta t) = 1$, $(t-\delta t) = 1$; (d) $(t+\delta t) = 0.6$, $(t-\delta t) = 1$; (e) $(t+\delta t) = 0$, $(t-\delta t) = 1$. In both cases (a) and (e), the energy eigenvalues don't depend on the wavenumber k. The energies are $E_{\pm}(k) = \pm 1$; this is the so-called *flatband limit* (see Section 1.3.3). In this special cases the nonuniversal information about the energy band is removed and only the topological information which classifies the different phases is present.

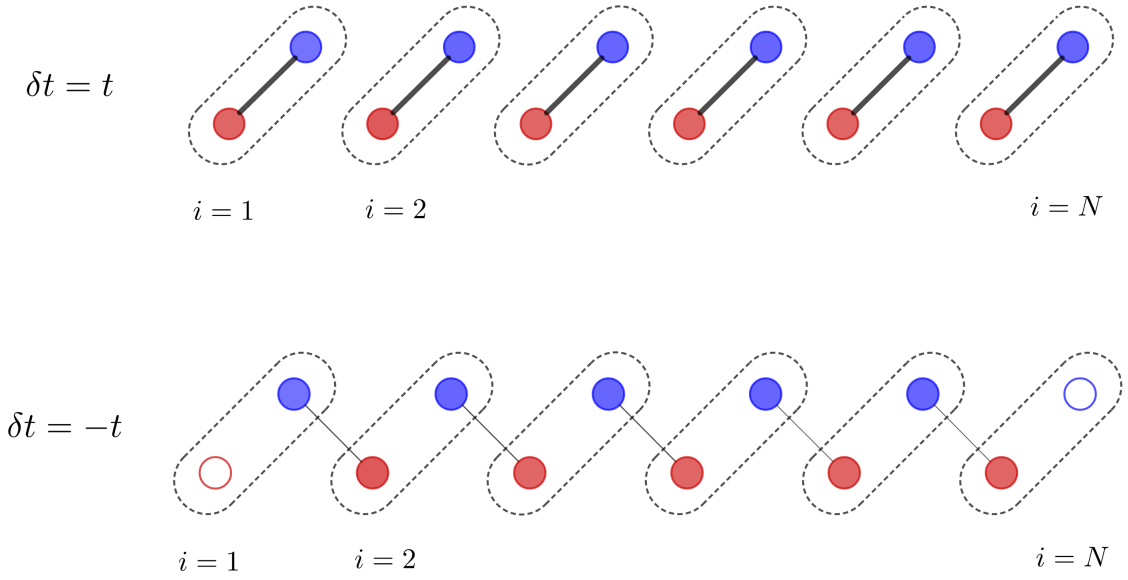

Figure 1.3: Fully dimerized limits for the SSH model. The trivial case $\delta t = t$ has no intracell hopping and there is no unpaired mode. The topological case $\delta t = -t$ has only intercell hopping and as a consequence there is one isolated site per edge (empty circles) that can host a zero energy excitation.

There is only intra-cell hopping. The eigensates are $|i, A\rangle \pm |i, B\rangle$ with $i \in 1, ..., N$. Here $|i, A\rangle$ and $|i, B\rangle$ denote the states of the chain where the electron is on the sublattice site A and B of the unit cell i, respectively. They satisfy

$$H(|i, A\rangle \pm |i, B\rangle) = \pm(-2t)(|i, A\rangle \pm |i, B\rangle) \tag{1.27}$$

for $i = 1, ..., N$. The system is in the trivial phase with constant energies $E_{\pm} = \pm 2|t|$.

2. $\delta t = -t$. The Hamiltonian is

$$H = -2t \sum_{i=1}^{N-1} [c^{\dagger}_{A,i+1} c_{B,i} + \text{h.c}] \tag{1.28}$$

In this case each dimer is shared between two neighboring unit cells

$$H(|i, B\rangle \pm |i + 1, A\rangle) = \pm(-2t)(|i, B\rangle \pm |i + 1, A\rangle) \tag{1.29}$$

for $i = 1, ..., N - 1$. There are two other eigenstates. Indeed, the previous Hamiltonian doesn't contain the modes $c_{A,1}$ and $c_{B,N}$ and therefore they can be excited with no cost of energy. Then there are two more zero energy eigenstates

$$|A, 1\rangle = c^{\dagger}_{A,1}|0\rangle \qquad |B, N\rangle = c^{\dagger}_{B,N}|0\rangle \tag{1.30}$$

which satisfy

$$H|A,1\rangle = 0 \qquad H|B,N\rangle = 0 \tag{1.31}$$

These states are called edge states because they are localized at the beginning or at the end of the chain.

From equation (1.25) we see that the gap closes for $\delta t = 0$ at $k = \pi$. Thus, the topological phase occurs at $\delta t < 0$ while the trivial phase occupies the region $\delta t > 0$. The edge states survive in the whole topological phase although they acquire an exponential tail protruding inside the bulk. These two edge states have non vanishing components only on the sublattice A or B because of the chiral symmetry (see the following discussion).

1.2.2 Chiral simmetry

A system has the chiral symmetry represented by the unitary and Hemitian operator Γ if (see Section 1.3.2 for a more detailed description)

$$\Gamma\Gamma^\dagger = \Gamma^\dagger\Gamma = \mathbb{1} \qquad \{\Gamma, H\} = 0 \tag{1.32}$$

The operator Γ is required to be local. In the SSH chain this means that for $i \neq i'$ the chiral operator Γ must satisfy $\langle i, a|\Gamma|i, b\rangle = 0$ for any $a, b \in \{A, B\}$. Starting from the anticommutation relation (1.32) one obtains that the spectrum of a chiral symmetric Hamiltonian is symmetric i.e. for any state $|u_E\rangle$ with energy E there is a chiral symmetric partner $\Gamma|u_E\rangle = |u_{-E}\rangle$ with energy $-E$. This property implies that nonzero energy eigenstates have equal support on both lattices A and B [4]. The only relevant symmetry (which does not alter the topological properties) of the SSH model is the chiral symmetry [5]. The bulk momentum-space Hamiltonain $H(k)$ satisfy

$$\sigma_z H(k) = -H(k)\sigma_z \tag{1.33}$$

This is a direct consequence of that $d_z(k) = 0$ for every value of k. Therefore the path of the endpoint of $\boldsymbol{d}(k)$, as the wavenumber goes through the Brillouin zone, $k \in [0, 2\pi]$, is a closed path (a circle of radius $(t - \delta t)$ centered at $(-(t + \delta t), 0)$) on the (d_x, d_y)-plane. The topology of this loop can be characterized by an integer: the bulk winding number v. This counts the number of times the loop winds around the origin of the (d_x, d_y)-plane. Fig. 1.4 shows the path of the endpoint of $\boldsymbol{d}(k)$ for different values of $(t + \delta t)$ and $(t - \delta t)$. For example, panels (a) and (b) in Fig. 1.4 show a curve with $v = 0$; in Fig. 1.4 panels (d) and (e) have $v = 1$. In Fig. 1.4(c) instead the winding number v is undefined. Therefore in the trivial phase $\delta t > 0$, $v = 0$; in the topological region $\delta t < 0$, $v = 1$. Let's define the unite vector

$$\tilde{\boldsymbol{d}}(k) = \frac{\boldsymbol{d}(k)}{|\boldsymbol{d}(k)|} \tag{1.34}$$

which, substantially, projects the curve of $\boldsymbol{d}(k)$ to the unit circle of the (d_x, d_y)-plane. Then the winding number is given by

$$v = \frac{1}{2\pi}\int_{-\pi}^{\pi}\left(\tilde{\boldsymbol{d}}(k) \times \frac{d}{dk}\tilde{\boldsymbol{d}}(k)\right)_z dk \tag{1.35}$$

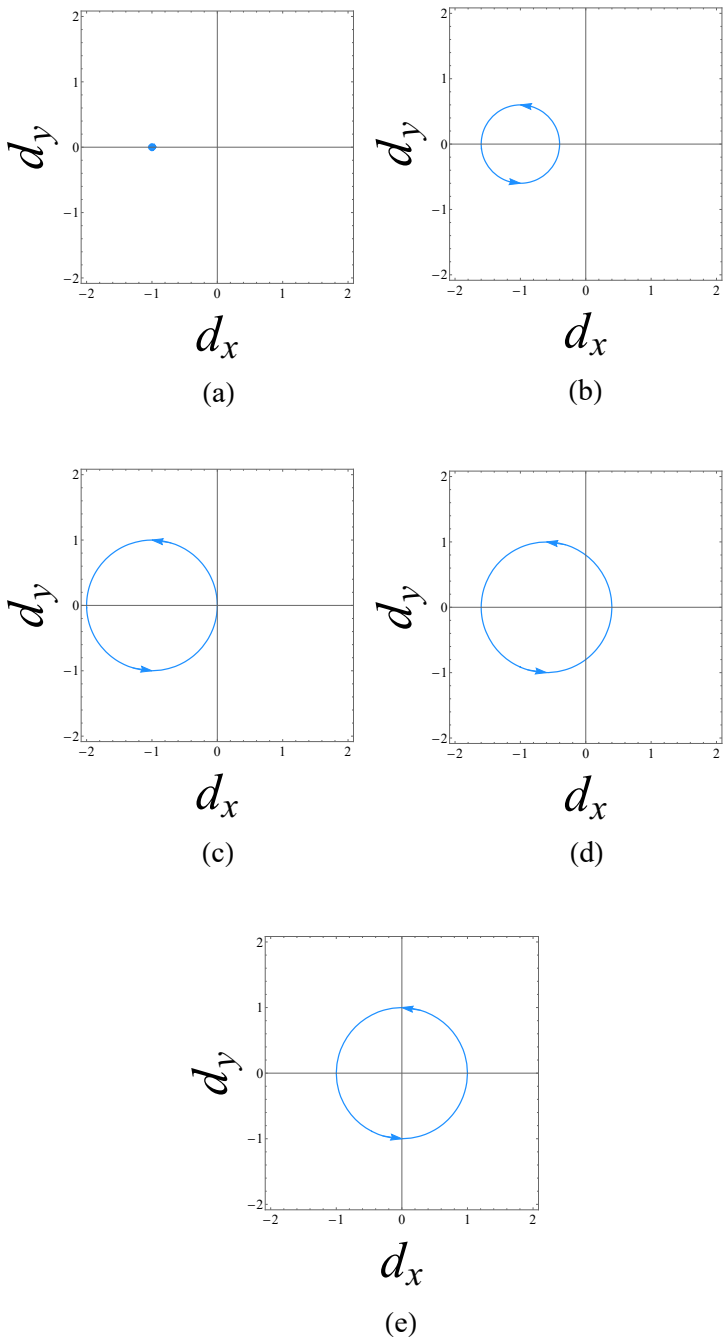

Figure 1.4: Paths of the endpoints of $\boldsymbol{d}(k)$ (1.24) in the (d_x, d_y)-plane as a function of $k \in [0, 2\pi]$ for different values of the hopping amplitudes: (a) $(t+\delta t) = 1$, $(t-\delta t) = 0$; (b) $(t+\delta t) = 1$, $(t-\delta t) = 0.6$; (c) $(t+\delta t) = 1$, $(t-\delta t) = 1$; (d) $(t+\delta t) = 0.6$, $(t-\delta t) = 1$; (e) $(t+\delta t) = 0$, $(t-\delta t) = 1$.

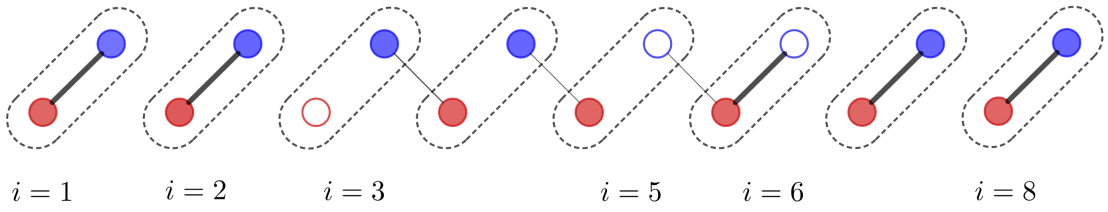

Figure 1.5: Three fully dimerized domains. The domain walls host zero energy eigenstates (empty circles) that can be localized on a single site (as for $i = 3$) or on a superposition of sites (as the odd superposition of the ends of the trimer shared between the $n = 5$ and $n = 6$ unit cells).

In the SSH model the points for which $\delta t > 0$ or $\delta t < 0$ are adiabatically connected because one can draw a path between them that doesn't cross the gapless phase $\delta t = 0$. To change the winding number one needs to pull the path of $\boldsymbol{d}(k)$ through the origin of the (d_x, d_y)-plane. This transformation is not adiabatic because it requires the closure of the gap. Therefore the points connected by an adiabatic transformation have the same winding number. The winding number v is an example of topological invariant i.e. an integer number that doesn't change under adiabatic transformations. Let's define N_A and N_B as the number of the edge modes at the left end of the chain in the sublattice A and B, respectively. Then, in the trivial region $N_A - N_B$ and v are 0; in the topological region $N_A - N_B$ and v are 1. Therefore, remembering that the bulk winding number was obtained from the bulk Hamiltonian only, the bulk properties of the model are related to the edge ones. This is an example of the bulk-edge correspondence, a recurring theme in the theory of topological insulators.

1.2.3 Bound states and domain walls

Edge states can occur also at domain walls between different insulating domains of the same chain. The domain walls are the boundaries between different insulating regions. Let's consider the three fully dimerized domains each characterized by a different value of δt (see Fig. 1.5). There are two types of domain walls which host zero energy excitations: one containing a single site and one containing a trimer. In fact, in the trimer case, the odd superposition of the two end sites satisfy

$$H(|5, B\rangle - |6, B\rangle) = 0 \tag{1.36}$$

Out of the fully dimerized limits the edge states penetrate the bulk with an exponentially decaying tails [4].

1.3 Classification of topological phases of matter

There are several ways to classify the topological phases of matter. In the first part of this section we discuss the general quantum entanglement-based viewpoint of Topological Phases of Matter. Then we give an overview of the classification problem of the Topological Insulators and Superconductors of non-interacting fermions which understanding is now very well established

and complete. In particular, we review in some detail the "Ten-Fold Way" in the bulk approach in the translationally invariant case which is the cornerstone of the classification of the non-interacting fermion systems. However, it must be said that the general classification problem of the topological phases of matter is still evolving and is currently a very active field of research. There is an interesting perspective on the classification problem which exploits the existence of the Quantum Anomalies (well known in the context of Elementary particle physics). In this approach, the boundary cannot be thought of as a consistent quantum theory in isolation from the topological quantum state in the bulk. It turns out that the Quantum anomalies persist even in the interacting regime and therefore they can be used to classify these systems. In many cases there are significant differences between the interacting and the non-interacting topological insulators. Nevertheless, it has been found that the fully interacting classification follows closely the non-interacting template. Recently, progress has been made also in the topological phases of systems of Bosons [10] where Group Cohomology appears to play an important role in the classification. Following the same line, for the fully interacting fermion phases, the Group Super Cohomology [16] has been proposed. However, a full description of the Quantum Anomalies, the Group Cohomology and the systems of Bosons is out of the scope of this thesis.
As a final remark, it must be stressed that the problem of classification of the topological phases of matter is not just strictly theoretical. In fact, in the last decades, new distinct types of Topological Insulators have been discovered thanks to the theoretical predictions made on the classification scheme of all possible Hamiltonians.

1.3.1 Quantum entanglement-based viewpoint of Topological phases of matter

Quantum entanglement turns out to provide an important perspective on Topological phases of matter. There are two types of quantum states: the Short Range Entangled (SRE) states and the Long Range Entangled (LRE) states. A SRE state is a quantum state $|s\rangle$ that can be continuously transformed into a final direct product state $|s\rangle_f$ [27]

$$|s\rangle_f = \mathcal{T}_g[e^{-i\int_{g_i}^{g_f} dg\hat{H}(g)}]|s\rangle, \qquad |s\rangle_f = |s_1\rangle_1 \otimes |s_2\rangle_2 \otimes |s_3\rangle_3 \otimes ... \tag{1.37}$$

where $\hat{H}(g)$ is a local Hamiltonian on which no symmetry condition are imposed and $\mathcal{T}_g$ is the time ordering acting on the parameter g. A quantum state is a Long Range Entangled (LRE) state if it's not a Short Range Entangled (SRE) state. LRE states have an *intrinsic bulk topological order* that is they usually show "interesting" properties like ground state degeneracies, anyonic excitations which can carry fractional excitations, etc.. Quantum systems can be grouped in the following two general categories:

1. **No symmetry constraints**. In this case the system under consideration is not subject to any symmetry constraint. There is only a single SRE phase because every state can be continuously transformed into each other.

2. **Symmetry Constraints**. Now the system is invariant under some symmetry group G. SRE states are called "standard" SRE states if they arise from spontaneously breaking of the symmetry of the system. Instead, if the symmetry is not broken, the SRE states

are called Symmetry Protected Topological (SPT) states. In the latter case, there can be several distinct phases with the same symmetry. The Topological Insulators of non-interacting fermions belong to this category. Finally, LRE with symmetry constraints are called Symmetry Enhanced Topological phases (SET).

In the following, we are interested in the systems of non-interacting fermions which, as explained above, provide the simplest examples of the SPT phases. SPT phases have a bulk gap and don't exhibit any "interesting" bulk properties. Nevertheless, the boundary is non-trivial i.e. it could spontaneously break the symmetry, have an intrinsic (boundary) topological order or be gapless. In particular, the boundary of a non-interacting fermion system is always gapless.
It turns out that all possible Hamiltonians can be classified according to the behavior under certain "special" symmetries. They are are the time-reversal, the charge-conjugation (particle-hole) and the chiral symmetry. The time-reversal and the charge-conjugation symmetries are not ordinary symmetries because they are realized (on the Hilbert space of the first quantized Hamiltonian) by antiunitary operators instead of unitary operators. There is a maximum of 10 types of Hamiltonians that respond differently to these three symmetries [27]. All these Hamiltonians can be classified within the "Ten fold way" framework which will be introduced below.

1.3.2 Role of symmetries

Let's consider a non-superconducting system. In second quantization it's described by the second quantization Hamiltonian [27]

$$\hat{H} = \sum_{A,B} \hat{\psi}^\dagger_A H_{AB} \hat{\psi}_B = \hat{\psi}^\dagger H \hat{\psi} \tag{1.38}$$

where $\hat{\psi}^\dagger$ and $\hat{\psi}$ are fermionic creation and destruction operators satisfying the usual anticommutation relations. The indexes A and B denote the lattice site (or a combined index, such as the lattice site and the spin). The Hamiltonian $H = H_{AB}$ is a matrix of numbers and is called *first quantized Hamiltonian*. The previous analysis can be extended also to superconductors. All that is necessary is to replace the column vector $\hat{\psi}$ by the Nambu spinor $\hat{\chi} = (\hat{\psi}, (\hat{\psi}^\dagger)^t)$. In this situation, the following discussion goes through analogously.
A Hamiltonian is invariant under a group G_0 of unitary realized symmetries if there exists a set of matrix U (one for each element of the group) that commute with the first quantized Hamiltonian

$$UHU^\dagger = H \tag{1.39}$$

In the second quantized language this corresponds to the following action of the operator $\hat{\mathcal{U}}$ on fermion creation and annihilation operators

$$\hat{\mathcal{U}} \hat{\psi}_A \hat{\mathcal{U}}^{-1} = \sum_B U^\dagger_{AB} \hat{\psi}_B \qquad \hat{\mathcal{U}} \hat{\psi}^\dagger_A \hat{\mathcal{U}}^{-1} = \sum_B \hat{\psi}^\dagger_B U_{BA} \tag{1.40}$$

The second quantized Hamiltonian commutes with $\hat{\mathcal{U}}$

$$\hat{\mathcal{U}} \hat{H} \hat{\mathcal{U}}^{-1} = \hat{H} \tag{1.41}$$

If H has a unitary (on the Hilbert space of the first quantized Hamiltonian) symmetry, we can block-diagonalize it and then consider the topological properties of each "symmetry-less" block individually.
In this situation, the vector space spanned by the single-particle eigenstates decomposes into a direct sum of vector spaces associated with certain irreducible representations λ of the group G_0. Each irreducible representation defines a Bloch Hamiltonian $H^{(\lambda)}$. If we consider all possible Hamiltonian, the set of all bloch Hamiltonians that can be obtained doesn't depend on the symmetry group G_0 [27]. In particular, there can be only ten possible set of these matrices.
In quantum mechanics, any symmetry must be realized by a unitary or an antiunitary operator acting on the Hilbert space. Since the block Hamiltonians $H^{(\lambda)}$ are completely independent of any unitary realized symmetries, they can only be classified according to the behavior under the antiunitary (on the Hilbert space of the first quantized Hamiltonian) symmetries. In order to classify all possible Hamiltonians, we need to consider only one time-reversal and only one charge conjugation operation as well as the unitary chiral symmetry [27].

Time-reversal symmetry The action of operator $\hat{\mathcal{T}}$ that implements the time-reversal symmetry on the fermion Fock space is

$$\hat{\mathcal{T}}\hat{\psi}_A\hat{\mathcal{T}}^{-1} = \sum_B (U_T^\dagger)_{AB}\hat{\psi}_B \qquad \hat{\mathcal{T}}\hat{\psi}_A^\dagger\hat{\mathcal{T}}^{-1} = \sum_B \hat{\psi}_B^\dagger (U_T)_{BA} \qquad \hat{\mathcal{T}}i\hat{\mathcal{T}}^{-1} = -i \tag{1.42}$$

where U_T is the associated unitary operator. The second quantized Hamiltonian is time-reversal invariant if

$$\hat{\mathcal{T}}\hat{H}\hat{\mathcal{T}}^{-1} = \hat{H} \tag{1.43}$$

The time evolution operator $\hat{U}(t) = e^{-it\hat{H}}$ is mapped into

$$\hat{\mathcal{T}}\hat{U}(t)\hat{\mathcal{T}}^{-1} = e^{-\hat{\mathcal{T}}i\hat{\mathcal{T}}^{-1}t\hat{H}} = e^{-i(-t)\hat{H}} = \hat{U}(-t) \tag{1.44}$$

as desired for time-reversal. The condition (1.43) implies for the first quantized Hamiltonian

$$THT^{-1} = H \qquad T = U_T K \tag{1.45}$$

where K is the antiunitary operator that implements complex conjugation, $KHK^{-1} = H^*$. In fact, being the time-reversal symmetry an antiunitary symmetry, the previous relation must involve the complex conjugation operation. It is easy to show that the square of the time-reversal operator $\hat{\mathcal{T}}^2$ is a unitary operator with associated matrix $T^2 = U_T^* U_T$. Applying time-reversal twice, any state must return to the same state up to an overall phase factor $e^{i\phi}$. The last condition implies that $T^2 = \pm 1$. Therefore, if the Hamiltonian is time-reversal invariant, there are two ways in which it can respond.

Charge conjugation The second fundamental antiunitary symmetry is the charge conjugation (particle-hole) symmetry $\hat{\mathcal{C}}$. The action of the second quantized operator $\hat{\mathcal{C}}$ on the fermion Fock space is

$$\hat{\mathcal{C}}\hat{\psi}_A\hat{\mathcal{C}}^{-1} = \sum_B (U_C^{*\dagger})_{AB}\hat{\psi_B^\dagger} \qquad \hat{\mathcal{C}}\hat{\psi}_A^\dagger\hat{\mathcal{C}}^{-1} = \sum_B \hat{\psi}_B (U_C^*)_{BA} \qquad \hat{\mathcal{C}}i\hat{\mathcal{C}}^{-1} = i \tag{1.46}$$

where U_C is the associated unitary matrix. The second quantized Hamiltonian $\hat{H}$ is charge-conjugation invariant if and only if

$$\hat{\mathcal{C}}\hat{H}\hat{\mathcal{C}}^{-1} = \hat{H} \tag{1.47}$$

Then the first quantized Hamiltonian satisfies

$$CHC^{-1} = -H \qquad C = U_C K \tag{1.48}$$

Repeating the same steps done for the time-reversal symmetry it follows that $C^2 = \pm 1$. Thus, also in this case, there are two ways in which a charge conjugation invariant Hamiltonian can respond to the symmetry.

Chiral symmetry The last symmetry that must be considered to fully characterize all the possible Hamiltonians is the chiral symmetry. The second quantized operator $\hat{\mathcal{S}}$ which implements chiral symmetry reads

$$\hat{\mathcal{S}} \equiv \hat{\mathcal{T}}\hat{\mathcal{C}} \tag{1.49}$$

The relations (1.42) and (1.46) imply that action on the fermion Fock space is [27]

$$\hat{\mathcal{S}}\hat{\psi}_A\hat{\mathcal{S}}^{-1} = \sum_B (U_S^{*\dagger})_{AB}\hat{\psi_B^\dagger} \qquad \hat{\mathcal{S}}\hat{\psi}_A^\dagger\hat{\mathcal{S}}^{-1} = \sum_B \hat{\psi}_B (U_S^*)_{BA} \qquad \hat{\mathcal{S}}i\hat{\mathcal{S}}^{-1} = -i \tag{1.50}$$

Here $U_S = U_T U_C^*$. The second quantized Hamiltonian $\hat{H}$ is chiral invariant if

$$\hat{\mathcal{S}}\hat{H}\hat{\mathcal{S}}^{-1} = \hat{H} \tag{1.51}$$

The first quantized Hamiltonian satisfies

$$SHS^{-1} = -H \qquad S = U_T U_C^* \tag{1.52}$$

Moreover, $S^2 = 1$. Thus, a chiral invariant Hamiltonian can respond only in one way to the chiral symmetry. The chiral symmetry, unlike the previous symmetries, is a unitary operator acting on the Hilbert space of the first quantized Hamiltonian. From now on, for simplicity, we will denote the Bloch Hamiltonians $H^{(\lambda)}$ by H. It turns out that there are 10 different ways in which the first quantized Hamiltonian H can respond to the time-reversal, the charge-conjugation and the chiral symmetry (see Tab.1.1). In fact, one obtains that the chiral symmetry is fixed by the behavior of the other two symmetries but for the case where the Hamiltonian is not invariant under time-reversal nor under particle-hole operations [27]. Each of these 10 possibilities is called symmetry class.

1.3.3 Classification by topology of the bulk in the translationally invariant case

Let's consider now a translational invariant system with, as usual, a gap in the excitation spectrum. In this situation, we can consider the single-particle Hamiltonian H in momentum space $H(\vec{k})$ where $\vec{k}$ is a d-dimensional vector in the Brillouin zone (a d-dimensional torus).

In the simplest case of a model with no symmetry conditions (class A) with n filled and m empty bands, the Bloch Hamiltonian $H(k)$ can be adiabatically deformed into the *flatband Hamiltonian* (see Section 1.2)

$$\mathcal{Q}(\vec{k}) = U(\vec{k})\Lambda U^{\dagger}(\vec{k}) \qquad \Lambda = \begin{pmatrix} 1_m & 0 \\ 0 & -1_n \end{pmatrix} \qquad U(\vec{k}) \in U(n+m) \tag{1.53}$$

which assigns $+1$ to the energy levels above the gap and -1 to those below the gap. By definition, any topological properties will remain unchanged by such continuous deformations. Due to the degeneration of the levels, if $U(\vec{k})$ is of the form

$$U(\vec{k}) = \begin{pmatrix} U_1(\vec{k}) & 0 \\ 0 & U_2(\vec{k}) \end{pmatrix} \qquad U_1(\vec{k}) \in U(m),\, U_2(\vec{k}) \in U(n) \tag{1.54}$$

then $\mathcal{Q}(\vec{k}) = \Lambda$ as in the case where $U(\vec{k}) = 1_{n+m}$. Hence $U(\vec{k})$ is an element of the coset space $G_{m,m+n}(C) = U(n+m)/[U(m) \times U(n)]$. Therefore we have established that every ground state of the simplified Hamiltonian $\mathcal{Q}(\vec{k})$ is described by a map from the Brillouin zone into space $G_{m,m+n}(C)$,

$$\mathcal{Q} : BZ \to G_{m,m+n}(C) \tag{1.55}$$

$$\vec{k} \to \mathcal{Q}(\vec{k}) \tag{1.56}$$

Each map describes a ground state. In a similar way we can consider the cases of the other symmetry classes, which yield a different space for $\mathcal{Q}(\vec{k})$ [27]. Let's assume, for simplicity, that the Brillouin zone is a d-dimensional sphere. The number of topologically different maps $\mathcal{Q}$, or, equivalently, the number of topologically distinct ground states, is given by the Homotopy group (for the class A)

$$\pi_d(G_{m,m+n}(C)) \tag{1.57}$$

Here d is the dimension of the Brillouin zone.
For example $\pi_{d=2}(G_{m,m+n}(C)) = \mathbb{Z}$ and therefore for every integer there is a different ground state. The ten classes are divided into *complex* and *real* ones.
The charge conjugation and the time-reversal symmetries impose a sort of reality condition on the Hamiltonian (see equations (1.45) and (1.48) that involve complex conjugation). Therefore the first two classes, which don't possess any invariance under either of the two antiunitary symmetries T or C, are called *complex*. Instead, the remaining eight classes are called *real*. The resulting classification is summarized in Tab. 1.1 which is taken from [5]. The symmetry classes are labeled with the Cartan's name.

	T^2	C^2	S^2	d	1	2	3	4	5	6	7	8
A	$\varnothing$	$\varnothing$	$\varnothing$		$\varnothing$	$\mathbb{Z}$	$\varnothing$	$\mathbb{Z}$	$\varnothing$	$\mathbb{Z}$	$\varnothing$	$\mathbb{Z}$
AIII	$\varnothing$	$\varnothing$	$+$		$\mathbb{Z}$	$\varnothing$	$\mathbb{Z}$	$\varnothing$	$\mathbb{Z}$	$\varnothing$	$\mathbb{Z}$	$\varnothing$
AII	$-$	$\varnothing$	$\varnothing$		$\varnothing$	$\mathbb{Z}_2$	$\mathbb{Z}_2$	$\mathbb{Z}$	$\varnothing$	$\varnothing$	$\varnothing$	$\mathbb{Z}$
DIII	$-$	$+$	$+$		$\mathbb{Z}_2$	$\mathbb{Z}_2$	$\mathbb{Z}$	$\varnothing$	$\varnothing$	$\varnothing$	$\mathbb{Z}$	$\varnothing$
D	$\varnothing$	$+$	$\varnothing$		$\mathbb{Z}_2$	$\mathbb{Z}$	$\varnothing$	$\varnothing$	$\varnothing$	$\mathbb{Z}$	$\varnothing$	$\mathbb{Z}_2$
BDI	$+$	$+$	$+$		$\mathbb{Z}$	$\varnothing$	$\varnothing$	$\varnothing$	$\mathbb{Z}$	$\varnothing$	$\mathbb{Z}_2$	$\mathbb{Z}_2$
AI	$+$	$\varnothing$	$\varnothing$		$\varnothing$	$\varnothing$	$\varnothing$	$\mathbb{Z}$	$\varnothing$	$\mathbb{Z}_2$	$\mathbb{Z}_2$	$\mathbb{Z}$
CI	$+$	$-$	$+$		$\varnothing$	$\varnothing$	$\mathbb{Z}$	$\varnothing$	$\mathbb{Z}_2$	$\mathbb{Z}_2$	$\mathbb{Z}$	$\varnothing$
C	$\varnothing$	$-$	$\varnothing$		$\varnothing$	$\mathbb{Z}$	$\varnothing$	$\mathbb{Z}_2$	$\mathbb{Z}_2$	$\mathbb{Z}$	$\varnothing$	$\varnothing$
CII	$-$	$-$	$+$		$\mathbb{Z}$	$\varnothing$	$\mathbb{Z}_2$	$\mathbb{Z}_2$	$\mathbb{Z}$	$\varnothing$	$\varnothing$	$\varnothing$

Table 1.1: The "Ten fold way". Symmetry classes of non-interacting fermionic first quantized Hamiltonians based on the works of Schnyder et al. [32] and Kitaev [22]. The symmetry classes are labeled with the Cartan's name (first column). The different symmetry classes can be characterized by their different behaviors of the first quantized Hamiltonian under time-reversal (T), charge-conjugation (C), and chiral symmetry ($S = TC$). If there is no symmetry the entry $\varnothing$ is found. If the symmetry is present, the sign of the square of the symmetry is listed. The remaining columns report the Homotopy groups for the dimensions $d = 1, ..., 8$ of space.

They differ by the sign of the squares of $\hat{\mathcal{T}}$, $\hat{\mathcal{C}}$ and $\hat{\mathcal{S}}$. The symbols Z and Z_2 indicate whether the space of quantum ground states is partitioned into topological sectors labeled by an integer or a Z_2 quantity. The previous analysis focused on the topology of the bulk states in the presence of translational invariance. The Table of Topological Insulators and Superconductors can also be obtained by analyzing the boundaries of the system which exhibit "anomalous" properties. For example, the boundaries of the non-interacting fermionic Topological insulators always conduct electrical current or heat. Following this approach, the classification problem of Topological Insulator in d spatial dimensions can be solved by studying the lack of the Anderson Localization in $\bar{d} = d - 1$ spatial dimensions. However, this description is out of the scope of this thesis.

1.4 The XY chain

Spin models are important because they are the simplest systems in which quantum phase transitions occur. In this chapter we present the XY chain in a transverse magnetic field which is the simplest non-trivial model showing a genuinely quantum mechanical behavior. Moreover, we introduce the Jordan Wigner transformation: a powerful tool, in 1 dimension, that allows us to map a system of interacting spins onto an equivalent system of interacting fermions. The idea behind this description is that often, in many-body systems, the best way of understanding a physical system is to map it onto a mathematically equivalent but physically different system whose properties are already understood. Furthermore, the model with PBCS will be diagonalized with the help of a Fourier transform followed by the Bogoliubov rotation

obtaining a simple system of non-interacting fermions (the quasi-particle description). This allows us to solve for the energy spectrum and the eigenstates of the original Hamiltonian.

1.4.1 The model

The XY model in a magnetic field consists of N spin 1/2 arranged in a row and having only nearest neighbor interactions involving only the x and the y components of the spin operators. The Hamiltonian is [12]

$$H = J\sum_i[(1+\gamma)S_i^xS_{i+1}^x + (1-\gamma)S_i^yS_{i+1}^y] + Jh\sum_i S_i^z \tag{1.58}$$

where γ is the parameter characterizing the degree of anisotropy in the xy-plane.
In the following we will consider only the ferromagnetic case $J=-1$. The operators S_i^x, S_i^y, S_i^z may be represented by the usual Pauli spin matrices ($\hbar=1$) setting $S^{x,y,z} = \frac{1}{2}\sigma^{x,y,z}$ where

$$\sigma^x = \begin{pmatrix} 0 & 1 \\ 1 & 0 \end{pmatrix} \quad \sigma^y = \begin{pmatrix} 0 & -i \\ i & 0 \end{pmatrix} \quad \sigma^z = \begin{pmatrix} 1 & 0 \\ 0 & -1 \end{pmatrix} \tag{1.59}$$

The commutation relations between the Pauli matrices are

$$(\sigma^i)^\dagger = \sigma^i \quad \{\sigma^i,\sigma^j\} = 2\delta^{ij} \quad [\sigma^i,\sigma^j] = 2i\epsilon^{ijk}\sigma^k \tag{1.60}$$

where ϵ^{ijk} is the Levi-Cita symbol. For $\gamma \neq 1$ the XY model shows his genuinely quantum mechanical behavior because the different components of S_i appearing in H do not commute with each other. The effect of the term multiplied by $(1-\gamma)$ is to oppose the ordering of the x-components but to favor the ordering of the y-components.
Let's define

$$a_i = S_i^x - iS_i^y \qquad a_i^\dagger = S_i^x + iS_i^y \tag{1.61}$$

where a_i and $a_i^\dagger$ are respectively the lowering and the raising operators. These operators partly resembles fermionic operators in that

$$\{a_i, a_i^\dagger\} = 1 \qquad a_i^2 = (a_i^\dagger)^2 = 0$$

and they partly resemble Bose operators in that

$$[a_i^\dagger, a_j] = [a_i^\dagger, a_j^\dagger] = [a_i, a_j] = 0 \qquad i \neq j$$

In one dimension the model can be solved by mapping the spins into fermionic operators by introducing the so-called Jordan-Wigner transformation

$$c_i = \exp[i\pi\sum_{j=1}^{i-1} a_j^\dagger a_j]a_i = \prod_{j=1}^{i-1}(1-2a_j^\dagger a_j)a_i \tag{1.62}$$

$$c_i^\dagger = a_i^\dagger\exp[-i\pi\sum_{j=1}^{i-1} a_j^\dagger a_j] = \prod_{j=1}^{i-1}(1-2a_j^\dagger a_j)a_i^\dagger \tag{1.63}$$

The Jordan-Wigner transformation is a highly non-local map which, substantially, associates a spin up to an empty site and a spin down to an occupied one. The non-local part of this mapping is called the Jordan-Wigner string and fixes the anticommutation relation between sites by counting the parity of the overturned spins to the left of the sites on which is applied. The equations (1.62), (1.62) imply the following fermionic anticommutation relations [26]

$$\{c_i, c_j^\dagger\} = \delta_{ij} \qquad \{c_i, c_j\} = 0 \qquad \{c_i^\dagger, c_j^\dagger\} = 0 \tag{1.64}$$

From the definitions (1.62) and (1.63) it follows that $c^\dagger c_i = a_i^\dagger a_i$ so the inverse transformation is simply

$$a_i = \exp[-i\pi \sum_{j=1}^{i-1} c_j^\dagger c_j] c_i = \prod_{j=1}^{i-1} (1 - 2c_j^\dagger c_j) c_i \tag{1.65}$$

$$a_i^\dagger = c_i^\dagger \exp[i\pi \sum_{j=1}^{i-1} c_j^\dagger c_j] = \prod_{j=1}^{i-1} (1 - 2c_j^\dagger c_j) c_i^\dagger \tag{1.66}$$

In the case of open boundary condition the range of the summation index in the Hamiltonian (1.58) is $1 \leq i \leq N-1$ (except for the magnetic term for which $1 \leq i \leq N$). On the other hand, if we consider the periodic boundary conditions then $1 \leq i \leq N$ and $S_{N+1}^x = S_1^x, S_{N+1}^y = S_1^y$. For $i = 1, ..., N-1$

$$\begin{cases} a_i^\dagger a_{i+1} = c_i^\dagger c_{i+1} & \text{(1.67a)} \\ a_i^\dagger a_{i+1}^\dagger = c_i^\dagger c_{i+1}^\dagger & \text{(1.67b)} \end{cases}$$

so that for the open chain

$$H = -\frac{1}{2} \sum_{i=1}^{N-1} [c_i^\dagger c_{i+1} + c_{i+1}^\dagger c_i + \gamma c_i^\dagger c_{i+1}^\dagger + c_{i+1}^\dagger c_i + \gamma c_{i+1} c_i] + h \sum_{i=1}^{N} c_i^\dagger c_j - \frac{hN}{2} \tag{1.68}$$

For the cyclic chain there are two more terms

$$\begin{cases} a_N^\dagger a_1 = -e^{i\pi\mathfrak{N}} c_N^\dagger c_1 & \text{(1.69a)} \\ a_N^\dagger a_1^\dagger = -e^{i\pi\mathfrak{N}} c_N^\dagger c_1^\dagger & \text{(1.69b)} \end{cases}$$

where $\mathfrak{N} \equiv \sum_{j=1}^N c_j^\dagger c_j$. The Hamiltonian is

$$\begin{aligned} H = &-\frac{1}{2} \sum_{i=1}^{N-1} [c_i^\dagger c_{i+1} + c_{i+1}^\dagger c_i + \gamma c_i^\dagger c_{i+1}^\dagger + \gamma c_{i+1} c_i] + h \sum_{i=1}^{N} c_i^\dagger c_i - \frac{hN}{2} \\ &+ e^{i\pi\mathfrak{N}} (c_N^\dagger c_1 + c_1^\dagger c_N + \gamma c_N^\dagger c_1^\dagger + \gamma c_1 c_N) \end{aligned} \tag{1.70}$$

where $e^{i\pi\mathfrak{N}} = \prod_{j=1}^N (1 - 2c_j^\dagger c_j)$ is the parity operator. The Hamiltonian describes spinless fermions hopping on a lattice, with superconducting-like interaction which creates/destroys them in pairs. Although the Hamiltonian doesn't conserve the number of fermions, since they

are created/destroyed in pairs, the parity is conserved. This observation allows to separate the theory in two disconnected sectors with parity ± 1, where the plus sign characterizes configurations with an even number of particles and the minus the one with an odd number. From the boundary terms in (1.70) it follows that for an even number of particles the anti-periodic boundary conditions must be imposed; for an odd number of particles instead the periodic boundary conditions are required. Namely

$$\begin{cases} c_{j+N} = -c_j & \text{for } e^{i\pi\mathfrak{N}} = 1 \quad \text{(even particle number)} \qquad (1.71a) \\ c_{j+N} = c_j & \text{for } e^{i\pi\mathfrak{N}} = -1 \quad \text{(odd particle number)} \qquad (1.71b) \end{cases}$$

With those definitions, the Hamiltonian (1.70) can be written as

$$H = -\frac{1}{2}\sum_{i=1}^{N}[c_i^\dagger c_{i+1} + c_{i+1}^\dagger c_i + \gamma c_i^\dagger c_{i+1}^\dagger + \gamma c_{i+1} c_i] + h\sum_{i=1}^{N} c_i^\dagger c_j - \frac{hN}{2} \qquad (1.72)$$

where the appropriate boundary conditions must be taken into account.
The next step is to move into Fourier space. Let's define [1]

$$c_j = \frac{e^{i\frac{\pi}{4}}}{\sqrt{N}}\sum_k e^{ikj} c_k \qquad\qquad c_k = \frac{e^{-i\frac{\pi}{4}}}{\sqrt{N}}\sum_{j=1}^{N} e^{-ikj} c_j \qquad (1.73)$$

where $k = 2\pi q/N$ and, taking into account the conditions (1.71),

$$\begin{cases} q = \frac{1}{2}, \frac{3}{2}, ..., N - \frac{1}{2} & \text{for } e^{i\pi\mathfrak{N}} = 1 \quad \text{(even particle number)} \qquad (1.74a) \\ q = 0, 1, ..., N-1 & \text{for } e^{i\pi\mathfrak{N}} = -1 \quad \text{(odd particle number)} \qquad (1.74b) \end{cases}$$

The Hamiltonian in Fourier space becomes [2]

$$H = \sum_k [(h - \cos k) c_k^\dagger c_k + \frac{\gamma}{2}\sin k (c_k c_{-k} + c_{-k}^\dagger c_k^\dagger)] - \frac{hN}{2} \qquad (1.76)$$

In matrix form, we can write

$$H = \frac{1}{2}\sum_k \begin{pmatrix} c_k^\dagger & c_{-k} \end{pmatrix} \begin{pmatrix} h - \cos k & -\gamma \sin k \\ -\gamma \sin k & \cos k - h \end{pmatrix} \begin{pmatrix} c_k \\ c_{-k}^\dagger \end{pmatrix} \qquad (1.77)$$

The Hamiltonian can be diagonalized through the Bogoliubov transformation

$$\begin{pmatrix} c_k \\ c_{-k}^\dagger \end{pmatrix} = \begin{pmatrix} \cos\theta_k & \sin\theta_k \\ -\sin\theta_k & \cos\theta_k \end{pmatrix} \begin{pmatrix} \eta_k \\ \eta_{-k}^\dagger \end{pmatrix} \qquad (1.78)$$

[1] The anticommutation relations in real space $\{c_j, c_l^\dagger\} = \delta_{j,l}$ imply that in momentum space $\{c_q, c_k^\dagger\} = \delta_{q,k}$ [12].

[2] The following relation has been used

$$\frac{1}{N}\sum_i e^{i(k-k')i} = \delta_{kk'} \qquad (1.75)$$

Then

$$\eta_k = \cos\theta_k c_k - \sin\theta_k c^\dagger_{-k} \qquad \eta^\dagger_{-k} = \sin\theta_k c_k + \cos\theta_k c^\dagger_{-k} \tag{1.79}$$

The Bogoliubov angle θ_k is defined by

$$\theta_k = \frac{1}{2}\arctan\left(\frac{\gamma\sin k}{h-\cos k}\right) \tag{1.80}$$

In terms of the Bogoliubov quasi-particles the Hamiltonian describes free fermions

$$H = \sum_k [\Lambda_k(\eta^\dagger_k\eta_k - \frac{1}{2})] \tag{1.81}$$

where

$$\Lambda_k = \sqrt{(h-\cos k)^2 + \gamma^2\sin^2 k} \tag{1.82}$$

Since the spectrum is always positive one obtains that the previous rotation is correct only if $h-\cos k > 0$; if $h-\cos k < 0$ then η_k and $\eta^\dagger_k$ must be exchanged.

Even particle number

The ground state of the model in this sector is defined by

$$\eta_k|GS\rangle_+ = 0 \qquad k = \frac{2\pi q}{N},\ q = \frac{1}{2},...,N-\frac{1}{2} \tag{1.83}$$

and is empty of quasi-particles. Instead the vacuum state is defined by

$$c_k|0\rangle = 0 \qquad \forall k \tag{1.84}$$

Imposing (1.83) one obtains [12] the ground state in terms of physical fermions

$$|GS\rangle_+ = \prod_{q=0}^{[(N-1)/2]} (\cos\theta_{k_{q+\frac{1}{2}}} + \sin\theta_{k_{q+\frac{1}{2}}} c^\dagger_{k_{q+\frac{1}{2}}} c^\dagger_{k_{-q-\frac{1}{2}}})|0\rangle \tag{1.85}$$

where $[x]$ is the integer part of x. The ground state energy is [12]

$$E_0^+ = -\frac{1}{2}\sum_{q=0}^{N-1} \Lambda_{k_{q+\frac{1}{2}}} \tag{1.86}$$

In this sector the Hilbert space is generated by applying the creations operators $\eta^\dagger_q$ in pairs to the ground state (in this sector the states have an even excitations number).

Odd particle number

The state of no quasi-particle excitations is defined as

$$\eta_k|GS\rangle_- = 0 \qquad k = \frac{2\pi q}{N},\ q = 0, ..., N-1 \tag{1.87}$$

and its energy is

$$E_0^- = -\frac{1}{2}\sum_{q=0}^{N-1}\Lambda_{k_q} \tag{1.88}$$

This state is not allowed by the conditions of odd excitations. The lowest energy state in this sector is

$$|GS'\rangle_- = c_0^\dagger \prod_{q=1}^{[N/2]}(\cos\theta_{k_q} + \sin\theta_{k_q} c_{k_q}^\dagger c_{k_{-q}}^\dagger)|0\rangle \tag{1.89}$$

where $[x]$ is the integer part of x.

Partition function

The partition function is

$$\begin{aligned} Z = \ & 2^{N-1}\prod_{q=0}^{N-1}\cosh\left[\frac{\beta}{2}\Lambda_{k_{q+\frac{1}{2}}}\right]\left\{1 + \prod_{q=0}^{N-1}\tanh\left[\frac{\beta}{2}\Lambda_{k_{q+\frac{1}{2}}}\right]\right\} \\ & + 2^{N-1}\prod_{q=0}^{N-1}\cosh\left[\frac{\beta}{2}\Lambda_{k_q}\right]\left\{1 - \prod_{q=0}^{N-1}\tanh\left[\frac{\beta}{2}\Lambda_{k_q}\right]\right\} \end{aligned} \tag{1.90}$$

In the thermodynamic limit, the free energy per site is

$$F \equiv -\frac{1}{\beta}\lim_{N\to\infty}\frac{1}{N}\ln Z = -\frac{1}{\beta}\ln 2 - \frac{1}{2\pi\beta}\int_0^{2\pi}\ln\cosh\left[\frac{\beta}{2}\epsilon(\omega)\right]d\omega \tag{1.91}$$

where the terms containing the hyperbolic tangent, being bounded, have been neglected in the thermodynamic limit.

1.5 The Kitaev model

One of the main problems in implementing quantum computers is the decoherence of the quantum systems. Kitaev in his paper [21] proposed a relatively simple theoretical one-dimensional quantum system ("quantum wire") which should avoid this problem or, at least, act as a reliable quantum memory. In general, quantum states are sensitive to two kinds of errors. The first one is the classical error represented by an operator σ_j^x which flips the j-th qubit changing $|0\rangle$ to $|1\rangle$ and viceversa. The second one is the phase error σ_j^z which changes the sign of all states with the j-th qubit equal to 1 relative to the states with the j-th qubit equal to 0. Classical

errors can be avoided by taking as qubit a site that can be either empty or occupied by an electron (the spin degree of freedom is neglected). In this way, single classical errors become impossible because the electric charge must be conserved. Even in superconducting systems, single classical errors can never occur because the fermionic parity (i.e. the electric charge modulo 2) must be conserved. It's important to notice that two classical errors can still happen at two sites simultaneously. This situation can be avoided by providing a medium between different fermionic sites with an energy gap in the excitation spectrum in order to avoid a strong interaction between them. However, this method does not protect from phase errors which are described within the context of fermionic chains by the number operator $c_j^\dagger c_j$. The situation can be improved by employing Majorana fermions which are defined as the real and the imaginary part of the fermionic operators c_i [3]

$$m_{2j-1} = e^{i\frac{\phi}{2}} c_j + e^{-i\frac{\phi}{2}} c_j^\dagger \qquad m_{2j} = ie^{-i\frac{\phi}{2}} c_j^\dagger - ie^{i\frac{\phi}{2}} c_j \tag{1.92}$$

The $2N$ operators m_{2j}, m_{2j-1} are called Majorana fermions because they satisfy the relations

$$m_{2j} = m_{2j}^\dagger \qquad m_{2j-1} = m_{2j-1}^\dagger \tag{1.93}$$

and so they are their own antiparticles. They satisfy

$$\{m_i, m_j\} = 2\delta_{ij} \tag{1.94}$$

The last anticommutation relation is substantially different from the standard fermionic ones. Indeed equation (1.94) implies that $m_i^2 = m_i^{\dagger 2} = 1$.This means that there is no Pauli exclusion principle for Majorana fermions. Indeed, acting twice with m_j gives us back the same state. In fact, it is not even possible to speak about the occupancy number of a Majorana mode because the standard construction $m_i^\dagger m_i = 1$ is trivial and then counting doesn't make any sense [25]. Inverting (1.92) one obtains that the number operator becomes $c_j^\dagger c_j = \frac{1}{2}(1 + 2m_{2j-1}m_{2j})$ and so the phase error would require interaction between two different Majorana sites which could be avoided. Therefore, in theory, a Majorana site is immune to any kind of error.
Unfortunately, Majorana fermions are not readily available in solid-state systems. Kitaev [21] proposed a toy model model which gives rise to Majorana fermions as effective low-energy degrees of freedom. This phenomenon can occur only if superconductive systems are considered [21].
The Kitaev model is a topological superconductor that belongs to the symmetry class BDI (see Section 1.3). However, for the topological properties that we explore below, only the charge conjugation symmetry is crucial [5].
The Hamiltonian is

$$H = \sum_j [-t(c_j^\dagger c_{j+1} + c_{j+1}^\dagger c_j) - \mu(c_j^\dagger c_j - \frac{1}{2}) + \Delta c_j c_{j+1} + \Delta^* c_{j+1}^\dagger c_j^\dagger] \tag{1.95}$$

where t is the real hopping amplitude, μ is the chemical potential and $\Delta = |\Delta| e^{i\phi}$ is the complex induced superconductive gap. The previous Hamiltonian (for Δ real) coincides with that of the XY model after the Jordan-Wigner transformation if $t = 1/2$, $\Delta = \gamma/2$ and $\mu = -h$.

[3] the phase ϕ is not strictly necessary in the present discussion but has been inserted for compatibility with the following treatment.

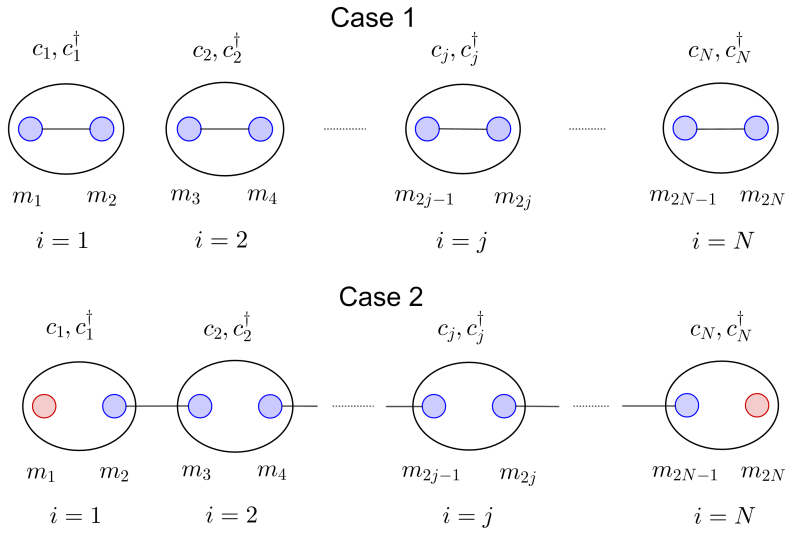

Figure 1.6: A picture of the two special cases. In the case 1 the model is in the trivial phase. In the case 2 the system is in the topological region and there are two unpaired Majorana fermions at the boundary.

1.5.1 Phases of the Kitaev chain

Inverting (1.92) one finds

$$c_j = \frac{e^{-i\frac{\phi}{2}}}{2}(m_{2j-1} + im_{2j}) \qquad c_j^\dagger = \frac{e^{i\frac{\phi}{2}}}{2}(m_{2j-1} - im_{2j}) \tag{1.96}$$

Then, the Hamiltonian (1.95) in terms of Majorana fermions reads

$$H = \frac{i}{2}\sum_j [-\mu m_{2j-1}m_{2j} + (|\Delta| + t)m_{2j}m_{2j+1} + (|\Delta| - t)m_{2j-1}m_{2j+2}] \tag{1.97}$$

where only the imaginary terms appear because the Hamiltonian must be Hermitian. In order to fully characterize the phases of the model let's consider the two special cases by imposing also OBCs:

1. $|\Delta| = t = 0$, $\mu < 0$. Then $H = -\mu\sum_{j=1}^N (c_j^\dagger c_j - \frac{1}{2}) = -\frac{i\mu}{2}\sum_{j=1}^N m_{2j-1}m_{2j}$. The Majorana operators m_{2j-1}, m_{2j} from the same site j are paired together to form a ground state with zero occupation number, as shown in Fig. 1.6, Case 1. Therefore in this case the system is in the trivial phase.

2. $|\Delta| = t > 0$ and $\mu = 0$. The Hamiltonian becomes

$$H = it\sum_{j=1}^{N-1} m_{2j}m_{2j+1} \tag{1.98}$$

The Majorana operators $m_{2j}m_{2j+1}$ from different sites are paired together, as shown in Fig. 1.6, Case 2. The operators m_1, m_N don't appear in the Hamiltonian so they can be collected in a non-local Dirac fermion $\tilde{c}_0 = \frac{1}{2}(m_1 + im_{2N})$ which can be populated without affecting the energy of the state. These Majorana fermions are called *edge states* because they're localized at the beginning or at the end of the chain. Thus, in this case, the edge state is also a zero mode. If one defines the operators $\tilde{c}_j = \frac{1}{2}(m_{2j} + im_{2j+1})$ and $\tilde{c}_j^\dagger = \frac{1}{2}(m_{2j} - im_{2j+1})$, the Hamiltonian becomes $H = 2t\sum_{j=1}^{N-1}(\tilde{c}_j^\dagger\tilde{c}_j - \frac{1}{2})$. There are two ground states $|\psi_i\rangle$ defined by the condition $\tilde{c}_j|\psi_i\rangle = 0$ for $j = 1, ...N-1$ with opposite parity (see the following discussion).

Parity operator In general, the parity operator measures if the number of occupied states, in this case the number of spinless fermions, is even or odd. It is usually defined as

$$P = \prod_j (1 - 2c_j^\dagger c_j) = \prod_j (-im_{2j-1}m_{2j}) \tag{1.99}$$

where the multiplication is over all the sites of the chain. Given the fact that the only eigenvalues of $c_j^\dagger c_j$ are 0 (empty j-th state) and 1 (occupied j-th state) then the parity operator can only take the following values:

$$P = \begin{cases} 1 & \text{even number of fermions} \\ 0 & \text{odd number of fermions} \end{cases} \tag{1.100}$$

In the previous case the parity operator can be written as

$$P = \prod_{j=0}^{N-1}(1 - 2\tilde{c}_j^\dagger\tilde{c}_j) = \left[\prod_{j=1}^{N-1}(-im_{2j-1}m_{2j})\right](-im_1m_{2N}) \tag{1.101}$$

The first ground state $|\psi_0\rangle$ can be defined as the one with no $\tilde{c}_j$ particles where $j = 0, ..., N$; the second one host instead a zero-energy fermion $|\psi_1\rangle = \tilde{c}_0^\dagger|\psi_0\rangle$. From (1.101)

$$\begin{cases} P|\psi_0\rangle = |\psi_0\rangle \\ P|\psi_1\rangle = (1 - 2\tilde{c}_0^\dagger\tilde{c}_0)|\psi_1\rangle = -|\psi_1\rangle \end{cases} \tag{1.102}$$

Then $|\psi_0\rangle$ has even fermionic parity while $|\psi_1\rangle$ has an odd parity. The degeneracy of the ground state is a sign of the presence of edge modes and of a topological phase. Therefore, for this particular values of the parameters, the system is in the topological region.

The bulk spectrum can be obtained by imposing PBCs and performing a Fourier transform followed by a Bogoliubov transformation in a similar way of what done in the previous section. The energy eigenvalues are:

$$\Lambda_k = \pm\sqrt{(2t\cos k + \mu)^2 + 4|\Delta|^2\sin^2 k} \qquad -\pi \leq k \leq \pi \tag{1.103}$$

Then, the gap closes for $2|t| = |\mu|$ at $k = \pm\pi$. Thus, we expect that the topological phase occurs at $2|t| < |\mu|$ while the trivial phase occupies the domain $2|t| > |\mu|$ ($|\Delta| \neq 0$). To verify the conjecture one has to find the boundary modes. The edge states survive in the whole ordered phase, although the other terms of the Hamiltonian hybridize them so that they acquire a tail protruding inside the chain [21](see the following discussion and chapters 3 and 4). In the thermodynamic limit the zero-modes read [21]

$$\begin{cases} b' = \sum_j (\alpha'_+ x_+^j + \alpha'_- x_-^j) m_{2j-1} \\ b'' = \sum_j (\alpha''_+ x_+^{-j} + \alpha''_- x_-^{-j}) m_{2j} \end{cases} \qquad x_\pm = \frac{-\mu \pm \sqrt{\mu^2 - 4t^2 + 4|\Delta|^2}}{2(t + |\Delta|)} \tag{1.104}$$

The coefficients $\alpha'_\pm, \alpha''_\pm$ take different values for the two phases:

1. If $|\mu| > 2|t|$, only one of the coefficients α'_+, α'_- (or α''_+, α''_-) is non vanishing. This makes it impossible to satisfy some boundary conditions and then the zero-modes cannot exist [21].

2. If $|\mu| < 2|t|$ instead the boundary conditions are satisfied and thus the Majorana fermions exist in the whole topological region. In particular if $|\mu| < 2t$ ($|x_+|, |x_-| < 1$) the Majorana fermions b' and b'' are localized at the beginning and at the end of the chain, respectively. On the other hand, if $|\mu| < -2t$ ($|x_+|, |x_-| > 1$) the positions of b' and b'' are exchanged.

In the following the Majorana modes localized at the beginning and at the end of the chain will be called ψ_L and ψ_R, respectively. The previous linear combinations of Majorana fermions can be collected in a zero energy non-local Dirac fermion Ψ by taking $\Psi = \frac{\psi_L + \psi_R}{2}$. However, the formulas (1.104) are valid only in the thermodynamic limit and in order to find the analytical solutions for finite chain length N a different approach must be adopted. For finite systems, the boundary state energy is not exactly zero and so, in this situation, the degeneracy of the system is split. In chapter 3 and 4 we will provide explicit solutions also for finite N.

Chapter 2

Diagonalization of a complex fermionic quadratic Hamiltonian

In the previous chapter the Kiteav model which, as already discussed, is equivalent to the XY model after the Jordan-Wigner transformation has been diagonalized only in the case of real coefficients and periodic boundary conditions. The goal of the next chapters will be to diagonalize it for complex parameters and a more general class of boundary conditions by analyzing the behavior of the energy spectrum and of the eigenstates of the Hamiltonian. In particular, the structure of the boundary states for different values of the model parameters and for generic boundary conditions will be discussed.
We will consider the following Hamiltonian:

$$\begin{aligned} H = \sum_{j=1}^{N-1} \big[& -tc_j^\dagger c_{j+1} - t^* c_{j+1}^\dagger c_j - \mu c_j^\dagger c_j + \Delta c_j^\dagger c_{j+1}^\dagger + \Delta^* c_{j+1} c_j \\ & + x(-tc_N^\dagger c_1 - t^* c_1^\dagger c_N + \Delta c_N^\dagger c_1^\dagger + \Delta^* c_1 c_N) \big] \end{aligned} \tag{2.1}$$

where $t = |t|e^{i\theta}$ is the complex hopping parameter, $\Delta = |\Delta|e^{i\phi}$ is the complex superconductive gap.
The second line of eq.(2.1) represents the hopping and the interaction between the first and last site of the chain, thus incorporating the boundary conditions: we choose the parameter x to vary in the interval $[0, 1]$ so to interpolate between OBCs for $x = 0$ and PBCs for $x = 1$.
The first line of eq.(2.1) is the most general (translational invariant) quadratic BCS-like Hamiltonian that we can write by assuming that the fermions may also interact with an external magnetic potential. In this case, the superconducting gap is complex, while, the action of the magnetic field on the fermions, can be treated by considering that they acquire a phase each time they jump from one site to the neighboring one. This is just the Ahranov-Bohm effect in a discrete lattice.
The superconductive gap Δ breaks the $U(1)$ global symmetry of the model into the $\mathbb{Z}_2$ symmetry. Thus, the phase in Δ doesn't affect the spectrum as we see by performing the global gauge $U(1)$ transformation $c_j \to e^{i\phi/2} c_j$ on the Hamiltonian. However, as we will see in the next chapters, the wavefunctions, and in particular the ground state, depend on the phase of

the superconductive gap.
The goal of this chapter is to extend what was done in the previous chapters for fermions that interact through a quadratic potential to the complex case and generic boundary conditions. As seen in the previous chapter, Fourier transform is a useful tool to diagonalize the Hamiltonian with PBCs: this is so because in this case, plane waves are in the domain of the Hamiltonian and indeed allow to write down the set of all eigenstates, which yields an orthonormal basis for the Hilbert space, after a Bogoliubov transformation. For more general BCs, it may happen that plane waves do not provide the complete set of eigenstates, as it may occur, for example, when there are bound states or edge states [21].
Starting from the Hamiltonian it is possible to diagonalize a complex quadratic fermionic model without using the Fourier and the Bogoliubov transformations in at least two different ways which will be described along with this chapter.
In the first section we will present an algebraic diagonalization method [28] while in the second one we discuss the complex extension of the Lieb, Schultz and Mattis procedure [26]. These two methods will allow us to calculate the energy eigenvalues of the system and the profile of the eigenstate wavefunctions in the real space. They don't show a manifest dependency on the chosen BCs of the system and thus they can capture the energy levels that live outside the bulk band and can be used to investigate possible edge modes.

2.1 Algebraic diagonalization

In this section we discuss an algebraic method for diagonalizing a fermionic quadratic Hamiltonian [28] using, for compatibility with the next section of the chapter, the notation adopted by Lieb, Schultz and Mattis [26]. A generic complex quadratic Hamiltonian can be written as

$$H = \sum_{i,j=1}^{N} [c_i^\dagger A_{ij} c_j + \frac{1}{2}(c_i^\dagger B_{ij} c_j^\dagger - c_i B_{ij}^* c_j)] \tag{2.2}$$

The Hermicity of the Hamiltonian requires that A is a Hermitian matrix, while the anticommutation rules among the c_i's require that B is an antisymmetric matrix. Namely

$$A_{ij} = A_{ji}^* \qquad B_{ij} = -B_{ji} \tag{2.3}$$

Let's introduce the Nambu spinor

$$\begin{pmatrix} c \\ (c^\dagger)^T \end{pmatrix} \equiv \begin{pmatrix} c_1 \\ \vdots \\ c_N \\ c_1^\dagger \\ \vdots \\ c_N^\dagger \end{pmatrix} \tag{2.4}$$

where ^{T} denotes the transpose.
The Hamiltonian can be written in matrix from as

$$H = \frac{1}{2}\begin{pmatrix} c^\dagger & c^T \end{pmatrix} T \begin{pmatrix} c \\ (c^\dagger)^T \end{pmatrix} + \frac{1}{2}\sum_i A_{ii} \tag{2.5}$$

where we have introduced the Hermitian matrix

$$T \equiv \begin{pmatrix} A & B \\ -B^* & -A^* \end{pmatrix} \tag{2.6}$$

The last additive constant in (2.5) is due to the fermionic commutation relation $\{c_i^\dagger, c_j\} = \delta_{ij}$.
The matrix T, being Hermitian, has real eigenvalues and can be diagonalized by a unitary matrix U such that $U^\dagger = U^{-1}$.
The spectrum of T is symmetric, i.e. for any eigenstate with eigenvalue λ there is another eigenstate with eigenvalue $-\lambda$.
Therefore the diagonalized Hamiltonian has the following structure

$$\begin{aligned} H =& \frac{1}{2}\begin{pmatrix} \eta^\dagger & \eta^T \end{pmatrix} D \begin{pmatrix} \eta \\ (\eta^\dagger)^T \end{pmatrix} + \frac{1}{2}\sum_i A_{ii} = \\ &= \sum_k \Lambda_k \eta_k^\dagger \eta_k + \frac{1}{2}(\sum_i A_{ii} - \sum_k \Lambda_k) \qquad\qquad \Lambda_k > 0 \qquad k = 1, ..., N \end{aligned} \tag{2.7}$$

where

$$D \equiv U^{-1}TU = \begin{pmatrix} \Lambda_1 & & & & & \\ & \ddots & & & & \\ & & \Lambda_N & & & \\ & & & -\Lambda_1 & & \\ & & & & \ddots & \\ & & & & & -\Lambda_N \end{pmatrix}, \qquad U^{-1} = \begin{pmatrix} \vec{g}_1^T & \vec{h}_1^T \\ \vdots & \vdots \\ \vec{g}_N^T & \vec{h}_N^T \\ \vec{h}_1^{*T} & \vec{g}_1^{*T} \\ \vdots & \vdots \\ \vec{h}_N^{*T} & \vec{g}_N^{*T} \end{pmatrix} \tag{2.8}$$

and

$$\begin{pmatrix} \eta \\ (\eta^\dagger)^T \end{pmatrix} = U^{-1} \begin{pmatrix} c \\ (c^\dagger)^T \end{pmatrix} \tag{2.9}$$

The N-dimensional vectors $\vec{g}_k, \vec{h}_k$ have in general complex coefficients and are defined up to a phase that doesn't change the product $\eta_k^\dagger \eta_k$.
We recall that the matrix U is built by putting the eigenvectors of T in column. Thus, the eigenvalue equation gives

$$\begin{cases} A\vec{g}_k^* + B\vec{h}_k^* = \Lambda_k \vec{g}_k^* \\ -B^*\vec{g}_k^* - A^*\vec{h}_k^* = \Lambda_k \vec{h}_k^* \end{cases} \tag{2.10}$$

or

$$\begin{cases} A^*\vec{g}_k + B^*\vec{h}_k = \Lambda_k \vec{g}_k \\ -A\vec{h}_k - B\vec{g}_k = \Lambda_k \vec{h}_k \end{cases} \tag{2.11}$$

These equations represent the generalization of the so-called Lieb-Schultz-Mattis conditions [26] to the complex case, as we will see in the next section. From the relation $U^{-1}U = U^{\dagger}U = \mathbb{1}$ the following relations can be derived

$$\sum_i [g^*_{ki} g_{k'i} + h^*_{ki} h_{k'i}] = \delta_{kk'} \tag{2.12}$$

$$\sum_i [g_{ki} h_{k'i} + h_{ki} g_{k'i}] = 0 \tag{2.13}$$

Here g_{ki} and h_{ki} denote the i-component of the vectors $\vec{g}_k$ and $\vec{h}_k$, respectively. Likewise, from $UU^{-1} = \mathbb{1}$, we get

$$\sum_k [g_{ki} g^*_{kj} + h^*_{ki} h_{kj}] = \delta_{ij} \tag{2.14}$$

$$\sum_k [h^*_{ki} g_{kj} + g_{ki} h^*_{kj}] = 0 \tag{2.15}$$

If the Hamiltonian is real the matrix T is symmetric and then it can be diagonalized through an orthogonal matrix U such that $U^T = U^{-1}$. Moreover the coefficients $\vec{g}_k$ and $\vec{h}_k$ can be chosen real because T is real. From the relation $U^{-1}U = U^T U = \mathbb{1}$ we obtain

$$\sum_i [g_{ki} g_{k'i} + h_{ki} h_{k'i}] = \delta_{kk'} \tag{2.16}$$

$$\sum_i [g_{ki} h_{k'i} + h_{ki} g_{k'i}] = 0 \tag{2.17}$$

and from $UU^T = \mathbb{1}$, we get

$$\sum_k [g_{ki} g_{kj} + h_{ki} h_{kj}] = \delta_{ij} \tag{2.18}$$

$$\sum_k [h_{ki} g_{kj} + g_{ki} h_{kj}] = 0 \tag{2.19}$$

Therefore the coefficients $\vec{g}_k$ and $\vec{h}_k$, which can be read out from the matrix U, and the energy eigenvalues can be found numerically by diagonalizing the matrix T.

2.2 Lieb-Schultz-Mattis method

Lieb, Schultz and Mattis proposed in their paper [26] another method to obtain the equations (2.11) in the real case. They presented also a procedure for decoupling them by obtaining an eigenvalue equation from which the eigenvalues can be found. The goal of the next section will be extending it to complex coefficients.

2.2.1 Lieb-Schultz-Mattis method in the complex case

Let's start again from the Hamitonian (2.5). We search for a linear transformation of the form (2.20)

$$\eta_k = \sum_{i=1}^{N} [g_{ki} c_i + h_{ki} c_i^\dagger] \qquad \eta_k^\dagger = \sum_{i=1}^{N} [g_{ki}^* c_i^\dagger + h_{ki}^* c_i] \tag{2.20}$$

which is canonical and which gives for H the form

$$H = \sum_{k=1}^{N} \Lambda_k \eta_k^\dagger \eta_k + \text{constant} \tag{2.21}$$

The transformation (2.20) must be canonical to preserve the fermionic commutation relations $\{\eta_k, \eta_{k'}^\dagger\} = \delta_{k,k'}, \{\eta_k, \eta_{k'}\} = 0$. This allows us to obtain some constraints on the coefficients g_{ki} and h_{ki}

$$\{\eta_k, \eta_{k'}^\dagger\} = \sum_i [g_{ki} g_{k'i}^* + h_{ki} h_{k'i}^*] = \delta_{k,k'} \tag{2.22}$$

and

$$\{\eta_k, \eta_{k'}\} = \sum_i [g_{ki} h_{k'i} + h_{ki} g_{k'i}] = 0 \tag{2.23}$$

These relations coincide with (2.12) and (2.13). The constant in H can be determined from the invariance of $\mathrm{Tr}H$ under the canonical transformation. From (2.5) one has

$$\mathrm{Tr}[H] = 2^{N-1} \sum_i A_{ii} \tag{2.24}$$

while, from (2.21), one obtains

$$\mathrm{Tr}[H] = 2^{N-1} \sum_k \Lambda_k + 2^N \cdot \text{constant} \tag{2.25}$$

The constant is thus

$$\text{constant} = \frac{1}{2} (\sum_i A_{ii} - \sum_k \Lambda_k) \tag{2.26}$$

A less trivial task is to determine the coefficients g_{ki} and h_{ki}. Let's start from (2.21) and consider the following commutator [1]

$$[\eta_k, H] = [\eta_k, \sum_{k'} \Lambda_{k'} \eta_{k'}^\dagger \eta_{k'} + \text{constant}] = \Lambda_k \eta_k \tag{2.28}$$

[1] If A, B, C are three operators the following relation holds

$$[AB, C] = \{A, B\} C - B\{A, C\} \tag{2.27}$$

Using the definitions (2.20), we find

$$\begin{aligned}[\eta_k, H] =& \sum_{il} [(g_{ki}A_{il} - h_{ki}B^*_{il})\, c_l + (-h_{ki}A_{li} + g_{ki}B_{il})\, c^\dagger_l] \\ =& \Lambda_k \sum_l [g_{kl}c_l + h_{kl}c^\dagger_l]\end{aligned} \tag{2.29}$$

Therefore the coefficients g_{kl} and h_{kl} must satisfy

$$\begin{cases} \Lambda_k g_{kl} = \sum_i (g_{ki}A_{il} - h_{ki}B^*_{il}) \\ \Lambda_k h_{kl} = \sum_i (-h_{ki}A_{li} + g_{ki}B_{il}) \end{cases} \tag{2.30}$$

In vector notation, the previous relation can be written as

$$\begin{cases} A^*\vec{g}_k + B^*\vec{h}_k = \Lambda_k \vec{g}_k \\ -A\vec{h}_k - B\vec{g}_k = \Lambda_k \vec{h}_k \end{cases} \tag{2.31}$$

Here $\vec{g}_k$ and $\vec{h}_k$ denote the N-dimensional vectors with components g_{kl} and h_{kl}, respectively. In matrix form, if k is fixed, equations (2.31) become

$$\begin{pmatrix} A^* & B^* \\ -B & -A \end{pmatrix} \begin{pmatrix} g \\ h \end{pmatrix} = \Lambda \begin{pmatrix} g \\ h \end{pmatrix} \tag{2.32}$$

where we have used the shorthands $\vec{g}_k \equiv g$ and $\vec{h}_k \equiv h$.
In particular we have

$$\begin{cases} A^*g + B^*h = \Lambda g \\ B^*g^* + A^*h^* = -\Lambda h^* \end{cases} \tag{2.33}$$

The last two equations can be decoupled to obtain an eigenvalue equation from which the spectrum of the Hamiltonian can be found. Taking the sum and the difference of the two previous equations

$$\begin{cases} A^*(g + h^*) + B^*(h + g^*) = \Lambda(g - h^*) \\ A^*(g - h^*) + B^*(h - g^*) = \Lambda(g + h^*) \end{cases} \tag{2.34}$$

and defining the new variables

$$z = g + h^* \qquad w = g - h^* \tag{2.35}$$

the following equations hold

$$\begin{cases} A^*z + B^*z^* = \Lambda w \\ A^*w - B^*w^* = \Lambda z \end{cases} \tag{2.36}$$

Splitting the real and the imaginary part

$$A = A_R + iA_I \quad B = B_R + iB_I \quad z = z_R + iz_I \quad w = w_R + iw_I \tag{2.37}$$

where

$$A_R^T = A_R \quad A_I^T = -A_I \quad B_R^T = -B_R \quad B_I^T = -B_I \tag{2.38}$$

the equations (2.36) can be written as

$$\begin{cases} (A_R - iA_I)(z_R + iz_I) + (B_R - iB_I)(z_R - iz_I) = \Lambda(w_R + iw_I) \\ (A_R - iA_I)(w_R + iw_I) - (B_R - iB_I)(w_R - iw_I) = \Lambda(z_R + iz_I) \end{cases} \tag{2.39}$$

Separating the real and the imaginary part, we obtain

$$\begin{pmatrix} A_R + B_R & A_I - B_I \\ -A_I - B_I & A_R - B_R \end{pmatrix} \begin{pmatrix} z_R \\ z_I \end{pmatrix} = \Lambda \begin{pmatrix} w_R \\ w_I \end{pmatrix} \tag{2.40}$$

$$\begin{pmatrix} A_R - B_R & A_I + B_I \\ -A_I + B_I & A_R + B_R \end{pmatrix} \begin{pmatrix} w_R \\ w_I \end{pmatrix} = \Lambda \begin{pmatrix} z_R \\ z_I \end{pmatrix} \tag{2.41}$$

Defining

$$\mathbb{M} \equiv \begin{pmatrix} A_R + B_R & A_I - B_I \\ -A_I - B_I & A_R - B_R \end{pmatrix} \tag{2.42}$$

(2.40) and (2.41) become

$$\mathbb{M} \begin{pmatrix} z_R \\ z_I \end{pmatrix} = \Lambda \begin{pmatrix} w_R \\ w_I \end{pmatrix} \qquad \mathbb{M}^T \begin{pmatrix} w_R \\ w_I \end{pmatrix} = \Lambda \begin{pmatrix} z_R \\ z_I \end{pmatrix} \tag{2.43}$$

These relations can be decoupled into the following eigenvalue equations

$$\mathbb{W} \begin{pmatrix} z_R \\ z_I \end{pmatrix} = \Lambda^2 \begin{pmatrix} z_R \\ z_I \end{pmatrix} \qquad \mathbb{V} \begin{pmatrix} w_R \\ w_I \end{pmatrix} = \Lambda^2 \begin{pmatrix} w_R \\ w_I \end{pmatrix} \tag{2.44}$$

where

$$\begin{aligned} \mathbb{W} \equiv \mathbb{M}^T\mathbb{M} &= \begin{pmatrix} A_R - B_R & A_I + B_I \\ -A_I + B_I & A_R + B_R \end{pmatrix} \begin{pmatrix} A_R + B_R & A_I - B_I \\ -A_I - B_I & A_R - B_R \end{pmatrix} \\ &= \begin{pmatrix} \mathcal{M}_{11} & \mathcal{M}_{12} \\ \mathcal{M}_{21} & \mathcal{M}_{22} \end{pmatrix} \end{aligned} \tag{2.45}$$

with

$$\begin{aligned} \mathcal{M}_{11} &= (A_R - B_R)(A_R + B_R) + (A_I + B_I)(-A_I - B_I) \\ \mathcal{M}_{12} &= (A_R - B_R)(A_I - B_I) + (A_I + B_I)(A_R - B_R) \\ \mathcal{M}_{21} &= (-A_I + B_I)(A_R + B_R) + (A_R + B_R)(-A_I - B_I) \\ \mathcal{M}_{22} &= (-A_I + B_I)(A_I - B_I) + (A_R + B_R)(A_R - B_R) \end{aligned} \tag{2.46}$$

and $\mathbb{V} \equiv \mathbb{M}\mathbb{M}^T$. Since the matrix $\mathbb{W}$ is symmetric, the block components $\mathcal{M}_{ij}$ satisfy

$$\mathcal{M}_{11}^T = \mathcal{M}_{11} \quad \mathcal{M}_{22}^T = \mathcal{M}_{22} \quad \mathcal{M}_{12}^T = \mathcal{M}_{21} \tag{2.47}$$

The real case can be obtained by simply putting $A_I = B_I = 0$. In this case the coefficients g and h are real and, using that $z_I = w_I = 0$, equations (2.44) in vector notation are reduced to

$$W\vec{\phi}_k = \Lambda_k^2 \vec{\phi}_k \tag{2.48}$$

$$V\vec{\psi}_k = \Lambda_k^2 \vec{\psi}_k \tag{2.49}$$

where $W \equiv (A-B)(A+B)$, $V \equiv (A+B)(A-B)$, $\vec{\phi}_k \equiv \vec{g}_k + \vec{h}_k$ and $\vec{\psi}_k \equiv \vec{g}_k - \vec{h}_k$. These are the LSM equations first obtained by Lieb, Schultz and Mattis in their article [26]. The eigenvalues can be found by diagonalizing the matrix $\mathbb{W}$ and W in the complex and in the real case, respectively. In the complex case, the relations between g and h and the LSM eigenfunctions z and w are (for k fixed)

$$g = \frac{1}{2}(z + w) \qquad h = \frac{1}{2}(z - w)^* \tag{2.50}$$

In the real case they read (restoring the vector notation)

$$\vec{g}_k = \frac{1}{2}(\vec{\phi}_k + \vec{\psi}_k) \qquad \vec{h}_k = \frac{1}{2}(\vec{\phi}_k - \vec{\psi}_k) \tag{2.51}$$

The coefficients g_{ki} and h_{ki} give the profile of the wavefunction in the real space (see equation (2.20)).
Therefore, once the analytical expressions of the normalized LSM eigenfunctions z and w (or, in the real case, $\vec{\phi}_k$ and $\vec{\psi}_k$) are known, the coefficients $\vec{g}_k$ and $\vec{h}_k$ can be easily obtained by simply adding or subtracting them. The next chapters will aim to find the LSM eigenfunctions z and w (or $\vec{\phi}_k$ and $\vec{\psi}_k$).

Chapter 3

Perturbation theory for the analytical solutions of the LSM equations for the finite Kitaev chain

In principle, the LSM equations (2.44) can be solved analytically to find the energy spectrum and the eigenstates of the original Hamiltonian. In this chapter, we discuss the solution of the real Kitaev model where the matrix to be diagonalized can be decomposed in an unperturbed symmetric Toeplitz one, whose eigensystem is known, plus a perturbation for which the effects are evaluated.
Firstly Golub [14] provided a general method to find the eigenvalues and the eigenfunctions of a perturbed symmetric matrix starting from the knowledge of the eigensystem of the unperturbed matrix. Subsequently Bunch et al. [8] improved this treatment including the explicit computation of the updated eigenvectors. In the first part of this chapter we present a slightly different version compared to the one developed in [8] which can be applied to every symmetric matrix. In the second part of the chapter, we will apply the general method to the Kitaev chain.

3.1 A general perturbation method

We suppose that V is a $N \times N$ real symmetric matrix for which the eigensystem problem is known. We assume that

$$V = QDQ^T \tag{3.1}$$

where $D \in \mathbb{R}^{N\times N}$ is diagonal and $Q^T = Q^{-1}$. In the following discussion we will consider only the rank-one perturbation case for which the perturbed matrix is defined as

$$\tilde{V} = V + \sigma uv^T \tag{3.2}$$

where u and v are two vectors that, unlike what was done in [8], may be different. Here $\sigma \in \mathbb{R}$ is the coefficient of the perturbation.
The matrix $\tilde{V}$ can be rewritten as

$$\tilde{V} = Q(D + \sigma zw^T)Q^T \qquad Qz = u \quad Qw = v \tag{3.3}$$

and therefore the problem is reduced to finding the eigenvalues of

$$C = D + \sigma z w^T \tag{3.4}$$

Using that $\det(1 + xy^T) = 1 + y^T x$, the secular equation can be written as

$$\begin{aligned} &\det(D + \sigma z w^T - \tilde{d}_k \mathbb{1}) = \\ &\det((D - \tilde{d}_k \mathbb{1})(1 + (D - \tilde{d}_k \mathbb{1})^{-1} \sigma z w^T) = \\ &(\prod_{i=1}^{N} (d_i - \tilde{d}_k)) \left(1 + \sigma \sum_{i=1}^{N} \frac{w_i z_i}{d_i - \tilde{d}_k} \right) = 0 \end{aligned} \tag{3.5}$$

where $\tilde{d}_k$ with $k = 1, ..., N$ are the eigenvalues of the matrix C and z_i and w_i are respectively the components of the vector z and w.
Thus, the perturbed eigenvalues $\tilde{d}_k$ solve the transcendental equation

$$1 + \sigma \sum_{i=1}^{N} \frac{w_i z_i}{d_i - \tilde{d}_k} = 0 \tag{3.6}$$

The previous equation is valid for every value of the coefficient σ. The perturbed eigenvectors $\tilde{q}_k$ are, by definition, the solution of

$$\tilde{V} \tilde{q}_k - \tilde{d}_k \tilde{q}_k = 0 \tag{3.7}$$

where $\tilde{d}_k$ are the perturbed eigenvalues. The previous equation can be rewritten as

$$(Q D Q^T + \sigma u v^T) \tilde{q}_k - \tilde{d}_k \tilde{q}_k = 0 \tag{3.8}$$

Then

$$(D_k + \sigma z w^T) x_k = 0 \tag{3.9}$$

where $x_k = Q^T \tilde{q}_k$ and $D_k = D - \tilde{d}_k \mathbb{1}$. The solution of (3.9) is [8]

$$x_k = \theta D_k^{-1} z \tag{3.10}$$

where θ is an arbitrary normalization constant. Therefore the normalized eigenvectors $\tilde{q}_k$ read

$$\tilde{q}_k = \frac{Q D_k^{-1} z}{\| D_k^{-1} z \|} \tag{3.11}$$

If the rank of the perturbation is greater than one, the more complicated multiple rank perturbation theory must be implemented. Nevertheless, it is still possible to obtain an approximate formula in order to find the perturbed eigenvalues by decomposing the multiple rank perturbation into a sum of rank-one ones. Let's define

$$\tilde{V} = V + \sum_{j=1}^{l} \sigma_j u_j v_j^T \tag{3.12}$$

where l is the number of rank-one perturbation terms. Repeating the same steps and taking into account that $\det(1+X) \approx 1 + \mathrm{tr}(X)$ for $X \ll 1$, the following approximate formula can be obtained

$$1 + \sum_{j=1}^{l} \sum_{i=1}^{N} \sigma_j \frac{z_{ij} w_{ij}}{d_i - \tilde{d}_k} = 0 \tag{3.13}$$

where z_{ij} and w_{ij} denote the i-component of the vectors $z_j = Q^T u_j$ and $w_j = Q^T v_j$, respectively. This expression is valid as long as $\sigma_j \ll 1$ for $j = 1, ..., l$.

3.2 Application to the Kitaev model

In this section we will apply the previous method to the real case $t = \Delta$ with generic BCs (see eq.(2.1)). The explicit form of the LSM matrices A and B of the Kitaev model is

$$A = \begin{pmatrix} -\mu & -t & & & & -xt \\ -t & -\mu & \ddots & & & \\ & \ddots & \ddots & \ddots & & \\ & & \ddots & \ddots & \ddots & \\ & & & \ddots & -\mu & -t \\ -xt & & & & -t & -\mu \end{pmatrix} \quad B = \begin{pmatrix} 0 & \Delta & & & & -x\Delta \\ -\Delta & 0 & \ddots & & & \\ & \ddots & \ddots & \ddots & & \\ & & \ddots & \ddots & \ddots & \\ & & & \ddots & 0 & \Delta \\ x\Delta & & & & -\Delta & 0 \end{pmatrix} \tag{3.14}$$

where t and Δ are real parameters.
They are Toeplitz matrices, i.e. matrices in which each descending diagonal from left to right is constant [15]. From the explicit forms of the matrices W and V in (2.48) and (2.49) it can be shown that ϕ_{kj} and ψ_{kj} differ only by the vector index exchange $j \to N - j + 1$. Therefore in the following only the matrix W will be considered. Set $\tilde{V} \equiv W$ where if $t = \Delta$

$$W = \begin{pmatrix} a & b & & & & d \\ b & a & \ddots & & & \\ & \ddots & \ddots & \ddots & & \\ & & \ddots & \ddots & \ddots & \\ & & & \ddots & a & b \\ d & & & & b & a+c \end{pmatrix} \tag{3.15}$$

having set

$$\begin{cases} a = 4t^2 + \mu^2 \\ b = 2t\mu \\ c = 4t^2(x^2 - 1) \\ d = 2xt\mu \end{cases} \tag{3.16}$$

In general, the previous matrix is not even Toeplitz and therefore difficult to diagonalize. Nevertheless, W can be seen as an unperturbed matrix

$$W_u = \begin{pmatrix} a & b & & & & \\ b & a & \ddots & & & \\ & \ddots & \ddots & \ddots & & \\ & & \ddots & \ddots & \ddots & \\ & & & \ddots & a & b \\ & & & & b & a \end{pmatrix} \tag{3.17}$$

plus three rank-one perturbation terms.
The unperturbed matrix $W_u \equiv 4t^2 + \mu^2 + 2t\mu\tilde{W}_u$ is a standard tridiagonal Toeplitz matrix for which the eigensystem is known [29]. The solution can be found through an ansatz of the form $\phi_{qj} = \alpha e^{iqj} + \beta e^{-iqj}$.
The term proportional to the identity matrix gives only an additive contribution to the eigenvalues Λ_q^2 of W_u.
Then, let's consider first the Toeplitz matrix

$$\tilde{W}_u = \begin{pmatrix} 0 & 1 & & & & \\ 1 & 0 & \ddots & & & \\ & \ddots & \ddots & \ddots & & \\ & & \ddots & \ddots & \ddots & \\ & & & \ddots & 0 & 1 \\ & & & & 1 & 0 \end{pmatrix} \tag{3.18}$$

From the eigenvalue equation $\tilde{W}_u\phi_{qj} = \lambda_q^2\phi_{qj}$ we obtain the following system

$$\begin{cases} \phi_{q(j-1)} + \phi_{q(j+1)} = \lambda_q^2\phi_{qj} \qquad j = 2, \cdots, N-1 \\ \phi_{q2} = \lambda_q^2\phi_{q1} \\ \phi_{q(N-1)} = \lambda_q^2\phi_{qN} \end{cases} \tag{3.19}$$

The first equation is the bulk condition and the last two are the boundary conditions from which the relation between the coefficients α and β of the eigenvector ϕ_{qj} and the allowed q can be found.
From the bulk relation we obtain that $\lambda_q^2 = 2\cos q$.
Using the second equation of (3.19), some long but straightforward algebra shows that $\alpha = -\beta$.
The last boundary condition in (3.19) fixes the allowed values of q. Namely:

$$q = \frac{\pi}{N+1}i \qquad i = 1, ..., N \tag{3.20}$$

Thus, the real unperturbed normalized eigenfunctions are

$$\phi_{qj} = \sqrt{\frac{2}{N+1}}\sin qj \qquad q = \frac{\pi}{N+1}i \quad i = 1, ..., N \tag{3.21}$$

The diagonal contribution gives only an additive constant to the eigenvalues Λ_q^2 of W_u and so

$$\Lambda_q^2 = 4t^2 + \mu^2 + 4t\mu\cos q \qquad q = \frac{\pi}{N+1}i \quad i = 1, ..., N \tag{3.22}$$

We will now consider two different cases.

1. Let's take into account the case with $x = 0$ and $\mu \neq 0$ so the only perturbation term is $4t^2(x^2 - 1)$ and the perturbation vectors u and v are $u = v = (0, 0, \cdot\cdot, 1)$. The matrix Q^T can be built by putting the eigenvectors (3.21) of the unperturbed matrix in the rows. Namely

$$Q^T = \sqrt{\frac{2}{N+1}} \begin{pmatrix} \sin\frac{\pi}{N+1} & \sin\frac{2\pi}{N+1} & \cdots & \sin\frac{N\pi}{N+1} \\ \sin\frac{2\pi}{N+1} & \sin\frac{4\pi}{N+1} & \cdots & \sin\frac{2N\pi}{N+1} \\ \vdots & \vdots & \ddots & \vdots \\ \sin\frac{N\pi}{N+1} & \sin\frac{2N\pi}{N+1} & \cdots & \sin\frac{N^2\pi}{N+1} \end{pmatrix} \tag{3.23}$$

   Using that

$$z = Q^T u = \begin{pmatrix} \sin\frac{N\pi}{N+1} \\ \sin\frac{2N\pi}{N+1} \\ \vdots \\ \sin\frac{N^2\pi}{N+1} \end{pmatrix} \tag{3.24}$$

   and applying (3.6), the following transcendental equation for the perturbed eigenvalues $\tilde{\Lambda}_k^2$ can be derived

$$F(\tilde{\Lambda}_k^2) = 1 - \frac{8t^2}{N+1}\sum_{i=1}^{N}\frac{\sin^2\frac{N\pi i}{N+1}}{\Lambda_{q_i}^2 - \tilde{\Lambda}_k^2} = 0 \tag{3.25}$$

   Fig. 3.1-3.4 show the case $x = 0$ and $\mu \neq 0$. The unperturbed eigenvalues $\Lambda_{q_i}^2$ (3.22), which are located inside the bulk spectrum (1.103), are represented in the graphs by the vertical asymptotes (they are the poles of eq.(3.25)). The perturbation drags the first energy level out of the bulk spectrum. Thus, the lowest energy state becomes a zero-mode.
   However, outside the topological phase, the zero-mode, as expected, enters the bulk band becoming a bulk state.
   Using (3.11), if $x = 0, \mu \neq 0$ we obtain the perturbed eigenvectors which can be written as (up to a normalization constant)

$$\tilde{\phi}_k = \begin{pmatrix} \sum_{i=1}^{N}\left[\left(\sin\frac{\pi i}{N+1}\right)\left(\sin\frac{N\pi i}{N+1}\right)\left(\frac{1}{\Lambda_{q_i}^2 - \tilde{\Lambda}_k^2}\right)\right] \\ \sum_{i=1}^{N}\left[\left(\sin\frac{2\pi i}{N+1}\right)\left(\sin\frac{N\pi i}{N+1}\right)\left(\frac{1}{\Lambda_{q_i}^2 - \tilde{\Lambda}_k^2}\right)\right] \\ \vdots \\ \sum_{i=1}^{N}\left[\left(\sin\frac{N\pi i}{N+1}\right)^2\left(\frac{1}{\Lambda_{q_i}^2 - \tilde{\Lambda}_k^2}\right)\right] \end{pmatrix} \tag{3.26}$$

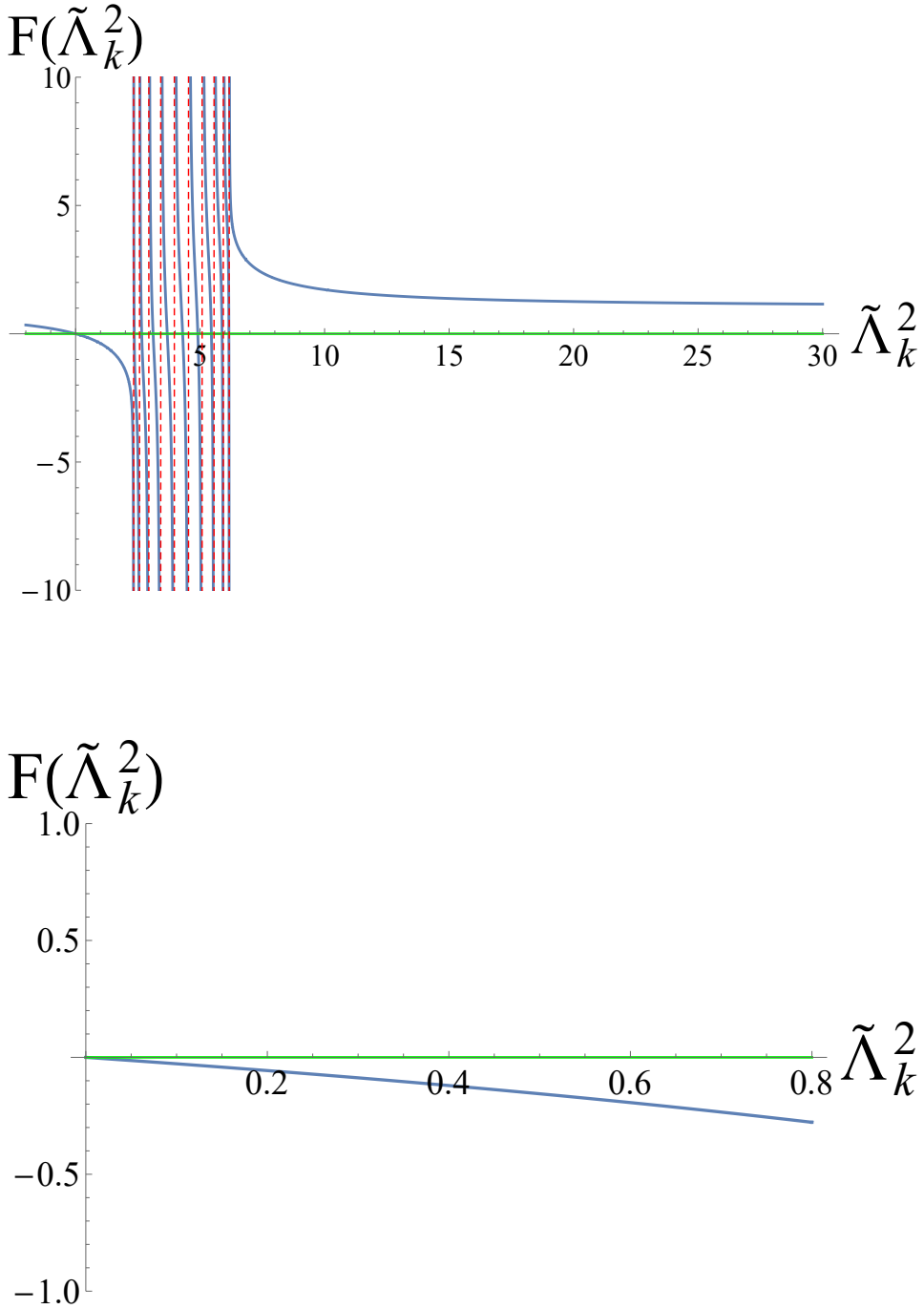

Figure 3.1: Graph of the secular equation for $N = 10$, $x = 0$ and $\mu = 0.5$. The second panel is a zoom of the lowest eigenvalue.

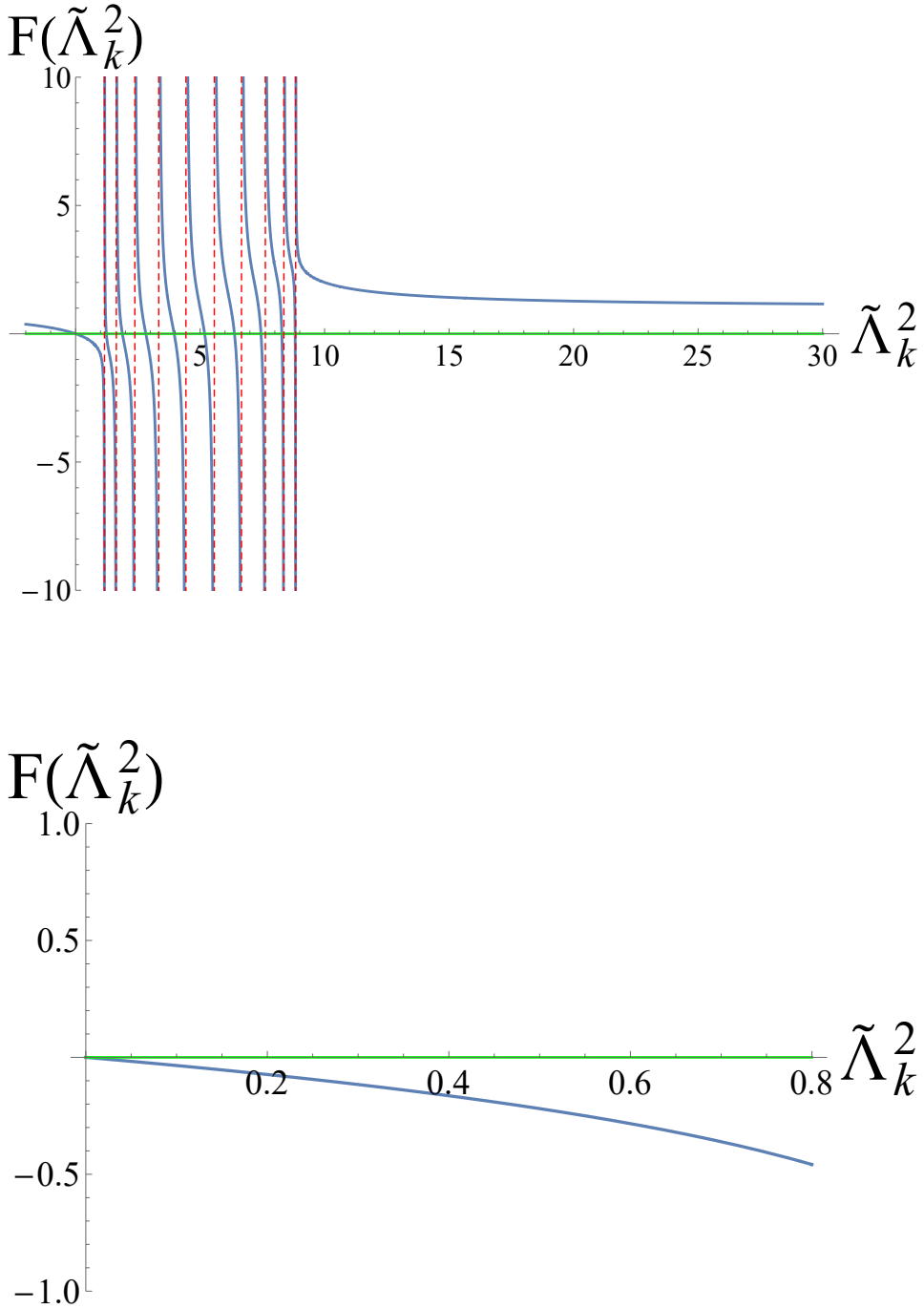

Figure 3.2: Graph of the secular equation for $N = 10$, $x = 0$ and $\mu = 1$. The second panel is a zoom of the lowest eigenvalue.

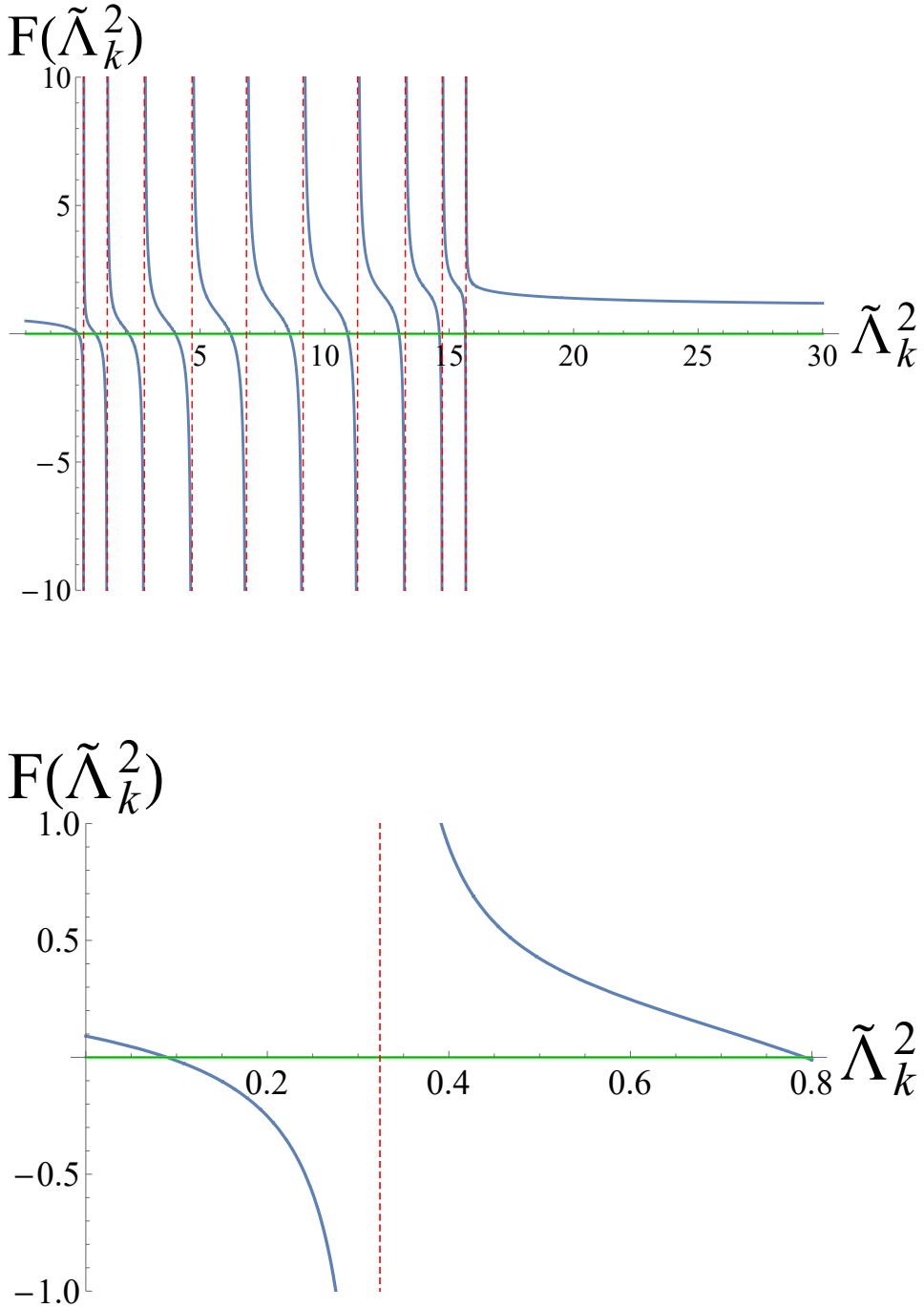

Figure 3.3: Graph of the secular equation for $N = 10$, $x = 0$ and $\mu = 2$. The second panel is a zoom of the lowest eigenvalue.

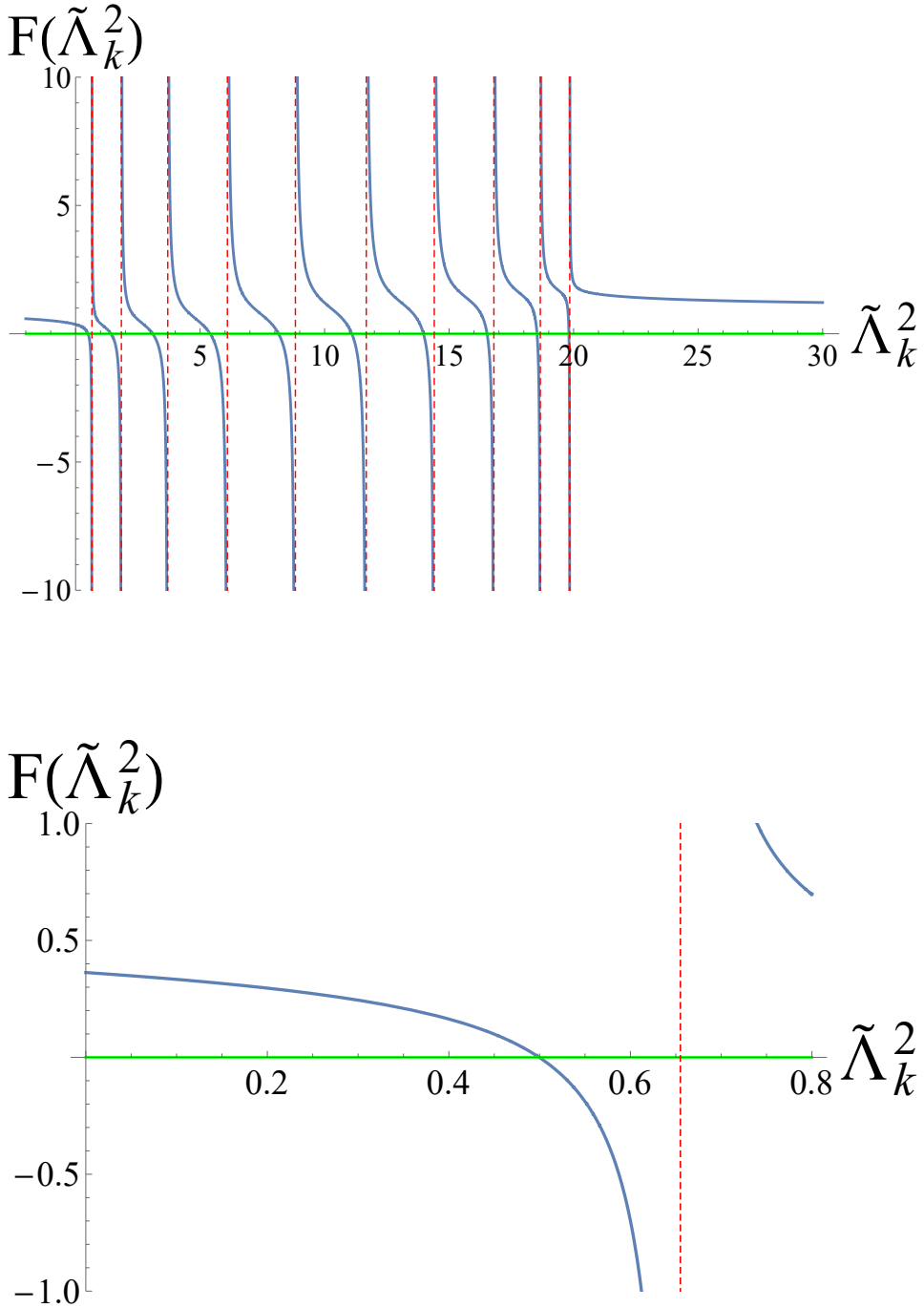

Figure 3.4: Graph of the secular equation for $N = 10$, $x = 0$ and $\mu = 2.5$. The second panel is a zoom of the lowest eigenvalue.

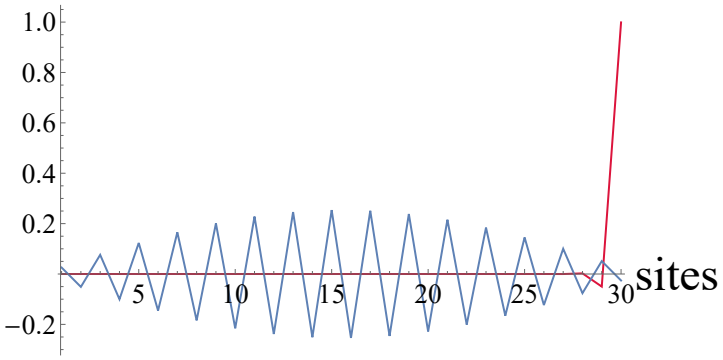

Figure 3.5: The blue line and the red line represent the unperturbed (3.21) and perturbed eigenfunction (3.27) of the first energy level for $x = 0$, $\mu = 0.1$ and $N = 30$, respectively. Adding the perturbation, the eigenfunction becomes peaked at the end of the chain.

where the $\Lambda^2_{q_i}$'s (3.22) are known exactly being the solution of the unperturbed problem. In general, the zero-mode energy $\tilde{\Lambda}^2_{k_0}$ is exactly zero only in the thermodynamic limit. However, for finite chain length N and OBCs $\tilde{\Lambda}^2_{k_0} \sim 0$ and equation (3.26) reduces to

$$\tilde{\phi}_{k_0} \simeq \begin{pmatrix} \sum_{i=1}^{N} \left[\left(\sin \frac{\pi i}{N+1} \right) \left(\sin \frac{N\pi i}{N+1} \right) \frac{1}{\Lambda^2_{q_i}} \right] \\ \sum_{i=1}^{N} \left[\left(\sin \frac{2\pi i}{N+1} \right) \left(\sin \frac{N\pi i}{N+1} \right) \frac{1}{\Lambda^2_{q_i}} \right] \\ \vdots \\ \sum_{i=1}^{N} \left[\left(\sin \frac{N\pi i}{N+1} \right)^2 \frac{1}{\Lambda^2_{q_i}} \right] \end{pmatrix} \tag{3.27}$$

Given that the first components of the vectors are almost zero due to the destructive interference in the summation, the zero-mode eigenvector $\tilde{\phi}_{k_0}$ is peaked at the end of the chain. The profile of the wavefunction is shown in Fig.(3.5)

2. Let's consider now the case with $x \neq 0, \mu \neq 0$ where all the three perturbations must be considered. Using (3.13) the transcendental equation reads

$$F(\tilde{\Lambda}^2_k) = 1 + \frac{8t^2(x^2-1)}{N+1} \sum_{i=1}^{N} \frac{\sin^2 \frac{N\pi i}{N+1}}{\Lambda^2_{q_i} - \tilde{\Lambda}^2_k} + \frac{8tx\mu}{N+1} \sum_{i=1}^{N} \frac{\sin \frac{N\pi i}{N+1} \sin \frac{\pi i}{N+1}}{\Lambda^2_{q_i} - \tilde{\Lambda}^2_k} = 0 \tag{3.28}$$

The case $x = 0.3, N = 10$ is plotted in Fig. 3.6-3.9 for different values of μ. We see that if $x \neq 0$, the zero-mode acquires a mass becoming a *Dirac mode*. A *Dirac mode* is a non-local and non-zero energy state located inside the gap whose eigenfunction is localized at the edges [37]. In the region $|\mu| < 2$, the energy of the massive mode increases as μ increase. At the point $\mu = 2$ the energy is almost zero. In the region $|\mu| > 2$ the Dirac mode enters the bulk band becoming a bulk state.

However the formula (3.28), unlike the exact formula (3.25), is valid as long as x and μ are not so large that they cannot be treated as a perturbation. In order to find the exact explicit

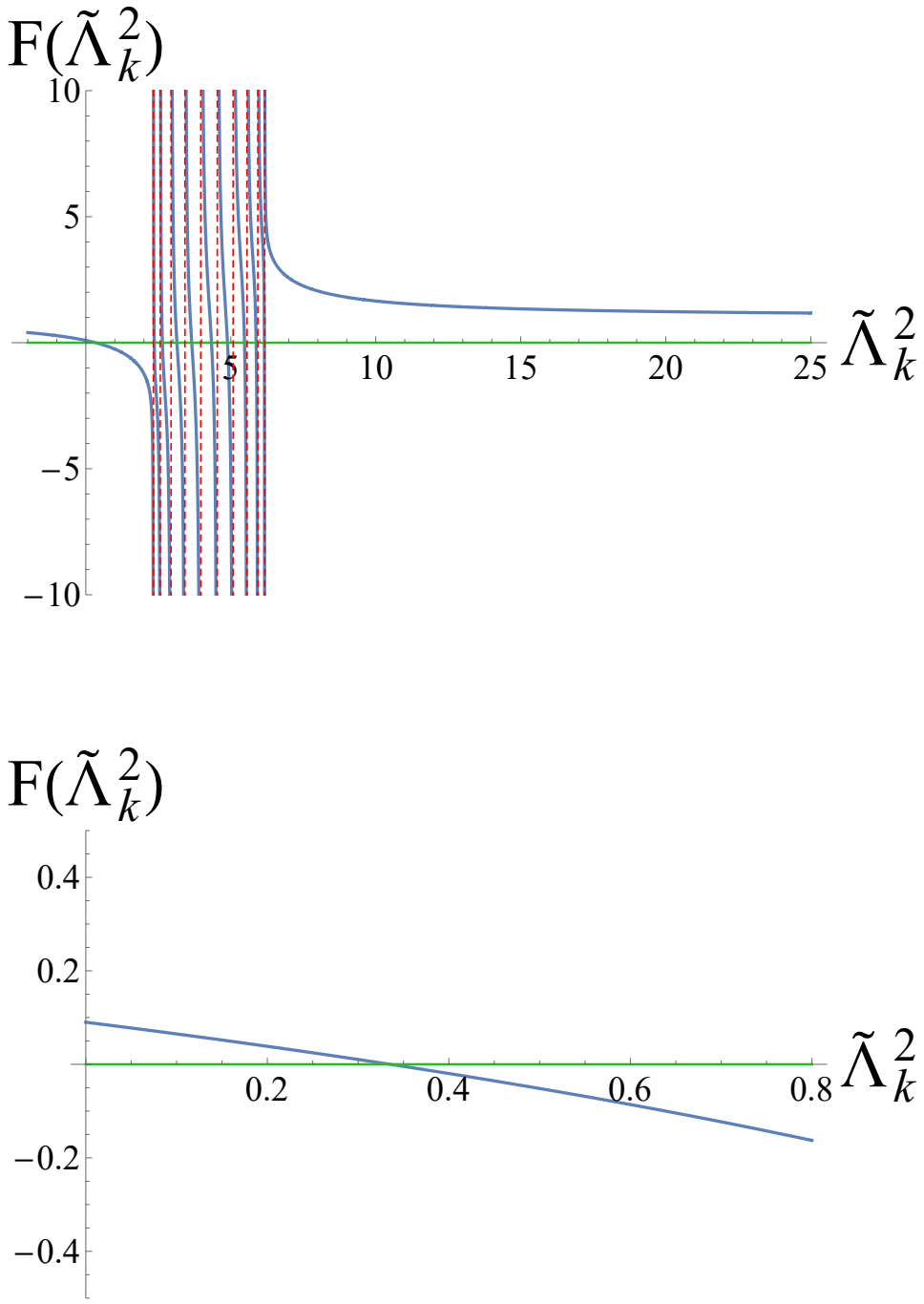

Figure 3.6: Graph of the transcendental equation for $N = 10$, $x = 0.3$ and $\mu = 0.5$. The second panel is a zoom of the lowest eigenvalue.

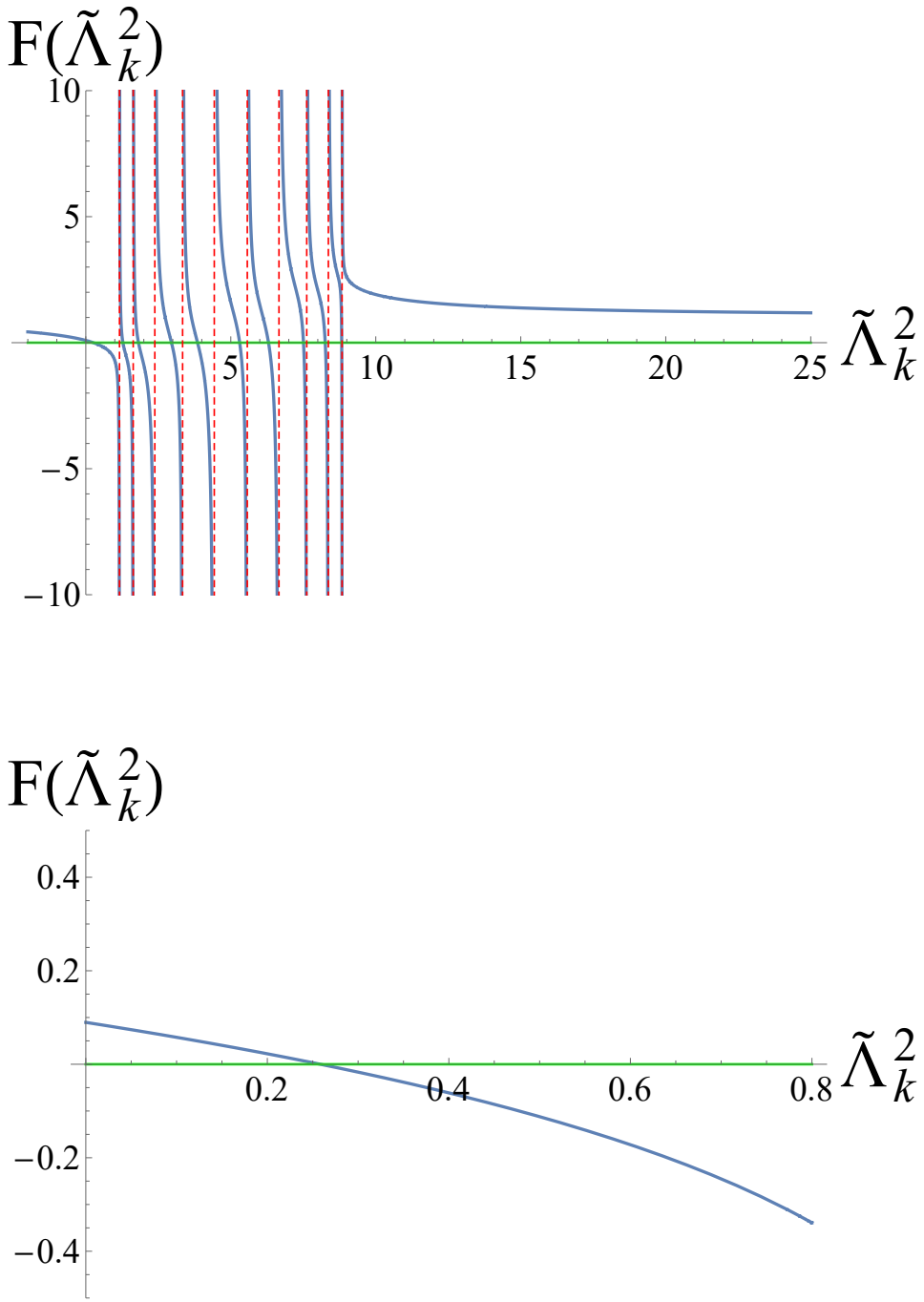

Figure 3.7: Graph of the transcendental equation for $N = 10$, $x = 0.3$ and $\mu = 1$. The second panel is a zoom of the lowest eigenvalue.

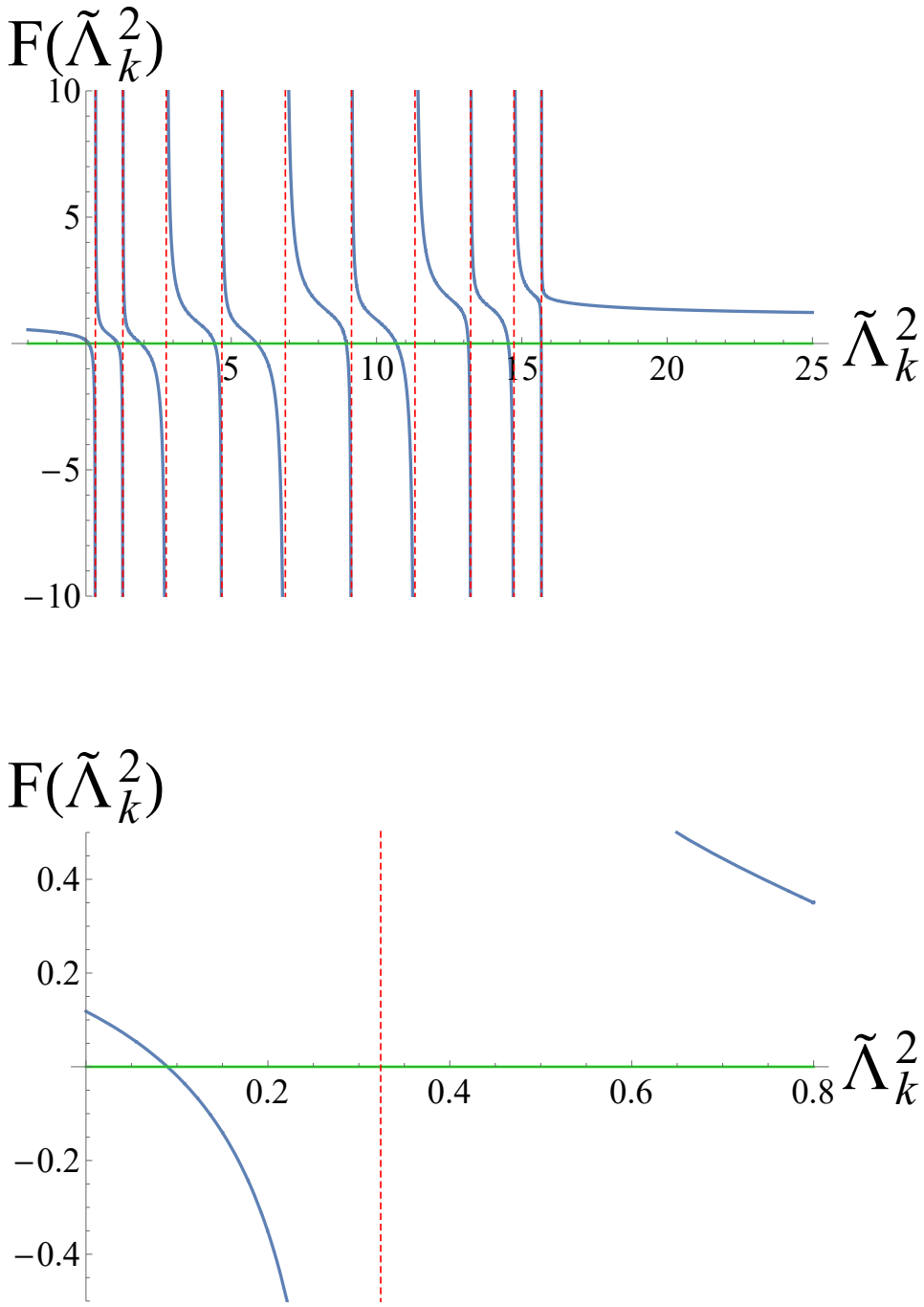

Figure 3.8: Graph of the transcendental equation for $N = 10$, $x = 0.3$ and $\mu = 2$. The second panel is a zoom of the lowest eigenvalue.

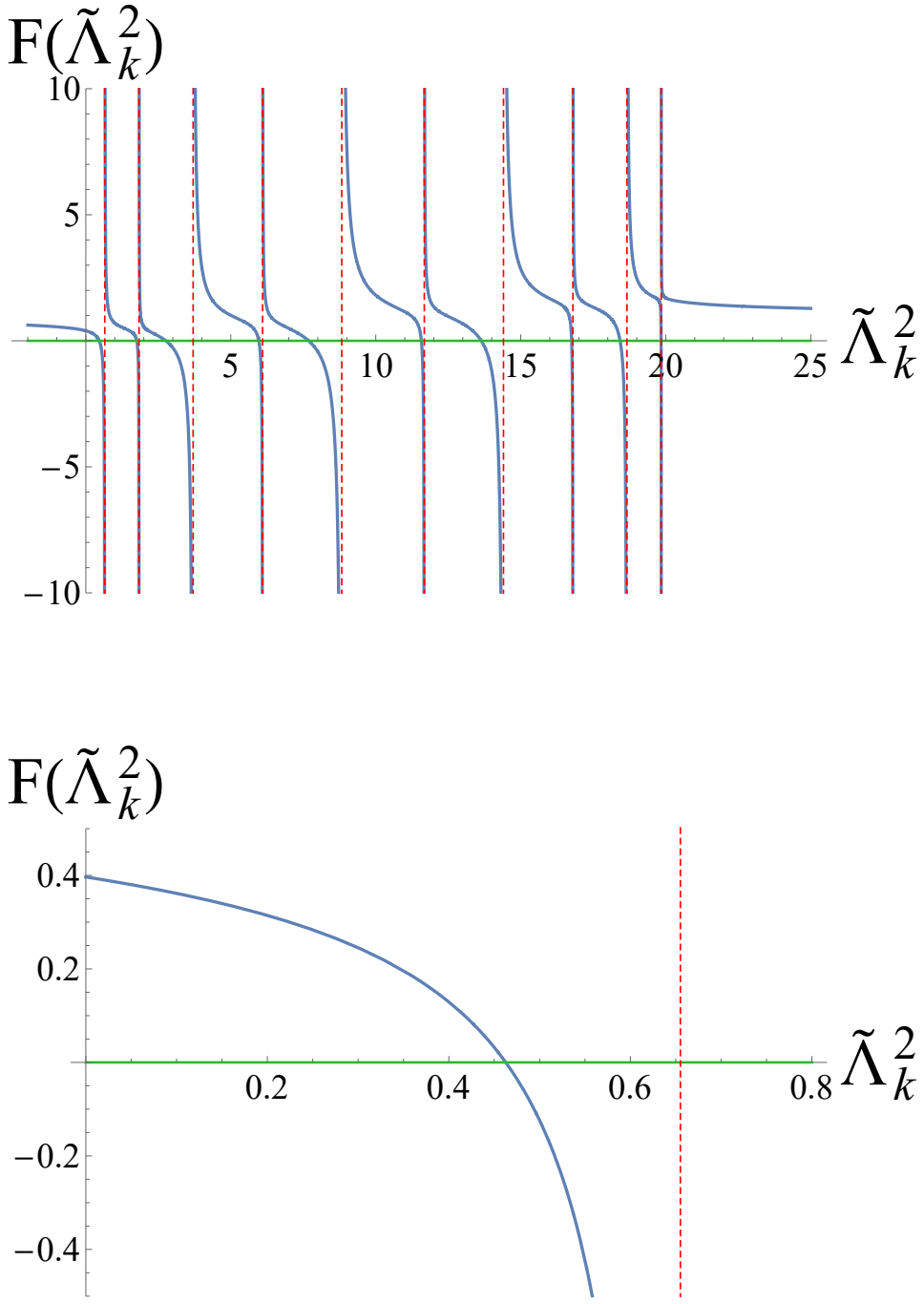

Figure 3.9: Graph of the transcendental equation for $N = 10$, $x = 0.3$ and $\mu = 2.5$. The second panel is a zoom of the lowest eigenvalue.

expressions of the perturbed eigenvalues and eigenvectors, the more complicated multiple-rank perturbation theory must be implemented [30]. Nevertheless, simpler solutions can be found by directly diagonalizing the matrix W without using the perturbative approach. This analysis will be carried out in the following chapter.

Chapter 4

Ansatz approach to the analytical solutions of the LSM equations for the finite Kitaev chain

In the previous chapter, we found the solutions of the LSM equation (2.48) for the finite Kitaev chain in the simplest cases by implementing the perturbation theory. However, to proceed further and analyze the other cases, the more complicated multiple-rank perturbation theory must be implemented [30]. This chapter aims to develop an equivalent approach which consists in directly diagonalizing the matrix W (real case) or $\mathbb{W}$ (complex case) introduced in section 2.2 to find simpler expressions for the eigenvectors and the eigenvalues for all the values of the model parameters.

4.1 Real case

According to the Lieb-Shultz-Mattis method the real case solutions $\vec{\phi}_k$ satisfy the equation (2.48) where A and B are given by eq.(3.14). Thanks to the translational invariance of the bulk, we can suggest as ansatz for the solutions the superposition of the plane waves $\phi_{kj} = \alpha e^{ikj} + \beta e^{-ikj}$. Here the coefficients α and β generally depend in the wavevector k. The bulk structure, i.e. the central part, of the matrix W is Toeplitz and fixes the functional form of the eigenvalues. The first and the last rows fix the coefficients α and β and the allowed values of k.

Let's define the bulk matrix W_B as the following pentadiagonal symmetric Toeplitz matrix:

$$W_B = \begin{pmatrix} \ddots & \ddots & \ddots & \ddots & \ddots & & & & & & \\ & \ddots & \ddots & \ddots & \ddots & \ddots & & & & & \\ & & c & b & a & b & c & & & & \\ & & & c & b & a & b & c & & & \\ & & & & c & b & a & b & c & & \\ & & & & & \ddots & \ddots & \ddots & \ddots & \ddots & \\ & & & & & & \ddots & \ddots & \ddots & \ddots & \ddots \\ & & & & & & & & & & \end{pmatrix} \tag{4.1}$$

Here

$$\begin{cases} a = 2(t^2 + \Delta^2) + \mu^2 \\ b = 2\mu t \\ c = t^2 - \Delta^2 \end{cases} \tag{4.2}$$

This is exactly the bulk structure (for which $3 < j < N - 3$ where j is the row index) of the matrix W for every value of the parameters.
The eigenvalue equation yields

$$\begin{aligned} \Lambda_k^2(\alpha e^{ikj} + \beta e^{-ikj}) =& [(t^2 - \Delta^2)(e^{i2k} + e^{-i2k}) + 2t\mu(e^{ik} + e^{-ik}) \\ &+ \mu^2 + 2(t^2 + \Delta^2)](\alpha e^{ikj} + \beta e^{-ikj}) \end{aligned} \tag{4.3}$$

which correspond to the eigenvalues

$$\Lambda_k^2 = (2t\cos k + \mu)^2 + 4\Delta^2 \sin^2 k \tag{4.4}$$

According to the Hermicity of the Hamiltonian the quadratic energy eigenvalues Λ_k^2 must be real. We split the real and imaginary part of the momentum $k = \kappa + i\eta$, so that

$$e^{ik} = \lambda e^{i\kappa} \tag{4.5}$$

where $\lambda = e^{-\eta} \geq 0$. As a consequence we find

$$\begin{aligned} \Lambda_k^2 =& t^2((\lambda + \lambda^{-1})^2 \cos^2\kappa - (\lambda - \lambda^{-1})^2 \sin^2\kappa) + 2t\mu(\lambda + \lambda^{-1})\cos\kappa \\ &+ \mu^2 - \Delta^2((\lambda - \lambda^{-1})^2 \cos^2\kappa - (\lambda + \lambda^{-1})^2 \sin^2\kappa) \\ &+ 2i(\lambda - \lambda^{-1})\sin\kappa((t^2 - \Delta^2)(\lambda + \lambda^{-1})\cos\kappa + \mu t) \end{aligned} \tag{4.6}$$

Then, the Λ_k^2 vanish if at least one of the following three conditions hold:

1. $(\lambda - \lambda^{-1}) = 0$
2. $\sin\kappa = 0$

3. $(t^2-\Delta^2)(\lambda+\lambda^{-1})\cos\kappa+\mu t=0$

The first condition corresponds to scattering states and the last two conditions to the edge states which, if they have zero energy, are also zero-modes. Let's examine each of them.

1. The first condition gives
$$\lambda=\lambda^{-1}\rightarrow\lambda=1\rightarrow e^{ik}=e^{i\kappa} \tag{4.7}$$
Using (4.7), (4.4) becomes
$$\Lambda_k^2=(2t\cos\kappa+\mu)^2+4\Delta^2\sin^2\kappa \tag{4.8}$$
Maxima and minima of Λ_k^2 are the solutions of
$$\frac{\partial\Lambda_k^2}{\partial\kappa}=-4\sin\kappa[2\cos\kappa(t^2-\Delta^2)+\mu t]=0 \tag{4.9}$$
In the interval $[0,2\pi]$, we have:
   - $\sin\kappa=0\rightarrow\kappa=0,\pi$ In these points the energy is equal to
   $$\Lambda_k^2=(\pm2t+\mu)^2 \tag{4.10}$$
   where the upper sign is valid if $\kappa=0$ and the lower sign if $\kappa=\pi$.
   - $\cos\kappa=-\frac{\mu t}{2(t^2-\Delta^2)}$. The energy is
   $$\Lambda_k^2=4\Delta^2-\frac{\mu^2\Delta^2}{(t^2-\Delta^2)} \tag{4.11}$$
   Then, because of $|\cos\kappa|\leq1$ there are also two other stationary points in the interval $[0,2\pi]$ if $|\mu t|<|2(t^2-\Delta^2)|$

2. The second condition of reality gives
$$\kappa=0,\pi\rightarrow e^{ik}=\pm e^{-\eta}=\pm\lambda \tag{4.12}$$
Here the upper sign is valid if $\kappa=0$ and the lower sign if $\kappa=\pi$.
The corresponding eigenvalues are:
$$\Lambda_k^2=(2t\cosh\eta\pm\mu)^2-4\Delta^2\sinh^2\eta \tag{4.13}$$

3. On the other hand, if the third condition is valid
$$\Lambda_k^2=(2t\cos(\kappa+i\eta)+\mu)^2+4\Delta^2\sin^2(\kappa+i\eta) \tag{4.14}$$
In this situation κ and η are not independent. Explicitly, we find (if $(t^2-\Delta^2)\cos\kappa\neq0$)
$$\cosh\eta=-\frac{\mu t}{2(t^2-\Delta^2)\cos\kappa} \tag{4.15}$$

In the following subsections, we will examine the solutions in some typical cases.

4.1.1 Case 1: $t = \Delta$, $x \neq 0$, $\mu \neq 0$

Let's consider the case $t = \Delta$. The solutions $\vec{\phi}_k$ must be the eigenfunctions of the matrix (3.15). The eigenvalue equation gives

$$\begin{cases} b\phi_{k(j-1)} + a\phi_{kj} + b\phi_{k(j+1)} = \Lambda_k^2 \phi_{kj} \qquad j = 2, \cdots, N-1 & \text{(4.16a)} \\ a\phi_{k1} + b\phi_{k2} + d\phi_{kN} = \Lambda_k^2 \phi_{k1} & \text{(4.16b)} \\ d\phi_{k1} + b\phi_{N-1} + (a+c)\phi_{kN} = \Lambda_k^2 \phi_{kN} & \text{(4.16c)} \end{cases}$$

The first equation is the bulk equation and the last two are the boundary equations. We can now use eq.(4.16b) to fix, up to a normalization factor, the coefficients α and β.
Some long but straightforward algebra shows that :

$$\phi_{kj} = \sin kj + \xi(k) \cos kj \tag{4.17}$$

where

$$\xi(k) \equiv \frac{d \sin kN}{b - d \cos kN} \tag{4.18}$$

The boundary equation (4.16c) gives

$$\begin{aligned} &d(\sin k + \xi(k) \cos k) + b(\sin k(N-1) + \xi(k) \cos k(N-1)) \\ &+ c(\sin kN + \xi(k) \cos kN) \\ &= 2b \cos k (\sin kN + \xi(k) \cos kN) \end{aligned} \tag{4.19}$$

Solving numerically equation (4.19) it can be shown that there are $N-1$ real independent solutions (the two trivial solutions $k = 0, k = \pi$ for which the eigenvector is null must be discarded). The last boundary solution can be determined assuming that k is a complex number.
The eigenvalues (4.4) read

$$\Lambda_k^2 = 4t^2 + \mu^2 + 4t\mu \cos k \tag{4.20}$$

The boundary state exists only in the region $|\mu| < |2t|$. From the explicit form of the eigenvalues (4.20) it can be demonstrated that the edge states drop out form the scattering spectrum only if $\kappa = \pi$ for $\mu t > 0$ or $\kappa = 0$ for $\mu t < 0$, where, as usual, κ is the real part of the wavenumber k. In these two cases the boundary states satisfy the condition 2 we have seen in the previous subsection.
The analytical expression for the edge states can be written in terms of hyperbolic functions. In particular, they can be obtained by substituting $k = \pi + i\eta$ if $\mu t > 0$ or $k = i\eta$ if $\mu t < 0$ in (4.17).
In the trivial case $\mu = 0$ the matrix (3.15) is diagonal with $N-1$ eigenvalues equal to $4t^2$ and one eigenvalue equal to $4t^2 + 4t^2(x^2 - 1)$. For $x = 0$ the energy of the edge state is zero; for $x \neq 0$ the mode acquires a mass until it reaches the rest of the bulk band for $x = 1$.
Solving numerically equation (4.19) it can be shown that the module of the imaginary part of the complex solution increases when x decreases. Therefore, being the hyperbolic cosine the derivative of the hyperbolic sine and vice versa, as $x \to 0$ the function $\phi_{k_0 j}$ becomes more peaked at the end of the chain.

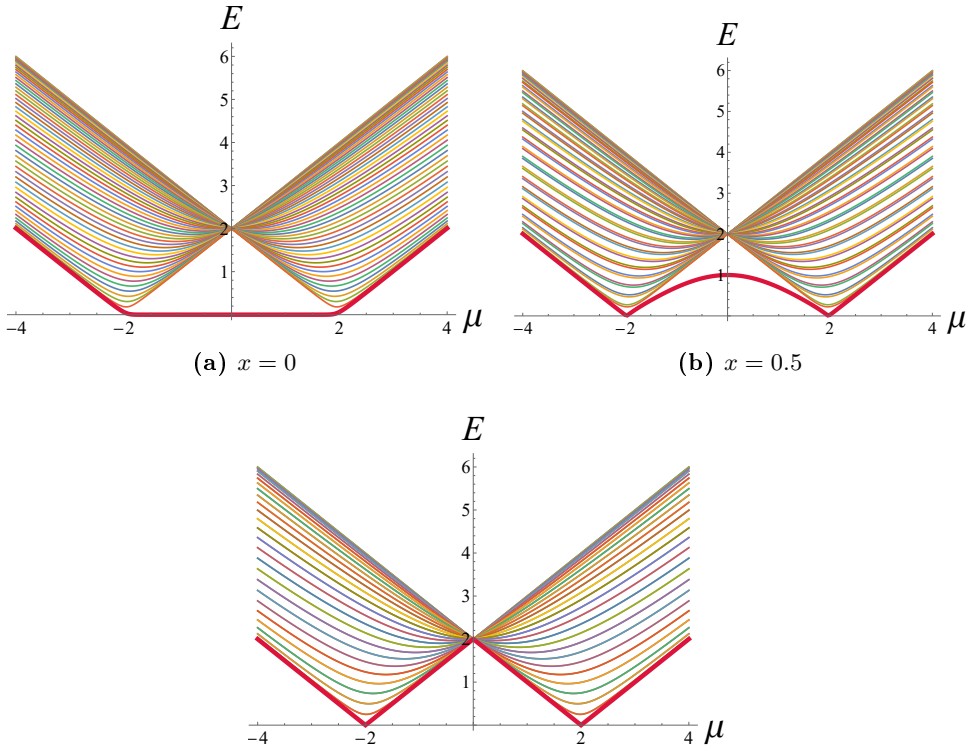

(a) $x = 0$ **(b)** $x = 0.5$ **(c)** $x = 1$

Figure 4.1: Energy levels for $N = 50, t = \Delta = 1$ as a function of μ for different values of x. To obtain the spectrum, we have numerically calculated the eigenvalues of the matrix W in (2.48). The red line shows that for OBCs, in the topological region, at least in the thermodynamic, the ground state of the model is doubly degenerate. If $x \neq 0$, the degeneracy is lifted.

The spectrum (4.4) can be easily calculated numerically by finding the eigenvalues of the matrix W.[1]

Fig. 4.1 shows the energy levels Λ_k as a function of μ for different values of x in the case $t = \Delta = 1$.

The red line shows the lowest one-particle excitation energy. For OBCs, in the region $|\mu| < 2|t|$, at least in thermodynamic limit, there is a zero one-particle excitation energy. Therefore the ground state of the model is doubly degenerate. In fact, there are two distinct ground states with opposite fermionic parity (see the discussion in Section 1.5). Nevertheless, for a finite chain length and out of the fully dimerized limit, this energy turns out to be slightly different from zero and therefore the ground state degeneracy is removed.

However, if $x \neq 0$ the degeneracy is lifted in the whole topological region for every value of N. Indeed, in this situation, the massless edge state, which is present only if $x = 0$, acquires a mass becoming a Dirac mode until it disappears in the bulk band for $x = 1$.

[1] The numerical analysis has been implemented via the software Wolfram Mathematica.

4.1.2 Case 2: $t = \Delta$, $x = 0$, $\mu \neq 0$

In this situation the previous equations take a simpler form. From (4.17), setting $d = 0$, the eigenvectors become, up to a normalization constant

$$\phi_{kj} = \sin kj \tag{4.21}$$

and (4.19) can be written as

$$\sin kN = -\frac{\mu}{2t} \sin k(N+1) \tag{4.22}$$

For OBCs the analytical expression of the boundary states are relatively simple.
If $\mu t > 0$, setting $k = \pi + i\eta$, the zero-mode reads

$$\phi_{k_0 j} = (-1)^j \sinh \eta j \tag{4.23}$$

where η is the solution of

$$\sinh \eta N = \frac{\mu}{2t} \sinh \eta(N+1) \tag{4.24}$$

Instead, if $\mu t < 0$, then $k = i\eta$, and the zero-mode can be written as

$$\phi_{k_0 j} = \sinh \eta j \tag{4.25}$$

where η solves

$$\sinh \eta N = -\frac{\mu}{2t} \sinh \eta(N+1) \tag{4.26}$$

The two hyperbolic sines in (4.24) and (4.26) intersect in only two equivalent and opposite points (the trivial point $k = 0$ must be discarded). Inverting (4.20)

$$k = \arccos\left(\frac{\Lambda_k^2 - 4t^2 - \mu^2}{4t\mu}\right) \tag{4.27}$$

The wavenumber of the zero-mode ($\Lambda_{k_0}^2 \sim 0$) is

$$k_0 \sim \arccos\left(-\frac{4t^2 + \mu^2}{4t\mu}\right) \tag{4.28}$$

We see that as $\mu \to 0$ the module of argument of the arccosine increases and the eigenfunction $\phi_{k_0 j}$ becomes more peaked at the end the chain.

4.1.3 Case 3: $t \neq \Delta$, $x \neq 0$, $\mu = 0$

If $t \neq \Delta, x \neq 0, \mu = 0$ the explicit form of the matrix W is

$$W = \begin{pmatrix} a+d & 0 & e & & & & f & 0 \\ 0 & a & 0 & \ddots & & & & f \\ e & 0 & a & \ddots & \ddots & & & \\ & \ddots & \ddots & \ddots & \ddots & \ddots & & \\ & & \ddots & \ddots & \ddots & \ddots & \ddots & \\ & & & \ddots & \ddots & a & 0 & e \\ f & & & & \ddots & 0 & a & 0 \\ 0 & f & & & & e & 0 & a+c \end{pmatrix} \tag{4.29}$$

having set

$$\begin{cases} a = 2t^2 + 2\Delta^2 \\ c = (x^2-1)(t+\Delta)^2 \\ d = (x^2-1)(t-\Delta)^2 \\ e = t^2 - \Delta^2 \\ f = t^2 x - x\Delta^2 \end{cases} \tag{4.30}$$

The eigenvalue equation gives

$$\begin{cases} e\phi_{k(j-2)} + a\phi_{kj} + e\phi_{k(j+2)} = \Lambda_k^2 \phi_{kj} \qquad j = 3, \cdots, N-3 & \text{(4.31a)} \\ (a+d)\phi_{k1} + e\phi_{k3} + f\phi_{k(N-1)} = \Lambda_k^2 \phi_{k1} & \text{(4.31b)} \\ a\phi_{k2} + e\phi_{k4} + f\phi_{kN} = \Lambda_k^2 \phi_{k2} & \text{(4.31c)} \\ f\phi_{k1} + e\phi_{k(N-3)} + a\phi_{k(N-1)} = \Lambda_k^2 \phi_{k(N-1)} & \text{(4.31d)} \\ f\phi_{k2} + e\phi_{k(N-2)} + (a+c)\phi_{kN} = \Lambda_k^2 \phi_{kN} & \text{(4.31e)} \end{cases}$$

In this case, we consider the following ansatz for the wavefunctions:

$$\phi_{kj} = \alpha e^{ikj} + \beta e^{-ikj} + \rho e^{i(k+\pi)j} + \sigma e^{-i(k+\pi)j} \tag{4.32}$$

The form of the ansatz is slightly different from the previous one, but it's still compatible with the analysis done at the beginning of the chapter.
If N is even, the first set of solutions read

$$\phi_{kj} = \cos kj - (-1)^j \cos kj + \xi(k)(\sin kj - (-1)^j \sin kj) \tag{4.33}$$

where, using (4.31b),

$$\xi(k) \equiv \frac{-d\cos k - e\cos 3k - f\cos k(N-1) + 2e\cos 2k\cos k}{d\sin k + e\sin 3k + f\sin k(N-1) - 2e\cos 2k\sin k} \tag{4.34}$$

The values of k can be found by replacing the previous ansatz in (4.31d). The second set of solutions is

$$\phi_{kj} = \cos kj + (-1)^j \cos kj + \xi(k)(\sin kj + (-1)^j \sin kj) \tag{4.35}$$

where, using (4.31c),

$$\xi(k) \equiv \frac{-e\cos 4k - f\cos kN + 2e\cos^2 2k}{e\sin 4k + f\sin kN - 2e\cos 2k\sin 2k} \tag{4.36}$$

Then, solving numerically (4.31e) the second set of solutions is completely determined.
If N is odd the general ansatz is more complicated. Namely

$$\begin{aligned}\phi_{kj} =&(\cos kj + (-1)^j \cos kj) + \delta(\sin kj + (-1)^j \sin kj)\\ &+ \tau(\cos kj - (-1)^j \cos kj) + \omega(\sin kj - (-1)^j \sin kj)\end{aligned} \tag{4.37}$$

The coefficients δ, τ, ω and the allowed values of k can be determined by solving numerically (4.31b), (4.31c), (4.31d) and (4.31e) .
The eigenvalues (4.4) are

$$\Lambda_k^2 = 2t^2 + 2\Delta^2 + 2(t^2 - \Delta^2)\cos 2k \tag{4.38}$$

Thus, now the edge states drop out form the scattering spectrum only if $\kappa = \pi/2$ for $|t| > |\Delta|$ or $\kappa = 0$ for $|t| < |\Delta|$.
Both values of κ of the edge states are compatible with the analysis done at the beginning of the chapter (see the conditions 2 and 3).
Also in this case an analytical expression for the edge states can be written in terms of hyperbolic functions.
In particular, they can be obtained by substituting $k = i\eta$ if $|t| < |\Delta|$ or $k = \pi/2 + i\eta$ if $|t| > |\Delta|$ in (4.35) for N even and in (4.37) for N odd.
Fig. 4.2 and Fig. 4.3 show the energy levels Λ_k as a function of μ for different values of x in the cases $t = 1, \Delta = 2$ and $t = 2, \Delta = 1$. In the topological region, for OBCs, as in the case $t = \Delta$, at least in the thermodynamic, the ground state of the model is doubly degenerate. However, if $x \neq 0$ the degeneracy is lifted.
Now if $\mu = 0$ the levels are no longer degenerate at the point $2|\Delta|$ as in the case $t = \Delta$.
Nonetheless, the topological transition is still at the point $|\mu| = 2|t|$ and the underlying physics of the model is the same as the case $t = \Delta$.

4.1.4 Case 4: $t \neq \Delta$, $x = 0$, $\mu = 0$

For OBCs the expressions of the previous subsection take a simpler form. The first set of solution is

$$\phi_{kj} = \cos kj - (-1)^j \cos kj + \xi(k)(\sin kj - (-1)^j \sin kj) \tag{4.39}$$

where, using (4.31b),

$$\xi(k) \equiv= \frac{-d\cos k - e\cos 3k + 2e\cos 2k\cos k}{d\sin k + e\sin 3k - 2e\cos 2k\sin k} \tag{4.40}$$

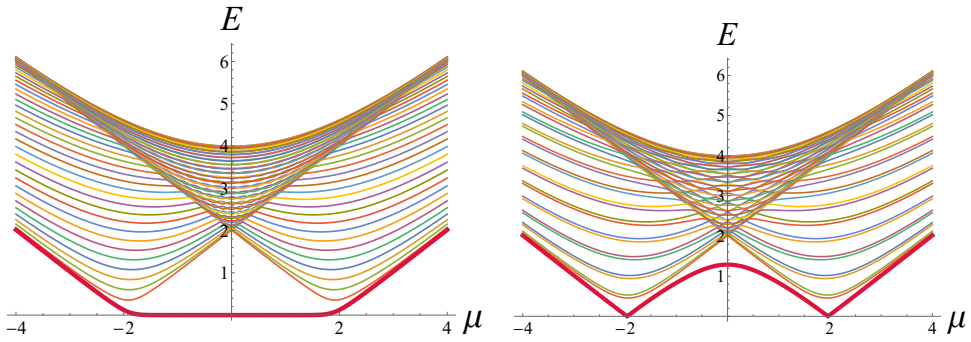

(a) $x = 0$ **(b)** $x = 0.5$

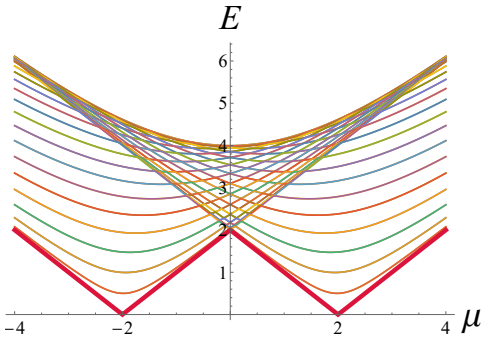

(c) $x = 1$

Figure 4.2: Energy levels for $N = 50, t = 1, \Delta = 2$ as a function of μ for different values of x. To obtain the spectrum, we have numerically calculated the eigenvalues of the matrix W in (2.48). The red line shows that for OBCs, in the topological region, at least in the thermodynamic, the ground state of the model is doubly degenerate. The degeracy is lifted for $x \neq 0$.

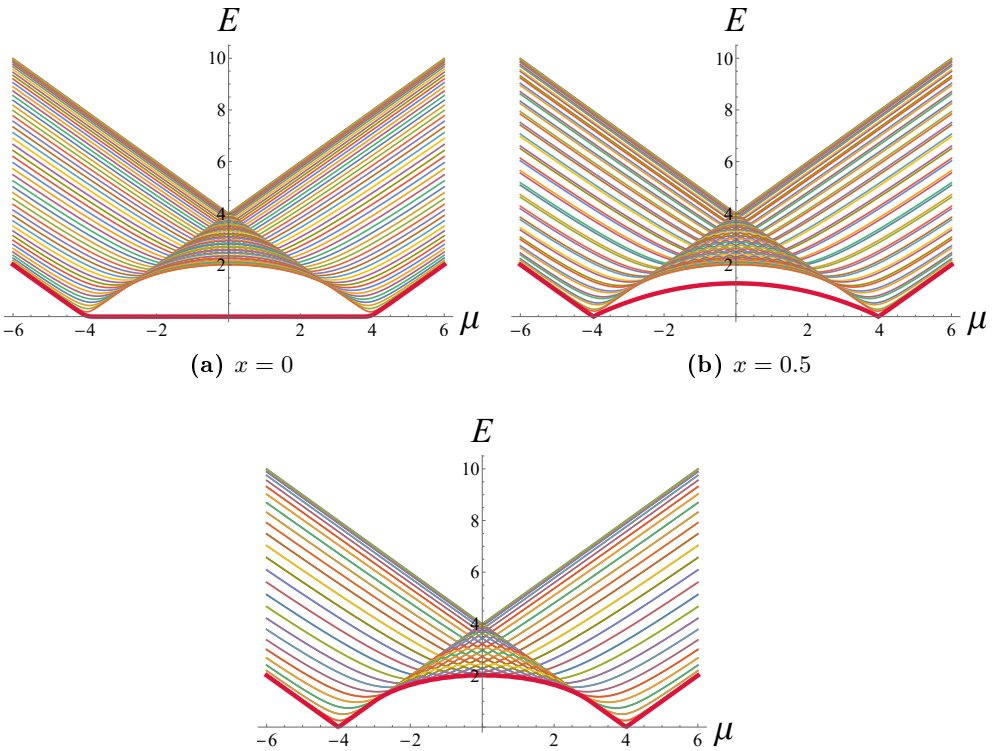

(a) $x = 0$ **(b)** $x = 0.5$

(c) $x = 1$

Figure 4.3: Energy levels for $N = 50, t = 2, \Delta = 1$ as a function of μ for different values of x. To obtain the spectrum, we have numerically calculated the eigenvalues of the matrix W in (2.48). The red line shows that for OBCs, in the topological region, at least in the thermodynamic, the ground state of the model is doubly degenerate. The degeracy is lifted for $x \neq 0$.

If N is even the values of k can be found by solving eq.(4.31d) which in this case reads

$$\begin{aligned} &e[\cos k(N-3)+\xi(k)\sin k(N-3)] \\ &=(2e\cos 2k)[\cos k(N-1)+\xi(k)\sin k(N-1)] \end{aligned} \tag{4.41}$$

If N is odd eq.(4.31e) becomes

$$\begin{aligned} &e[\cos k(N-2)+\xi(k)\sin k(N-2)]+c[\cos kN+\xi(k)\sin kN] \\ &=(2e\cos 2k)[\cos kN+\xi(k)\sin kN] \end{aligned} \tag{4.42}$$

The two previous equations give only $N/2$ independent solutions.
The second set of solutions is

$$\phi_{kj}=\sin kj+(-1)^j\sin kj \tag{4.43}$$

The allowed values of k can be found by solving the following two equations. For N even, eq.(4.31e) becomes

$$e\sin k(N-2)+c\sin kN=2e\cos 2k\sin kN \tag{4.44}$$

Instead, if N is odd, eq.(4.31d) reads

$$e\sin k(N-3)=2e\cos 2k\sin k(N-1) \tag{4.45}$$

The last two equations give the remaining $N/2$ solutions.
For OBCs the analytical expression of the boundary states are relatively simple.
Let's consider N even.
If $|t|<|\Delta|$, setting as usual $k=i\eta$, the functional form of the zero-mode reads

$$\phi_{k_0 j}=\sinh\eta j+(-1)^j\sinh\eta j \tag{4.46}$$

where η is the solution of

$$e\sinh\eta(N-2)+c\sinh\eta N=2e\cosh 2\eta\sinh\eta N \tag{4.47}$$

The solution $\phi_{k_0 j}$ in this case never changes the sign.
If $|t|>|\Delta|$

$$\phi_{k_0 j}=(-1)^{\frac{j}{2}}\sinh\eta j+(-1)^{\frac{3j}{2}}\sinh\eta j \tag{4.48}$$

where η solves

$$e\sinh\eta(N-2)-c\sinh\eta N=2e\cosh 2\eta\sinh\eta N \tag{4.49}$$

Thus, when $|t|>|\Delta|$ the solution $\phi_{k_0 j}$ take both positive and negative values.
Let's consider now N odd.
If $|t|<|\Delta|$

$$\phi_{k_0 j}=\cosh\eta j-(-1)^j\cosh\eta j+\zeta(\eta)(\sinh\eta j-(-1)^j\sinh\eta j) \tag{4.50}$$

where

$$\zeta(\eta)\equiv\frac{-d\cosh\eta-e\cosh 3\eta+2e\cosh 2\eta\cosh\eta}{d\sinh\eta+e\sinh 3\eta-2e\cosh 2\eta\sinh\eta} \tag{4.51}$$

Here η is the solution of (4.42) with $k = i\eta$.
If $|t| > |\Delta|$

$$\begin{aligned}\phi_{k_0 j} =&(-1)^{\frac{j-1}{2}} \sinh \eta j - (-1)^{\frac{3j-1}{2}} \sinh \eta j \\ &+ \zeta(\eta)((-1)^{\frac{j-1}{2}} \cosh \eta j - (-1)^{\frac{3j-1}{2}} \cosh \eta j)\end{aligned} \tag{4.52}$$

where

$$\zeta(\eta) \equiv \frac{-d \sinh \eta + e \sinh 3\eta - 2e \cosh 2\eta \sinh \eta}{d \cosh \eta - e \cosh 3\eta + 2e \cosh 2\eta \cosh \eta} \tag{4.53}$$

and η solves (4.42) with $k = \pi/2 + i\eta$.
Inverting (4.38)

$$k = \frac{1}{2} \arccos\left(\frac{\Lambda_k^2 - 2(t^2 + \Delta^2)}{2(t^2 - \Delta^2)}\right) \tag{4.54}$$

The momentum of the zero-mode ($\Lambda_{k_0}^2 \sim 0$) is

$$k_0 \sim \frac{1}{2} \arccos\left(-\frac{t^2 + \Delta^2}{t^2 - \Delta^2}\right) \tag{4.55}$$

If $|t| \to |\Delta|$ the module of argument increases and the eigenfunction $\phi_{k_0 j}$ becomes more peaked at the end of the chain.

4.2 Majorana edge states in the Kitaev model for finite chain length

For OBCs, in the topological phase, as discussed in section 1.5 for the fully dimerized limit, there are two Majorana edge states which are localized at the beginning and at the end of the chain. It is thus possible to define a complex fermion out of them which is an eigenstate of the Hamiltonian and, at least in the thermodynamic limit, can be populated without affecting the energy of the state. However, for finite chain length, in general, this non-local fermion has quasi-zero energy and thus the degeneracy in the spectrum (see Section 1.5) is split. Moreover, as previously explained, if $x \neq 0$, the degeneracy is removed in the whole topological region. In this section, we will extend the analytical expressions of the Majorana tails for OBCs (1.104), which hold in the thermodynamic limit, for finite chain length N. Furthermore, we will find the analytical expression of the Majorana edge states for generic boundary conditions.

4.2.1 Analytical expressions

Now we want to express the mode η_k in terms of the Majorana modes m_{2j-1} and m_{2j}. Let's start from the following transformation

$$c_j = \frac{e^{i\frac{\phi}{2}}}{2}(m_{2j-1} + i m_{2j}) \qquad c_j^\dagger = \frac{-e^{i\frac{\phi}{2}}}{2}(m_{2j-1} - i m_{2j}) \tag{4.56}$$

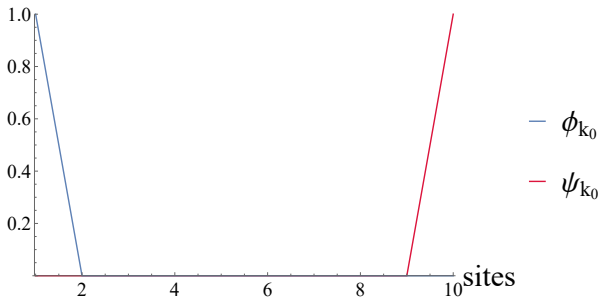

Figure 4.4: Profiles of the wavefunction of the two Majorana zero-modes for $N = 10$, $x = 0$ and $\mu = 0$.

Taking into account that if $\Delta \to |\Delta| e^{i\phi}$ with $\Delta = |\Delta|$ then, up to an overall constant, $g'_{kj} = e^{-i\frac{\phi}{2}} g_{kj}$ and $h'_{kj} = e^{i\frac{\phi}{2}} h_{kj}$ where g_{kj} and h_{kj} are the LSM coefficients of the real problem one finds that

$$\begin{aligned}\eta_k &= \sum_j [g'_{kj} c_j + h'_{kj} c_j^\dagger] = \\ &= \sum_j \left[\frac{1}{2}(g_{kj} + h_{kj}) m_{2j-1} + \frac{i}{2}(g_{kj} - h_{kj}) m_{2j} \right] = \\ &= \frac{1}{2} \sum_j [\phi_{kj} m_{2j-1} + i\psi_{kj} m_{2j}] \end{aligned} \tag{4.57}$$

Thus, the boundary state becomes

$$\eta_{k_0} \equiv \frac{1}{2} (\psi_\alpha + i\psi_\beta) \tag{4.58}$$

where $\psi_\alpha \equiv \sum_j \phi_{k_0 j} m_{2j-1}$, $\psi_\beta \equiv \sum_j \psi_{k_0 j} m_{2j}$ and $\alpha, \beta = \{L, R\}$.
The Majorana modes localized at the beginning and at the end of the chain will be called ψ_L and ψ_R, respectively.
Therefore the normalized exact boundary solutions $\phi_{k_0 j}$ and $\psi_{k_0 j}$ of the real problem found in the Sections 3.2 and 4.1 for almost all the values of the model parameters are the analytical expressions of the exponentially decaying Majorana tails for finite chain length N.
We can now obtain the results of the articles [21, 37] for which $\Delta \to |\Delta| e^{i\phi}$ and therefore the functions ϕ_{kj} and ψ_{kj} are exchanged.
In particular, we consider first the case $\Delta = t > 0$ and $\mu = 0$ for which the matrix W is diagonal and the zero-mode is given by $\vec{\phi}_{k_0} = (1, 0, ..., 0)$ and $\vec{\psi}_{k_0} = (0, 0, ..., 1)$.

Fig. 4.4 shows the coefficients $\phi_{k_0 j}$ and $\psi_{k_0 j}$. Therefore using (4.57)

$$\eta_{k_0} = \frac{1}{2}(m_1 + i m_{2N}) \tag{4.59}$$

which is the same result obtained in chapter 1.5.
If $t = \Delta = 1$, then $x_+ = 0$ and $x_- = -\frac{\mu}{2}$ and the expressions (1.104), which hold in the

thermodynamic limit, become

$$\psi_L = \sum_j (\alpha'_- x_-^j) m_{2j-1} \quad \psi_R = \sum_j (\alpha''_- x_-^{-j}) m_{2j} \tag{4.60}$$

The previous formulas coincide with those obtained in [37]

$$\psi_L = \sum_j \left(-\frac{\mu}{2}\right)^{j-1} m_{2j-1} \qquad \psi_R = \sum_i \left(-\frac{\mu}{2}\right)^{N-j} m_{2j} \tag{4.61}$$

if $\alpha'_- = \left(-\frac{\mu}{2}\right)^{-1}$, $\alpha''_- = \left(-\frac{\mu}{2}\right)^{N}$.
Thus, up to a normalization constant, we obtain

$$\phi'_{k_0 j} = \left(-\frac{\mu}{2}\right)^{j-1} \qquad \psi'_{k_0 j} = \left(-\frac{\mu}{2}\right)^{N-j} \tag{4.62}$$

where the prime symbol indicates that the expressions refer to the thermodynamic limit. Using the results of section 4.1, if $x = 0$ and $\mu > 0$

$$\phi_{k_0 j} = (-1)^{N-j+1} \sinh \eta (N - j + 1) \qquad \psi_{k_0 j} = (-1)^j \sinh \eta j \tag{4.63}$$

The previous two equation are equivalent if

$$\left(-\frac{\mu}{2}\right)^{N-j} \sim (-1)^j \sinh \eta j \tag{4.64}$$

Fig. 4.5 shows an example of the normalized eigenfunctions $\psi_{k_0 j}$ and $\psi'_{k_0 j}$ for $N = 6$ for which the finite size effects are evident. For N finite they are both localized at the right edge of the chain where they are quite coincident but they differ slightly in the tail that penetrate inside the bulk. Writing the hyperbolic sine in exponential form and neglecting the exponential decaying factor from (4.64) we obtain that

$$\eta \simeq \ln \frac{2}{\mu} \tag{4.65}$$

Indeed, doing the same approximations made before, eq.(4.65) is the solution of (4.24). The last relation is also valid for finite N in the limit $\eta \gg 1$ and so $\mu \ll 1$. If $\mu < 0$

$$\left(-\frac{\mu}{2}\right)^{N-j} \sim \sinh \eta j \tag{4.66}$$

and in this case

$$\eta \simeq \ln \frac{2}{|\mu|} \tag{4.67}$$

In the sections 3.2 and 4.1 the analytical expressions of the coefficients ϕ_{kj} and ψ_{kj} have been derived from an eigenvalue equation so, if ϕ_{kj} and ψ_{kj} are chosen real and normalized, they are defined up to a sign. The exact sign can be determined by finding the coefficients g_{kj} and h_{kj} numerically and then taking the linear combinations $\phi_{kj} = g_{kj} + h_{kj}$ and $\psi_{kj} = g_{kj} - h_{kj}$ (see Chapter 2).

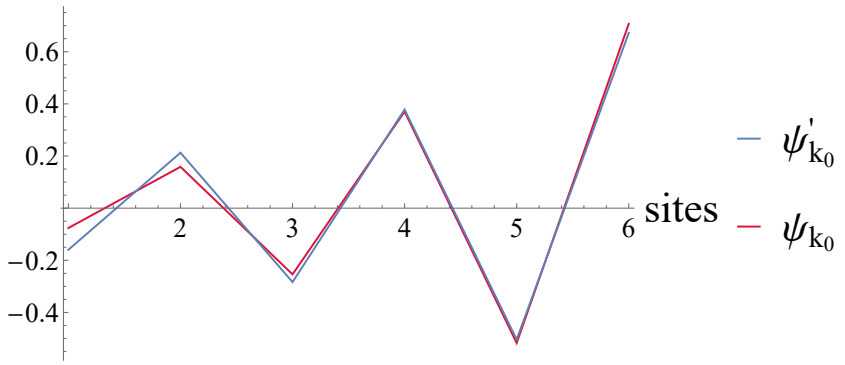

Figure 4.5: Majorana tails $\psi'_{k_0 j} = \left(-\frac{\mu}{2}\right)^{N-j}$ (blue) and $\psi_{k_0 j} = (-1)^j \sinh \eta j$ (red) for $t = \Delta = 1, x = 0, \mu = 1.5$ and $N = 6$.

We now examine how the edge states change while we change either the chemical potential μ or the boundary parameter x.

Fig. 4.6 represents the coefficients $\phi_{k_0 j}$ and $\psi_{k_0 j}$ for $x = 0$ and different values of μ. As expected, the Majorana tails, which are localized at the ends of the chains, become less peaked as $|\mu| \to 2|t|$. Out of the topological phase instead, there are no more hyperbolic solutions and so the lowest energy level is no longer a boundary state.
The graph 4.7 represents instead the tail for different values of x. As $x \to 1$ the Majorana tails become less peaked. If $x = 1$ the matrix W becomes circulant. A circulant matrix is a special kind of Toeplitz matrix where each row vector is rotated one element to the right relative to the preceding row vector [15].
In this situation the solutions for the eigenvalues and the eigenvectors are well known [15]. If $x = 1$ and N is even (see Fig. 4.7) the previous eigenfunctions tend to the expressions

$$\phi_{kj} = \frac{(-1)^{j+1}}{\sqrt{N}} \tag{4.68}$$

$$\psi_{kj} = \frac{(-1)^{j+1}}{\sqrt{N}} \tag{4.69}$$

Their energy is

$$\Lambda_k^2 = (4t^2 + \mu^2 - 4t\mu) \tag{4.70}$$

Finally, Fig. 4.8 shows the situation for some examples with $t \neq \Delta$. As expected, the behavior of the edge states and so the physics underlying the model is the same as the case $t = \Delta$.

4.3 Complex case

To find analytically the eigenvectors and the eigenvalues of the systems (2.44) for arbitrary values of the parameters is a quite difficult and involved problem. In the following, only the

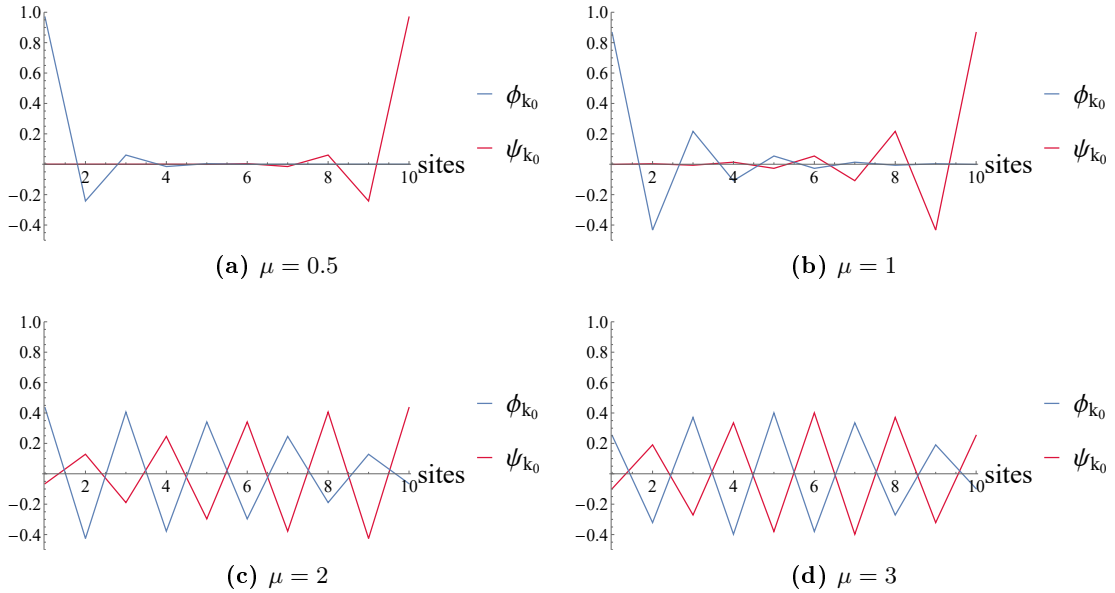

(a) $\mu = 0.5$ **(b)** $\mu = 1$

(c) $\mu = 2$ **(d)** $\mu = 3$

Figure 4.6: Majorana tails $\phi_{k_0 j}$ (blue) and $\psi_{k_0 j}$ (red) for $N = 10, x = 0, t = \Delta = 1$ and different values of μ.

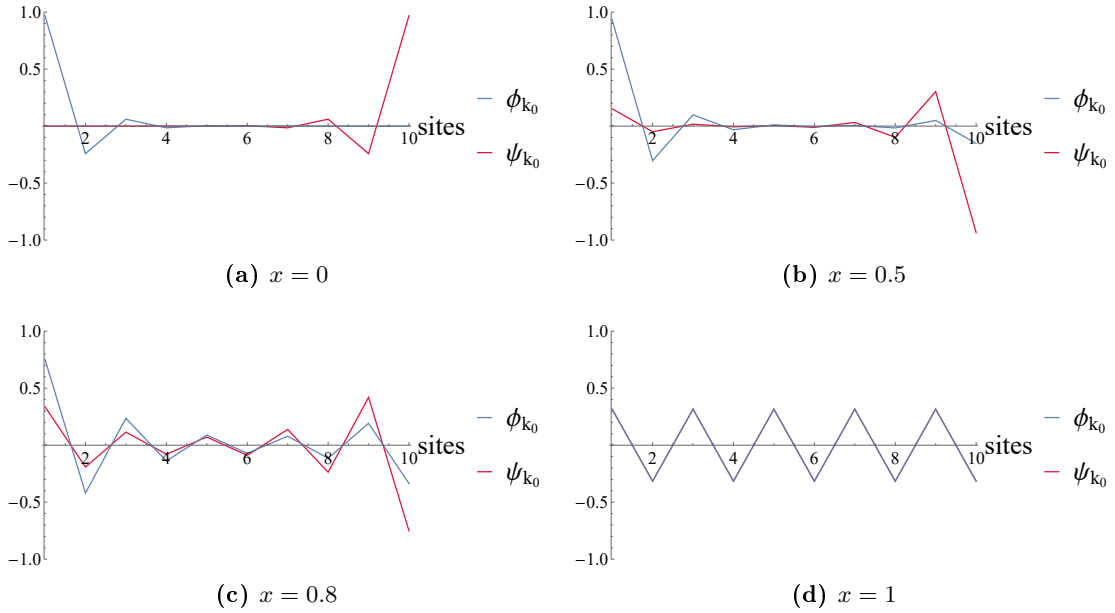

(a) $x = 0$ **(b)** $x = 0.5$

(c) $x = 0.8$ **(d)** $x = 1$

Figure 4.7: Majorana tails $\phi_{k_0 j}$ (blue) and $\psi_{k_0 j}$ (red) for $N = 10, t = \Delta = 1, \mu = 0.5$ and different values of x.

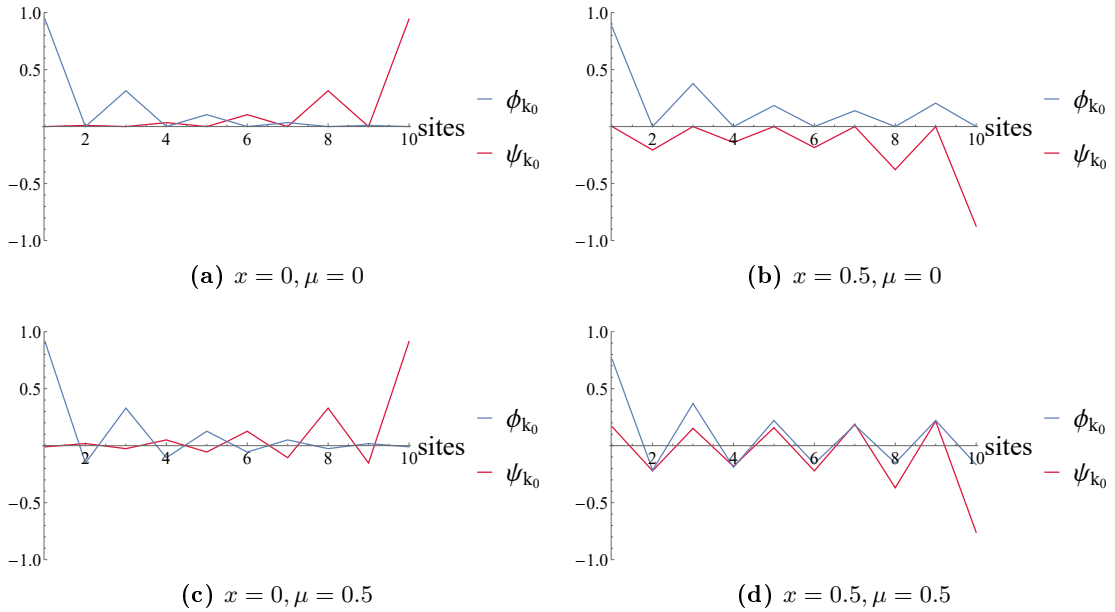

(a) $x = 0, \mu = 0$ **(b)** $x = 0.5, \mu = 0$

(c) $x = 0, \mu = 0.5$ **(d)** $x = 0.5, \mu = 0.5$

Figure 4.8: Majorana tails for $N = 10, t = 1, \Delta = 2$ and different values of x and μ.

periodic boundary conditions case and the simplest non-trivial one will be analyzed analytically. At the end of the chapter instead, a numerical analysis will be performed for a large number of situations.
Let us recall that, in the complex case, we have to consider the Toeplitz matrices

$$A = \begin{pmatrix} -\mu & -t & & & & -xt^* \\ -t^* & -\mu & \ddots & & & \\ & \ddots & \ddots & \ddots & & \\ & & \ddots & \ddots & \ddots & \\ & & & \ddots & -\mu & -t \\ -xt & & & & -t^* & -\mu \end{pmatrix} \quad B = \begin{pmatrix} 0 & \Delta & & & & -x\Delta \\ -\Delta & 0 & \ddots & & & \\ & \ddots & \ddots & \ddots & & \\ & & \ddots & \ddots & \ddots & \\ & & & \ddots & 0 & \Delta \\ x\Delta & & & & -\Delta & 0 \end{pmatrix} \tag{4.71}$$

where $t = |t|e^{i\theta}, \Delta = |\Delta|e^{i\phi}$.

4.3.1 Bogoliubov transformation with complex operators

In the case of periodic boundary conditions ($x = 1$), the Hamiltonian can be diagonalized through the Fourier transform and the Bogoliubov rotation extending the standard procedure carried out for the XY model (see Section 1.4). In this case, there are no edge states but the following analysis is very useful because, from the explicit form of the eigenvalues, we can understand how the complex parameters of the Hamiltonian can affect the phase transition.

For PBCs, the complex Kitaev Hamiltonian (2.1) becomes

$$H = \sum_{j=1}^{N} [-tc_j^\dagger c_{j+1} - t^* c_{j+1}^\dagger c_j - \mu c_j^\dagger c_j + \Delta c_j^\dagger c_{j+1}^\dagger + \Delta^* c_{j+1} c_j] \tag{4.72}$$

where

$$c_{j+N} \equiv c_j \tag{4.73}$$

Given that Fourier transforms are defined as

$$c_j = \frac{e^{i\frac{\pi}{4}}}{\sqrt{N}} \sum_k e^{ikj} c_k \qquad\qquad c_k = \frac{e^{-i\frac{\pi}{4}}}{\sqrt{N}} \sum_j e^{-ikj} c_j \tag{4.74}$$

with

$$k = \frac{2\pi q}{N} \qquad\qquad q = 0, ..., N-1 \tag{4.75}$$

the Hamiltonian can be rewritten as

$$\begin{aligned} H = \frac{1}{2} \sum_k [&(-2|t| \cos(k+\theta) - \mu) c_k^\dagger c_k + (-2|t| \cos(k-\theta) - \mu) c_{-k}^\dagger c_{-k} \\ &+ 2|\Delta| e^{i\phi} (\sin k) c_k^\dagger c_{-k}^\dagger + 2|\Delta| e^{-i\phi} (\sin k) c_{-k} c_k] \end{aligned} \tag{4.76}$$

which can be expressed in matrix form

$$H = \frac{1}{2} \sum_k \begin{pmatrix} c_k^\dagger & c_{-k} \end{pmatrix} \begin{pmatrix} -2|t| \cos(k+\theta) - \mu & 2|\Delta| e^{i\phi} \sin k \\ 2|\Delta| e^{-i\phi} \sin k & 2|t| \cos(k-\theta) + \mu \end{pmatrix} \begin{pmatrix} c_k \\ c_{-k}^\dagger \end{pmatrix} \tag{4.77}$$

The eigenvalues are

$$\Lambda_k = 2|t| \sin k \sin\theta \pm \sqrt{(2|t| \cos k \cos\theta + \mu)^2 + 4|\Delta|^2 \sin^2 k} \tag{4.78}$$

where $k = 2\pi q/N, q = 0, ..., N-1$. For $N \to \infty$ the values of k fill continuously the interval $[0, 2\pi]$. Instead if the previous function is considered in the interval $[-\pi, \pi]$ then the values of k must be taken as

$$k = \frac{2\pi q}{N} \qquad \begin{cases} q = -\frac{N}{2}, ..., \frac{N}{2} - 1 & N \text{ even} \\ q = -\frac{N-1}{2}, ..., \frac{N-1}{2} & N \text{ odd} \end{cases} \tag{4.79}$$

As expected, the spectrum doesn't depend on the phase ϕ.
However from equations (2.11), which hold for generic boundary conditions, we can show that although the eigenvalues don't depend on the phase ϕ the coefficients g_{ki} and h_{ki} do. If $\Delta \to |\Delta| e^{i\phi}$ with $\Delta = |\Delta|$ the LSM equations for the new coefficients g'_{ki}, h'_{ki} become

$$\begin{cases} A^* \vec{g'_k} + B^* e^{-i\phi} \vec{h'_k} = \Lambda_k \vec{g'_k} \\ -A \vec{h'_k} - B e^{i\phi} \vec{g'_k} = \Lambda_k \vec{h'_k} \end{cases} \tag{4.80}$$

and so, up to an overall constant, $g' = e^{-i\phi} g$ and $h' = h$.
The Hamiltonian (4.77) can be diagonalized through the Bogoliubov transformation

$$\begin{pmatrix} c_k \\ c^\dagger_{-k} \end{pmatrix} = \begin{pmatrix} \cos\theta_k & e^{i\phi}\sin\theta_k \\ -e^{-i\phi}\sin\theta_k & \cos\theta_k \end{pmatrix} \begin{pmatrix} \eta_k \\ \eta^\dagger_{-k} \end{pmatrix} \tag{4.81}$$

whose inverse is

$$\begin{cases} \eta_k = \cos\theta_k c_k - e^{i\phi}\sin\theta_k c^\dagger_{-k} & \text{(4.82a)} \\ \eta^\dagger_{-k} = e^{-i\phi}\sin\theta_k c_k + \cos\theta_k c^\dagger_{-k} & \text{(4.82b)} \end{cases}$$

with

$$\theta_k = \frac{1}{2}\arctan\left(\frac{2|\Delta|\sin k}{\mu + 2|t|\cos\theta\cos k}\right) \tag{4.83}$$

In this case, unlike the real case, the eigenvaules Λ_k and $-\Lambda_{-k}$ have different values as well as different signs. In terms of the Bogoliubov quasi-particles the Hamiltonian describes free fermions

$$H = \frac{1}{2}\sum_k [\Lambda_k \eta^\dagger_k \eta_k - \Lambda_{-k}\eta_{-k}\eta^\dagger_{-k}] = \sum_k [\Lambda_k(\eta^\dagger_k\eta_k - \frac{1}{2})] \tag{4.84}$$

Using the relations (4.82a), (4.74) the LSM coefficients g_{kj} and h_{kj} for periodic boundary conditions can be written as

$$\begin{cases} g_{kj} = \dfrac{e^{-\frac{i\pi}{4}}}{\sqrt{N}} e^{-ikj}\cos\theta_k & \text{(4.85a)} \\ h_{kj} = -e^{i\phi}\dfrac{e^{\frac{i\pi}{4}}}{\sqrt{N}} e^{-ikj}\sin\theta_k & \text{(4.85b)} \end{cases}$$

Since the spectrum is always positive one obtains that the previous rotation is correct only if $\mu + 2|t|\cos\theta\cos k < 0$.
If $\mu + 2|t|\cos\theta\cos k > 0$ then η_k and $\eta^\dagger_k$ are exchanged and so the replacement $g \to h^*, h \to g^*$ must be performed.
The ground state of the model is defined by

$$\eta_k|GS\rangle = 0 \qquad k = \frac{2\pi q}{N},\ q = 0, ..., N-1 \tag{4.86}$$

Instead the vacuum state is defined by the relations

$$c_k|0\rangle = 0 \qquad k = \frac{2\pi q}{N},\ q = 0, ..., N-1 \tag{4.87}$$

Imposing (4.86) one obtains that the ground state in terms of physical fermions can be written as

$$|GS\rangle = \prod_{q=1}^{[N/2]} (\cos\theta_{k_q} + e^{i\phi}\sin\theta_{k_q} c^\dagger_{k_q} c^\dagger_{-k_q})|0\rangle \tag{4.88}$$

where $[x]$ is the integer part of x.
If we perform the global gauge $U(1)$ transformation $c_j \to e^{-i\phi}c_j$ on the Hamiltonian, the BCS term $\Delta c_j^\dagger c_{j+1}^\dagger$ acquires an additional phase equal to 2ϕ.
Thus, as expected, we see that in the ground state to global gauge $U(1)$ symmetry is broken into the $\mathbb{Z}_2$ symmetry.
The same analysis can be done using antiperiodic boundary conditions. The results are similar.

4.3.2 Case 1: $|t| = |\Delta| = 1, x = 0, \mu = 0, \theta \neq 0, \phi = 0$

Let's consider the simplest non-trivial case $|t| = |\Delta| = 1, x = 0, \mu = 0, \theta \neq 0, \phi = 0$ where the explicit form of the matrices (2.46) is

$$\mathcal{M}_{11} = \begin{pmatrix} a+c & 0 & b & & & & & & \\ 0 & a & 0 & \ddots & & & & & \\ b & 0 & a & \ddots & \ddots & & & & \\ & \ddots & \ddots & \ddots & \ddots & \ddots & & & \\ & & \ddots & \ddots & \ddots & \ddots & \ddots & & \\ & & & \ddots & \ddots & a & 0 & b & \\ & & & & \ddots & 0 & a & 0 & \\ & & & & & b & 0 & a+d & \end{pmatrix} \tag{4.89}$$

having set

$$\begin{cases} a = 4 \\ b = -2\sin^2\theta \\ c = -2 + 2\cos\theta \\ d = -(2 + 2\cos\theta) \end{cases} \tag{4.90}$$

and

$$\mathcal{M}_{12} = \begin{pmatrix} e+f & 0 & g & & & & & & \\ 0 & e & 0 & \ddots & & & & & \\ h & 0 & e & \ddots & \ddots & & & & \\ & \ddots & \ddots & \ddots & \ddots & \ddots & & & \\ & & \ddots & \ddots & \ddots & \ddots & \ddots & & \\ & & & \ddots & \ddots & e & 0 & g & \\ & & & & \ddots & 0 & e & 0 & \\ & & & & & h & 0 & e+f & \end{pmatrix} \tag{4.91}$$

where

$$\begin{cases} e = -4\sin\theta \\ f = 2\sin\theta \\ g = 2\sin\theta(1+\cos\theta) \\ h = 2\sin\theta(1-\cos\theta) \end{cases} \tag{4.92}$$

The ansatz for the eigenvalue equations (2.44) is the $2N$ dimensional vector

$$\begin{pmatrix} z_R \\ z_I \end{pmatrix} = \begin{pmatrix} \alpha e^{ikj} + \beta e^{-ikj} \\ \rho e^{ikj} + \sigma e^{-ikj} \end{pmatrix} \tag{4.93}$$

where $j = 1, ..., N$.
Owing to the block structure of the matrix $\mathbb{W}$, the first eigenvalue problem in (2.44) splits into two sets of bulk equations related to the rows j and $N+j$, for $j = 3, \cdots, N-3$, and in four boundary equations for the rows $j = 1, 2, N+1, N+2$.
The first set of bulk equations gives

$$\begin{aligned} \Lambda_k^2(\alpha e^{ikj} + \beta e^{-ikj}) =& (-4\sin^2\theta\cos 2k + 4)(\alpha e^{ikj} + \beta e^{-ikj}) \\ &+ (4\sin\theta\cos 2k - 4\sin\theta)(\rho e^{ikj} + \sigma e^{-ikj}) \\ &+ (4i\cos\theta\sin\theta\sin 2k)(\rho e^{ikj} - \sigma e^{-ikj}) \end{aligned} \tag{4.94}$$

It is then possible to separate the real and the imaginary part of e^{ikj}, namely

$$e^{ikj} = \cos kj + i\sin kj \tag{4.95}$$

so, remembering that $\cos kj$ and $\sin kj$ are two linearly independent functions, we can easily derive two equations from (4.94):

$$\begin{aligned} \Lambda_k^2(\alpha+\beta) =& (-4\sin^2\theta\cos 2k + 4)(\alpha+\beta) + (4\sin\theta\cos 2k - 4\sin\theta)(\rho+\sigma) \\ &+ (4i\cos\theta\sin\theta\sin 2k)(\rho-\sigma) \end{aligned} \tag{4.96}$$

$$\begin{aligned} \Lambda_k^2(\alpha-\beta) =& (-4\sin^2\theta\cos 2k + 4)(\alpha-\beta) + (4\sin\theta\cos 2k - 4\sin\theta)(\rho-\sigma) \\ &+ (4i\cos\theta\sin\theta\sin 2k)(\rho+\sigma) \end{aligned} \tag{4.97}$$

The second set of bulk equations gives

$$\begin{aligned} \Lambda_k^2(\rho e^{ikj} + \sigma e^{-ikj}) =& (4\sin\theta\cos 2k - 4\sin\theta)(\alpha e^{ikj} + \beta e^{-ikj}) \\ &+ (-4i\cos\theta\sin\theta\sin 2k)(\alpha e^{ikj} - \beta e^{-ikj}) \\ &+ (-4\sin^2\theta\cos 2k + 4)(\rho e^{ikj} + \sigma e^{-ikj}) \end{aligned} \tag{4.98}$$

which, repeating the same steps, are equivalent to:

$$\begin{aligned} \Lambda_k^2(\rho+\sigma) =& (4\sin\theta\cos 2k - 4\sin\theta)(\alpha+\beta) + (-4i\cos\theta\sin\theta\sin 2k)(\alpha-\beta) \\ &+ (-4\sin^2\theta\cos 2k + 4)(\rho+\sigma) \end{aligned} \tag{4.99}$$

$$\begin{aligned} \Lambda_k^2(\rho-\sigma) =& (4\sin\theta\cos 2k - 4\sin\theta)(\alpha-\beta) + (-4i\cos\theta\sin\theta\sin 2k)(\alpha+\beta) \\ &+ (-4\sin^2\theta\cos 2k + 4)(\rho-\sigma) \end{aligned} \tag{4.100}$$

Adding (4.96) to (4.97) and (4.99) to (4.100), we get the following equivalent equations, written in matrix notation:

$$\begin{pmatrix} -4\sin^2\theta\cos 2k+4 & 4\sin\theta\cos 2k-4\sin\theta+4i\cos\theta\sin\theta\sin 2k \\ 4\sin\theta\cos 2k-4\sin\theta-4i\cos\theta\sin\theta\sin 2k & -4\sin^2\theta\cos 2k+4 \end{pmatrix}\begin{pmatrix}\alpha\\ \rho\end{pmatrix} = \Lambda_k^2\begin{pmatrix}\alpha\\ \rho\end{pmatrix} \tag{4.101}$$

The solutions of the secular equation are

$$\Lambda_k^2 = (2\sin k\sin\theta \pm \sqrt{4\cos^2 k\cos^2\theta + 4\sin^2 k})^2 \tag{4.102}$$

The previous equation, as expected, coincides with the result (4.78) if $|t| = |\Delta| = 1, \mu = 0$.
Ideed, it can be demonstrated, starting from the eigenvalue equations (2.44) and taking as ansatz for the eigenvectors a linear combination of plane waves, that the functional form of the eigenvalues, for generic boundary conditions and values of the model parameters, is exactly the one in (4.78). However, in general, the values of k can be determined by solving non-simple transcendental equations.
Since the physics of the model is the same for odd and even N and the eigenvector solution is in general very complicated, in the following we consider the case N odd for which the eigenvectors can be written in a simpler form.
There are 5 possible different set of solutions (if $\theta \neq \pi/2$)

1. For the first case, we can write

$$\begin{pmatrix} z_R \\ z_I \end{pmatrix} = \begin{pmatrix} \gamma(\sin kj+\sin(k+\pi)j)+\delta(\cos kj+\cos(k+\pi)j) \\ \gamma(\sin k(N+1-j)+\sin(k+\pi)(N+1-j))+\delta(\cos k(N+1-j)+\cos(k+\pi)(N+1-j)) \end{pmatrix} \tag{4.103}$$

where the ratio of the two coefficients $\xi \equiv \delta/\gamma$ is

$$\xi = (-1)\frac{(a-\Lambda_k^2)\sin 2k + b\sin 4k + e\sin k(N-1) + g\sin k(N-3)}{(a-\Lambda_k^2)\cos 2k + b\cos 4k + e\cos k(N-1) + g\cos k(N-3)} \tag{4.104}$$

The solutions for k can be found by solving the boundary condition:

$$\begin{aligned}\Lambda_k^2(\sin k(N-1) + \xi\cos k(N-1)) = {} & e(\sin 2k + \xi\cos 2k) \\ & + h(\sin 4k + \xi\cos 4k) \\ & + a(\sin k(N-1) + \xi\cos k(N-1)) \\ & + b(\sin k(N-3) + \xi\cos k(N-3))\end{aligned} \tag{4.105}$$

2. The second set of solutions is obtained by taking

$$\begin{pmatrix} z_R \\ z_I \end{pmatrix} = \begin{pmatrix} \gamma(\sin kj+\sin(k+\pi)j)+\delta(\cos kj+\cos(k+\pi)j) \\ -\gamma(\sin k(N+1-j)+\sin(k+\pi)(N+1-j))-\delta(\cos k(N+1-j)+\cos(k+\pi)(N+1-j)) \end{pmatrix} \tag{4.106}$$

We get ($\xi \equiv \delta/\gamma$)

$$\xi = (-1)\frac{(a-\Lambda_k^2)\sin 2k + b\sin 4k - e\sin k(N-1) - g\sin k(N-3)}{(a-\Lambda_k^2)\cos 2k + b\cos 4k - e\cos k(N-1) - g\cos k(N-3)} \tag{4.107}$$

The k are fixed now by the equation:

$$\begin{aligned}-\Lambda_k^2(\sin k(N-1)+\xi\cos k(N-1)) &= e(\sin 2k+\xi\cos 2k)\\ &+ h(\sin 4k+\xi\cos 4k)\\ &- a(\sin k(N-1)+\xi\cos k(N-1))\\ &- b(\sin k(N-3)+\xi\cos k(N-3))\end{aligned} \tag{4.108}$$

3. The third set of solutions is of the form

$$\begin{pmatrix} z_R \\ z_I \end{pmatrix} = \begin{pmatrix} \gamma(\sin kj-\sin(k+\pi)j)+\delta(\cos kj-\cos(k+\pi)j) \\ \gamma(\sin k(N+1-j)-\sin(k+\pi)(N+1-j))+\delta(\cos k(L+1-j)-\cos(k+\pi)(N+1-j)) \end{pmatrix} \tag{4.109}$$

Then we obtain ($\xi \equiv \delta/\gamma$)

$$\xi = (-1)\frac{(a+c-\Lambda_k^2)\sin k + b\sin 3k + (e+f)\sin kN + g\sin k(N-2)}{(a+c-\Lambda_k^2)\cos k + b\cos 3k + (e+f)\cos kN + g\cos k(N-2)} \tag{4.110}$$

The equation for k is

$$\begin{aligned}\Lambda_k^2(\sin kN+\xi\cos kN) &= (e+f)(\sin k+\xi\cos k)\\ &+ h(\sin 3k+\xi\cos 3k)\\ &+ (a+d)(\sin kN+\xi\cos kN)\\ &+ b(\sin k(N-2)+\xi\cos k(N-2))\end{aligned} \tag{4.111}$$

4. The fourth set of solution is

$$\begin{pmatrix} z_R \\ z_I \end{pmatrix} = \begin{pmatrix} \gamma(\sin kj-\sin(k+\pi)j)+\delta(\cos kj-\cos(k+\pi)j) \\ -\gamma(\sin k(N+1-j)-\sin(k+\pi)(N+1-j))-\delta(\cos k(N+1-j)-\cos(k+\pi)(N+1-j)) \end{pmatrix} \tag{4.112}$$

with ($\xi \equiv \delta/\gamma$)

$$\xi = (-1)\frac{(a+c-\Lambda_k^2)\sin k + b\sin 3k - (e+f)\sin kN - g\sin k(N-2)}{(a+c-\Lambda_k^2)\cos k + b\cos 3k - (e+f)\cos kN - g\cos k(N-2)} \tag{4.113}$$

The equation for k is

$$\begin{aligned}-\Lambda_k^2(\sin kN+\xi\cos kN) &= (e+f)(\sin k+\xi\cos k)\\ &+ h(\sin 3k+\xi\cos 3k)\\ &- (a+d)(\sin kN+\xi\cos kN)\\ &- b(\sin k(N-2)+\xi\cos k(N-2))\end{aligned} \tag{4.114}$$

5. There are also two boundary states (in the complex case the spectrum is doubly degenerate) of the form

$$\begin{pmatrix} z_R \\ z_I \end{pmatrix} = \begin{pmatrix} 0 \\ \vdots \\ 1 \\ 0 \\ \vdots \\ -b/g \end{pmatrix} \qquad \begin{pmatrix} z_R \\ z_I \end{pmatrix} = \begin{pmatrix} -b/g \\ \vdots \\ 0 \\ 1 \\ \vdots \\ 0 \end{pmatrix} \tag{4.115}$$

with zero energy.

The vectors w_R and w_I differ from z_R and z_I only by the vector index exchange $j \to N - j + 1$. Then we can find the coefficients g and h through the relations (2.50). However, since the spectrum is doubly degenerate, the coefficients of the linear combination of the eigenvectors belonging to the same eigenspace must be determined numerically.

4.3.3 Numerical analysis of the complex Kitaev model

As previously discussed, the analytical solution of the complex case for arbitrary values of the parameters is very difficult. Nevertheless, the Hamiltonian can be easily diagonalized numerically with the methods developed in chapter 2. Let's consider the Hamiltonian of the complex Kitaev model for generic boundary conditions (2.1).
The functional form of the eigenvalues is (see the previous section)

$$\Lambda_k = 2|t| \sin k \sin\theta + \sqrt{(2|t| \cos k \cos\theta + \mu)^2 + 4|\Delta|^2 \sin^2 k} \tag{4.116}$$

where, in general, the values of k are determined by solving transcendental equations.
Several comments are now in order.
The energy levels don't depend on the phase ϕ because it can be removed by the global gauge transformation $c_j \to c_j e^{i\frac{\phi}{2}}$. Moreover if $\Delta = 0, x = 0$ the energy levels don't depend also on θ as can be seen by performing the $U(1)$ local gauge transformation $c_j \to c_j e^{-i\theta j}$.
If $x \neq 0$ or $\Delta \neq 0$ the phase θ can no longer be removed by a $U(1)$ local gauge transformation. From (4.116) it is easy to see that the gap closes at the point $|\mu| = |2t \cos\theta|$ for $k = \pi$ or $k = -\pi$ signaling a phase transition. Indeed for $|\mu| < |2t \cos\theta|$ the model is in the topological phase; for $|\mu| > |2t \cos\theta|$ it is in the trivial phase.

Fig. 4.9 shows the energy levels for open boundary conditions as a function of μ for different values of θ. The numerical data confirm that the gap closes at $|\mu| = |2t \cos\theta|$ and that in the region $|\mu| < |2t \cos\theta|$ a zero-mode is present.

Fig. 4.10 shows instead the energy levels for $x = 0.3$. As expected, the point of the phase transition does not change, but the zero-mode acquires a mass becoming a Dirac mode.

Fig. 4.11 represents the case $|t| = |\Delta| = 1$ for $\theta \in [0, 2\pi]$. The transition point is $|\mu| = |2t \cos\theta|$ and then when $\arccos(|\mu|/2|t|) < \theta < \pi - \arccos(|\mu|/2|t|)$ the edge state goes inside the bulk band.
Let's consider the real limits $\theta = 0$ and $\theta = \pi$ where $t = |t|$ and $t = -|t|$ respectively. In this situation, the eigenvalues are have the form (4.4). If $x = 0$ the equation that fix k is (4.22) and if $t \to -t$ then $k \to k + \pi$ and therefore the eigenvalues don't change. Instead, if $x \neq 0$ the equation that must be considered is (4.19). If N is even the same reasoning done above holds. For N odd instead the levels are slightly shifted but the general structure doesn't change.

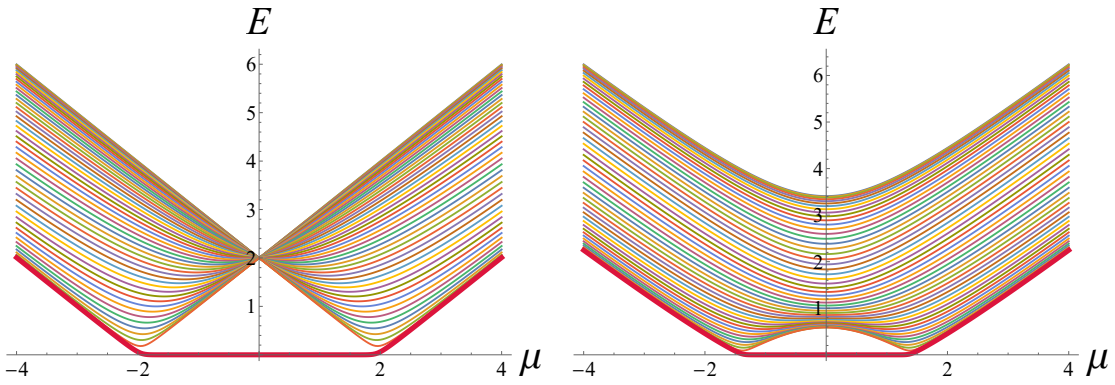

(a) $\theta = 0$ **(b)** $\theta = \frac{\pi}{4}$

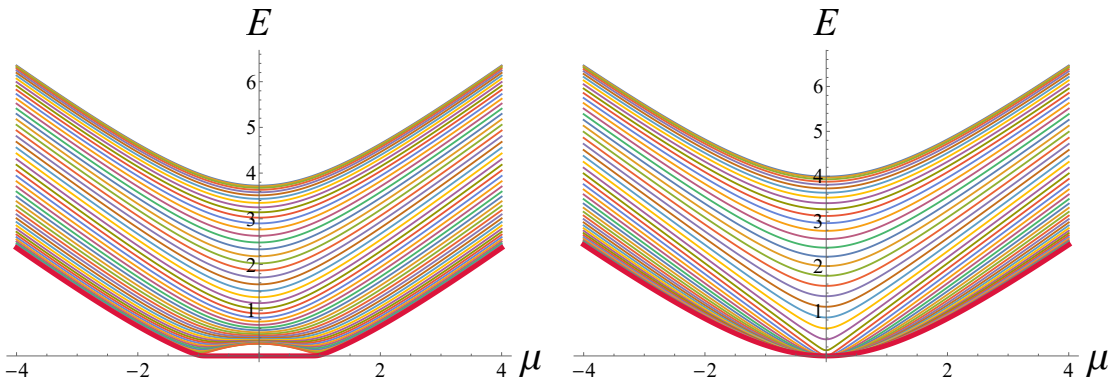

(c) $\theta = \frac{\pi}{3}$ **(d)** $\theta = \frac{\pi}{2}$

Figure 4.9: The graphs represent the energy levels as a function of μ for $N = 50, |t| = |\Delta| = 1, \phi = 0, x = 0$ and different values of θ.

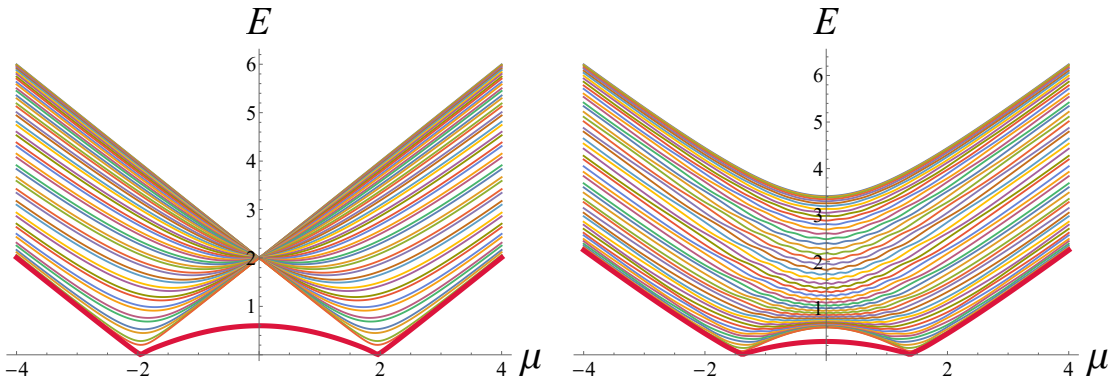

(a) $\theta = 0$

(b) $\theta = \frac{\pi}{4}$

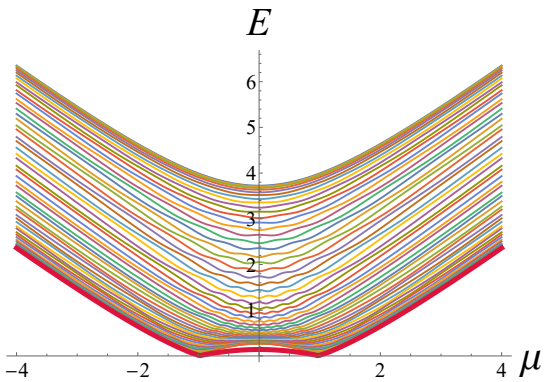

(c) $\theta = \frac{\pi}{3}$

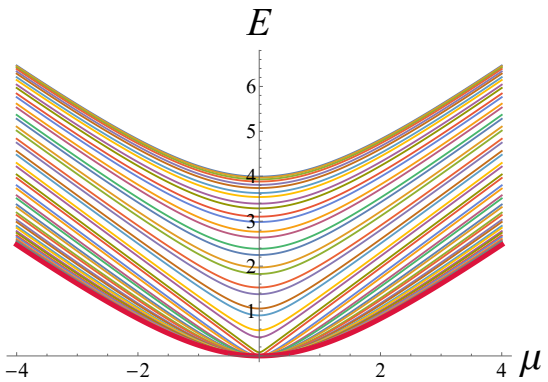

(d) $\theta = \frac{\pi}{2}$

Figure 4.10: The graphs represent the energy levels as a function of μ for $N = 50, |t| = |\Delta| = 1, \phi = 0, x = 0.3$ and different values of θ.

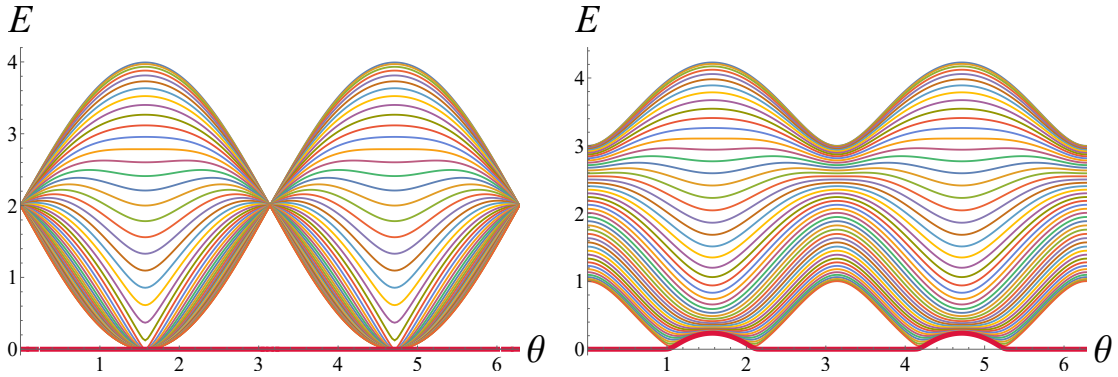

(a) $\mu = 0, x = 0$ **(b)** $\mu = 1, x = 0$

(c) $\mu = 1, x = 0.5$ **(d)** $\mu = 1, x = 1$

Figure 4.11: Energy levels as a function of θ for $N = 50, |t| = |\Delta| = 1, \phi = 0$ and different values of μ and x.

Chapter 5

Quantum correlations in complex fermionic systems

5.1 Correlation functions for the complex Kitaev model

Correlation functions are powerful tools useful to understand different thermodynamic aspects of quantum many-body systems. They measure the order of a system and describe how microscopic variables, such as spin and density, at different positions are related. The Kitaev model is a short-range model and therefore from the general theory, the two-point correlators in the gapped phase should have an exponential decay with the distance. Instead, at the critical point, the model becomes scale-invariant and the correlation functions should have a power-law decay. In the first part of this section we will analyze the behaviors of the correlators for finite chain, generic boundary conditions and for different values of the Hamiltonian parameters. In the second part we will obtain some integral expressions for the correlation functions in the thermodynamic limit and we will evaluate their behavior both outside and inside the critical point.

5.1.1 Finite chain behavior of the correlation functions

The two-point standard and anomalous correlation functions are defined as

$$\mathbb{C}_{ij} \equiv \langle GS|c_i^\dagger c_j|GS\rangle \tag{5.1}$$

$$\mathbb{F}_{ij} \equiv \langle GS|c_i^\dagger c_j^\dagger|GS\rangle \tag{5.2}$$

A simple explicit expression of the correlators $\mathbb{C}_{ij}$ and $\mathbb{F}_{ij}$ in terms of the LSM coefficients g_{ki} and h_{ki} can be obtained. Inverting equation (2.9) one finds

$$\begin{pmatrix} c \\ c^\dagger \end{pmatrix} = U \begin{pmatrix} \eta \\ \eta^\dagger \end{pmatrix} \quad U = \begin{pmatrix} \vec{g}_1^* & \cdots & \vec{g}_N^* & \vec{h}_1 & \cdots & \vec{h}_N \\ \vec{h}_1^* & \cdots & \vec{h}_N^* & \vec{g}_1 & \cdots & \vec{g}_N \end{pmatrix} \tag{5.3}$$

and thus the following relations hold

$$c_i = \sum_k [g^*_{ki}\eta_k + h_{ki}\eta^\dagger_k] \tag{5.4}$$

$$c^\dagger_i = \sum_k [g_{ki}\eta^\dagger_k + h^*_{ki}\eta_k] \tag{5.5}$$

Thus, the two-point fermionic correlators can be written as

$$\mathbb{C}_{ij} = \sum_k h^*_{ki}h_{kj} \tag{5.6}$$

$$\mathbb{F}_{ij} = \sum_k h^*_{ki}g_{kj} \tag{5.7}$$

The previous equations are valid for a generic quadratic fermionic Hamiltonian and not only for the Kitaev model.
Owing to the fermionic anticommutation rules, the matrix $\mathbb{C}_{ij}$ is Hermitian and $\mathbb{F}_{ij}$ is antisymmetric.
Then, using the results of the chapters 3 and 4, we can write the analytical expressions of the correlation functions of the Kitaev model for finite chain, generic boundary conditions and for almost all the values of t,Δ and μ (at least in the real case).
Fig. 5.1 shows the correlations $|\mathbb{C}_{ij}|$ between the sites $i = 1$ and $j = 2, .., N$ in the real case for different values of x and μ.
In the topological phase, the correlations between the first and the last sites are different from zero because there is a non-local fermion i.e. an eigenstate of the Hamiltonian, that couples the edges of the chain.
Indeed in this phase the coefficients $h_{k_0 i}$ are peaked at the end of the chain (they can be written in terms of hyperbolic functions) and they give a high contribution to the summation if $i \sim 1$ and $j \sim N$.
In the limit $x = 1$ the correlations are symmetric around the center of the chain.
Using the explicit expression of the coefficients g_{ki} and h_{ki} it can be demonstrated that also the anomalous correlation function $|\mathbb{F}_{ij}|$ follows the same behavior of $\mathbb{C}_{ij}$ with the distance.
If t and Δ are complex parameters $\mathbb{C}_{ij}$ and $\mathbb{F}_{ij}$ are generally complex and so in order to observe the behavior of the correlations between the lattice sites the complex modulus of $\mathbb{C}_{ij}$ and $\mathbb{F}_{ij}$ must be taken.
In this case the point of transition between the topological phase and the trivial phase is shifted to the value $|\mu| = |2t\cos\theta|$ (see Fig. 5.2).
We can obtain some simple analytical expressions for PBCs ($x = 1$) of $\mathbb{C}_{ij}$ and $\mathbb{F}_{ij}$. Using (4.85) we obtain

$$\mathbb{C}_{ij} = \frac{1}{N}\sum_k \frac{1 \mp \cos(2\theta_k)}{2} e^{\pm ik(i-j)} \tag{5.8}$$

$$\mathbb{F}_{ij} = \frac{ie^{-i\phi}}{N}\sum_k \frac{\sin(2\theta_k)}{2} e^{\pm ik(i-j)} \tag{5.9}$$

where, due to the fact that, as previously explained, the spectrum is always defined positive , the upper sign is valid when $\mu + 2|t|\cos\theta\cos k < 0$ and the lower sign when $\mu + 2|t|\cos\theta\cos k > 0$.

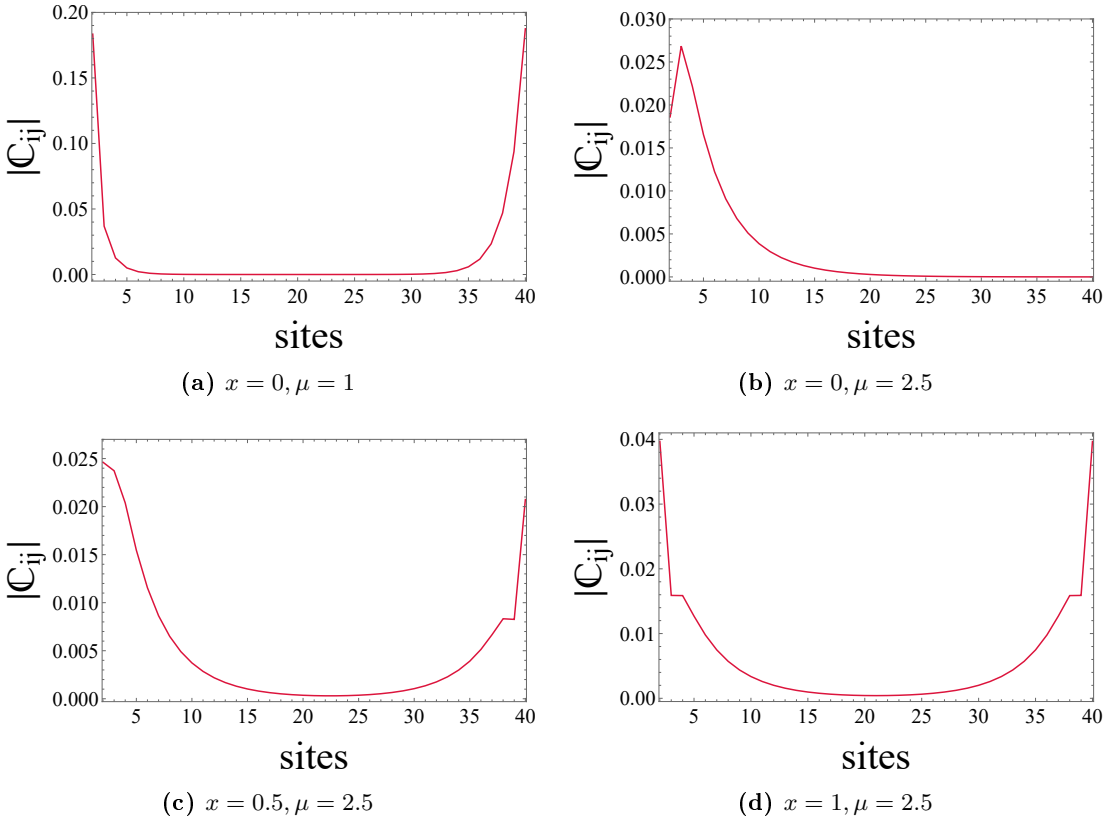

(a) $x = 0, \mu = 1$ **(b)** $x = 0, \mu = 2.5$

(c) $x = 0.5, \mu = 2.5$ **(d)** $x = 1, \mu = 2.5$

Figure 5.1: Behavior of $\mathbb{C}_{ij}$ in the real case for $N = 40$, $|t| = |\Delta| = 1$, $\theta = \phi = 0$ and different values of x and μ.

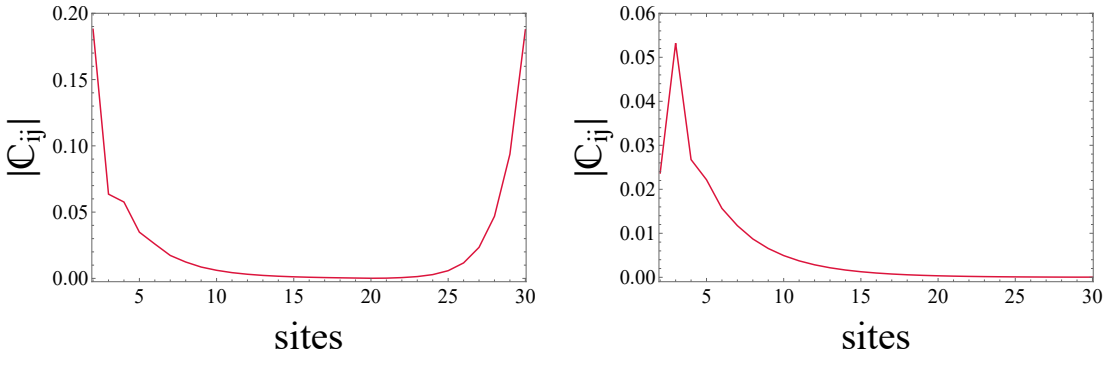

(a) $x = 0, \mu = 0.5$ **(b)** $x = 0, \mu = 1.5$

Figure 5.2: The graphs represent the behavior of $|\mathbb{C}_{ij}|$ for $|t| = |\Delta| = 1$, $x = 0$, $\theta = \frac{\pi}{3}$ and different values of μ.

5.1.2 Asympotic behaviour of the correlation functions

The asymptotic behavior of the correlation functions can be analyzed analytically by taking the thermodynamic limit of the periodic boundary expressions (5.8),(5.9) and solving the resulting integrals for $j \gg i$. In the thermodynamic limit where $N \to \infty$ equations (5.8), (5.9) become

$$\mathbb{C}_{ij} = \int_0^{2\pi} \frac{dk}{2\pi} \frac{1 \mp \cos(2\theta_k)}{2} e^{\pm ik(i-j)} = \frac{\delta_{ij}}{2} + \int_0^{2\pi} \frac{dk}{2\pi} \frac{\mp \cos(2\theta_k)}{2} e^{\pm ik(i-j)} \tag{5.10}$$

$$\mathbb{F}_{ij} = ie^{-i\phi} \int_0^{2\pi} \frac{dk}{2\pi} \frac{\sin(2\theta_k)}{2} e^{\pm ik(i-j)} \tag{5.11}$$

In this limit, obviously, the edge effects are no longer visible. If $\phi = 0$ both $\mathbb{C}_{ij}$ and $\mathbb{F}_{ij}$ are real. Moreover considering that $\theta_k \in [-\frac{\pi}{4}, \frac{\pi}{4}]$, $\cos(2\theta_k) = \frac{1}{\sqrt{1+\tan^2(2\theta_k)}}$ and $\sin(2\theta_k) = \frac{\tan(2\theta_k)}{\sqrt{1+\tan^2(2\theta_k)}}$ we obtain that

$$\cos 2\theta_k = \operatorname{sgn}(\mu + 2|t|\cos\theta\cos k) \frac{\mu + 2|t|\cos\theta\cos k}{\sqrt{(\mu + 2|t|\cos\theta\cos k)^2 + 4|\Delta|^2 \sin^2 k}} \tag{5.12}$$

$$\sin 2\theta_k = \operatorname{sgn}(\mu + 2|t|\cos\theta\cos k) \frac{2|\Delta|\sin k}{\sqrt{(\mu + 2|t|\cos\theta\cos k)^2 + 4|\Delta|^2 \sin^2 k}} \tag{5.13}$$

Therefore the correlation functions can be written as

$$\mathbb{C}_{ij} = \frac{\delta_{ij}}{2} + g(i-j) \tag{5.14}$$

$$\mathbb{F}_{ij} = ie^{-i\phi} \int_0^{2\pi} \frac{dk}{2\pi} \frac{2|\Delta|\sin k}{2\lambda(k)} e^{-ik(i-j)} \tag{5.15}$$

where

$$g(i-j) \equiv \int_0^{2\pi} \frac{dk}{2\pi} \frac{\mu + 2|t|\cos\theta\cos k}{2\lambda(k)} e^{-ik(i-j)}$$

and $\lambda(k) \equiv \sqrt{(\mu + 2|t|\cos\theta\cos k)^2 + 4|\Delta|^2 \sin^2 k}$. If $\theta \neq 0$ then, unlike the real case, $\lambda(k) \neq \Lambda_k$ where Λ_k are the eigenvalues (4.116) of the complex Kitaev Hamiltonian. The asymptotic behavior of the previous integrals can be evaluated by considering an integration contour in the complex plane. Let's consider the case $i < j$.
In this situation we follow the path in the upper half-plane shown in Fig. 5.3 in the limit $M \to \infty$ for which the contributions of the segments $C_\perp$ and $C'_\perp$ vanish.
The Cauchy Theorem implies that

$$g(i-j) = -\frac{1}{2\pi} \lim_{M\to\infty} \left(\int_{C_0} + \int_{L_-} + \int_{L_+} + \int_{C_{2\pi}} \right) dz e^{-iz(i-j)} G(z) \tag{5.16}$$

where

$$G(z) = \frac{\mu + 2|t|\cos\theta\cos z}{2\lambda(z)} \tag{5.17}$$

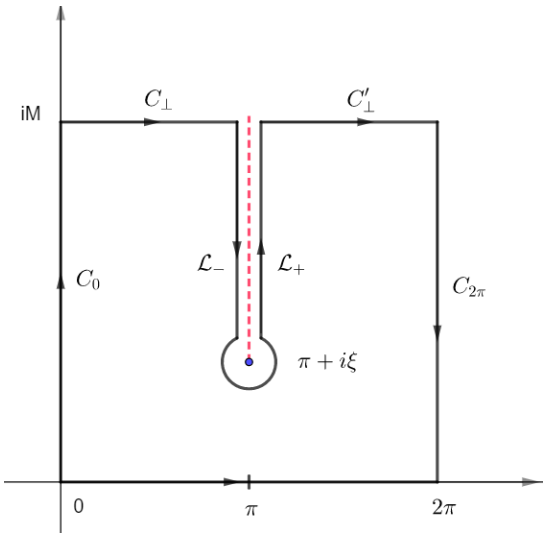

Figure 5.3: Integration contour in the complex plane used to evaluate the integrals (5.14) and (5.15). The red dashed line indicates the branch cut of the function $\lambda(z)$.

and $z = k + iy$.
If $|t|\cos\theta, \mu > 0$, the function $G(z)$ has one pole at the point $z = \pi + i\xi$ where ξ is the solution of

$$(2|t|\cos\theta\cosh\xi - \mu)^2 - 4|\Delta|^2\sinh^2\xi = 0 \tag{5.18}$$

The presence of this pole leads to a branch cut on the line $\pi + iy$ being the square root a two-valued function in the complex plane. The cut can be chosen in the following way

$$\lambda(z) = \begin{cases} i\sqrt{-(2|t|\cos\theta\cosh y - \mu)^2 + 4|\Delta|^2\sinh^2 y} & z = \pi^+ + iy, y > \xi \\ -i\sqrt{-(2|t|\cos\theta\cosh y - \mu)^2 + 4|\Delta|^2\sinh^2 y} & z = \pi^- + iy, y > \xi \end{cases} \tag{5.19}$$

The integrals along the paths C_0 and $C_{2\pi}$ are zero because the integrating functions are periodic with period 2π. Thus the function $g(i-j) \equiv g(R)$ where $R \equiv i - j$ can be written as

$$\begin{aligned} g(R) &= -2I_{L_+} \\ &= -e^{i\pi R}\int_\xi^\infty \frac{dy}{2\pi}\frac{(2|t|\cos\theta\cosh y - \mu)e^{-Ry}}{\sqrt{-(2|t|\cos\theta\cosh y - \mu)^2 + 4|\Delta|^2\sinh^2 y}} \end{aligned} \tag{5.20}$$

If $j \gg i$ and so $|R| \gg 1$ the integration function becomes exponentially small and is significantly different from zero only in the region near the point $y \sim \xi$.
To solve the integral, let's define the variable $k = y - \xi$. The condition $y \sim \xi$ implies that $k \sim 0$. In this limit, we can perform the following expansions:

$$-(2|t|\cos\theta\cosh(\xi + k) - \mu)^2 + 4|\Delta|^2\sinh^2(\xi + k) \simeq ak + bk^2 \tag{5.21}$$

where

$$a = \sinh 2\xi(4|\Delta|^2 - 4|t|^2\cos^2\theta) + 4|t|\mu\cos\theta\sinh\xi \tag{5.22}$$

$$b = \cosh 2\xi(4|\Delta|^2 - 4|t|^2\cos^2\theta) + 2|t|\mu\cos\theta\cosh\xi \tag{5.23}$$

so that

$$\begin{aligned}&\frac{(2|t|\cos\theta\cosh(\xi+k)-\mu)}{\sqrt{-(2|t|\cos\theta\cosh(\xi+k)-\mu)^2+4|\Delta|^2\sinh^2(\xi+k)}}\\ &\simeq \frac{2|t|\cos\theta\cosh\xi-\mu}{\sqrt{ak}} + \sqrt{k}\left(\frac{2|t|\cos\theta\sinh\xi}{\sqrt{a}} - \frac{b(2|t|\cos\theta\cosh\xi-\mu)}{2a^{\frac{3}{2}}}\right)\end{aligned} \tag{5.24}$$

Inserting this expansion in (5.20), using that [1]

$$\int_0^\infty e^{-yR}y^\alpha = \frac{\Gamma(\alpha+1)}{R^{\alpha+1}} \tag{5.25}$$

the leading contribution for large distances of $\mathbb{C}(R)$ is

$$\begin{aligned}\mathbb{C}(R) =& \frac{\delta_{R,0}}{2} - \frac{1}{2\sqrt{\pi R}}e^{i\pi R}e^{-R\xi}\left(\frac{2|t|\cos\theta\cosh\xi-\mu}{\sqrt{a}}\right)\\ &- \frac{1}{4\sqrt{\pi}R^{\frac{3}{2}}}e^{i\pi R}e^{-R\xi}\left(\frac{2|t|\cos\theta\sinh\xi}{\sqrt{a}} - \frac{b(2|t|\cos\theta\cosh\xi-\mu)}{2a^{\frac{3}{2}}}\right)\\ \simeq& \frac{\delta_{R,0}}{2} - \frac{1}{2\sqrt{\pi R}}e^{i\pi R}e^{-R\xi}\left(\frac{2|t|\cos\theta\cosh\xi-\mu}{\sqrt{a}}\right)\end{aligned} \tag{5.26}$$

Therefore, since $e^{i\pi R} = (-1)^R$, the correlation function $\mathbb{C}(R)$ is real.
The correlation length $\xi' = \frac{1}{\xi}$ can be found by inverting equation (5.18).
If $|t|\cos\theta = |\Delta|$ we obtain

$$\xi' = \frac{1}{\xi} = \left[\operatorname{arcosh}\left(\frac{4|t|^2\cos^2\theta+\mu^2}{4|t|\mu\cos\theta}\right)\right]^{-1} \tag{5.27}$$

Fig. 5.4 shows the correlator $\mathbb{C}_{ij}$ for different values of μ. From the previous formula we see that $\xi' \to 0$ if $\mu = 0$ or $\mu \to \infty$.
Indeed, if $\mu \to \infty$ only the term $H \sim -\mu\sum_i c_i^\dagger c_i$ is significant and then the Hamiltonian becomes local and has zero correlation length.

At the critical point $\mu = 2|t|\cos\theta$, from (5.27), we see that the correlation length ξ' diverges. In this case the function $g(R)$ reads

$$g(R) = -e^{i\pi R}\int_0^\infty \frac{dk}{2\pi}\frac{(2|t|\cos\theta\cosh k-\mu)e^{-Rk}}{\sqrt{-(2|t|\cos\theta\cosh k-\mu)^2+4|\Delta|^2\sinh^2 k}} \tag{5.28}$$

In the limit $k \ll 1$, using the following expansion

$$-(2|t|\cos\theta\cosh k-\mu)^2 + 4|\Delta|^2\sinh^2 k \simeq 4|\Delta|^2k^2 + ck^4 \tag{5.29}$$

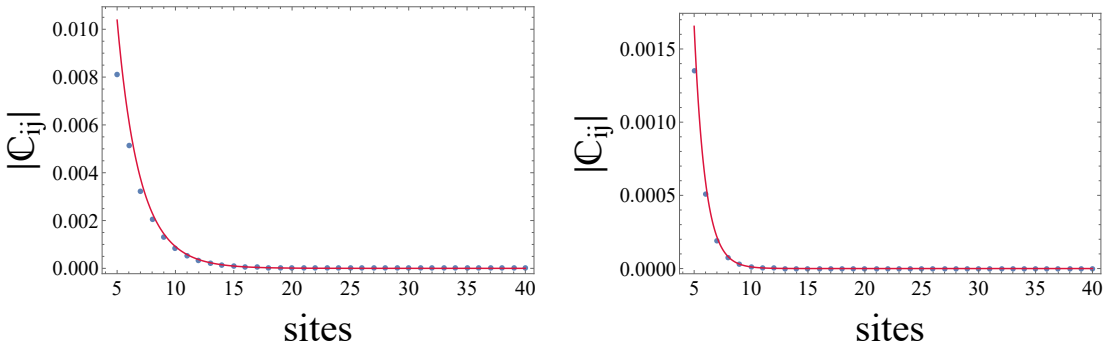

(a) $\mu = 3$ **(b)** $\mu = 5$

Figure 5.4: Plot of the correlation functions $|\mathbb{C}_{ij}|$ for $|t| = |\Delta| = 1$, $\theta = \phi = 0$, $N = 40$, $i = 1$ and $j = 5, ..., N$ for different values of μ.
The blue dots represent the values computed numerically form (5.14); the red line is the function (5.26).

where

$$c = \frac{4}{3}|\Delta|^2 - |t|^2 \cos^2\theta \tag{5.30}$$

we find that

$$\begin{aligned} &\frac{(2|t|\cos\theta\cosh k - \mu)}{\sqrt{-(2|t|\cos\theta\cosh k - \mu)^2 + 4|\Delta|^2\sinh^2 k}} \\ &\qquad \simeq k\frac{|t|\cos\theta}{2|\Delta|} + k^3\left(\frac{|t|\cos\theta}{24|\Delta|} - \frac{c|t|\cos\theta}{16|\Delta|^3}\right) \end{aligned} \tag{5.31}$$

Substituting the previous expansion in (5.28) it follows that the correlation function has the algebraic decay

$$\begin{aligned} \mathbb{C}_c(R) =& \frac{\delta_{R,0}}{2} - \frac{|t|\cos\theta}{4\pi|\Delta|}e^{i\pi R}\frac{1}{R^2} - \frac{3e^{i\pi R}}{\pi R^4}\left(\frac{|t|\cos\theta}{24|\Delta|} - \frac{c|t|\cos\theta}{16|\Delta|^3}\right) \\ \simeq& \frac{\delta_{R,0}}{2} - \frac{|t|\cos\theta}{4\pi|\Delta|}e^{i\pi R}\frac{1}{R^2} \end{aligned} \tag{5.32}$$

where the subscript c points out that the previous expression holds at the critical point.
The same analysis can be done for the anomalous correlator $\mathbb{F}(R)$.
Repeating the same steps, one finds

$$\mathbb{F}(R) = -e^{-i\phi}\int_\xi^\infty \frac{dy}{2\pi}\frac{2|\Delta|\sinh y}{\sqrt{-(2|t|\cos\theta\cos k - \mu)^2 + 4|\Delta|^2\sinh^2 y}}e^{i\pi R}e^{-Ry} \tag{5.33}$$

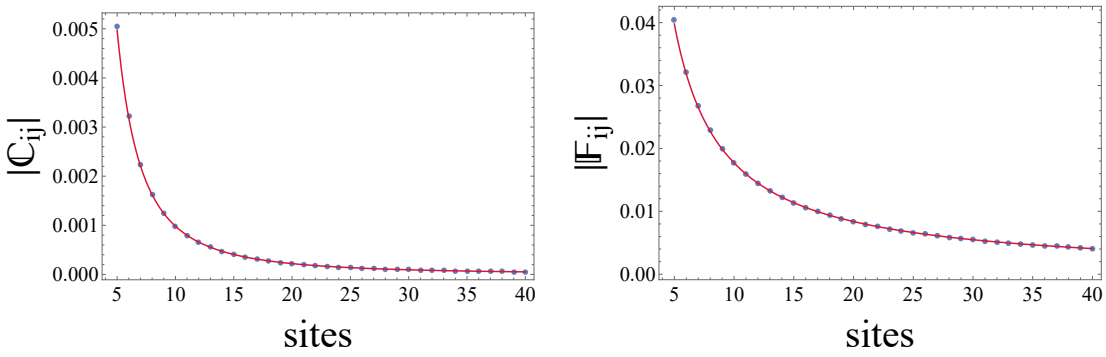

(a) $|\mathbb{C}_{ij}|$ **(b)** $|\mathbb{F}_{ij}|$

Figure 5.5: Plot (a) shows the numerical results of the critical correlation function $|\mathbb{C}_{ij}|$ (blue dots) and the plot of (5.32) (red line) for $|t| = |\Delta| = 1$, $\theta = \phi = 0$, $N = 40$, $\mu = 2$, $i = 1$ and $j = 5, ..., N$; (b) numerical results of the critical correlation function $|\mathbb{F}_{ij}|$ (blue dots) and the plot of (5.37) (red line) for $|t| = |\Delta| = 1$, $\theta = \phi = 0$, $N = 40$, $\mu = 2$, $i = 1$ and $j = 5, ..., N$.

If $k \ll 1$, we have

$$\frac{2|\Delta|\sinh(\xi+k)}{\sqrt{-(2|t|\cos\theta\cos(\xi+k)-\mu)^2+4|\Delta|^2\sinh^2(\xi+k)}} \simeq \frac{2|\Delta|\sinh\xi}{\sqrt{ak}} + \sqrt{k}\left(\frac{2|\Delta|\cosh\xi}{\sqrt{a}} - \frac{2b|\Delta|\sinh\xi}{2a^{\frac{3}{2}}}\right) \tag{5.34}$$

where a and b are given by the expressions (5.22) and (5.23). Then the anomalous correlation function takes the form

$$\begin{aligned}\mathbb{F}(R) &\simeq -e^{-i\phi}\frac{e^{i\pi R}e^{-R\xi}|\Delta|\sinh\xi}{\sqrt{a\pi R}} - e^{-i\phi}\frac{e^{i\pi R}e^{-R\xi}}{4\sqrt{\pi}R^{\frac{3}{2}}}\left(\frac{2|\Delta|\cosh\xi}{\sqrt{a}} - \frac{2b|\Delta|\sinh\xi}{2a^{\frac{3}{2}}}\right)\\ &\simeq -e^{-i\phi}\frac{e^{i\pi R}e^{-R\xi}|\Delta|\sinh\xi}{\sqrt{a\pi R}}\end{aligned} \tag{5.35}$$

At the critical point, we can use the expansion

$$\frac{2|\Delta|\sinh k}{\sqrt{-(2|t|\cos\theta\cosh k-\mu)^2+4|\Delta|^2\sinh^2 k}} \simeq 1 + k^2\left(\frac{1}{6} - \frac{c}{8|\Delta|^2}\right) \tag{5.36}$$

to find

$$\mathbb{F}_c(R) \simeq -e^{-i\phi}\frac{e^{i\pi R}}{2\pi R} - e^{-i\phi}\frac{e^{i\pi R}}{\pi R^3}\left(\frac{1}{6} - \frac{c}{8|\Delta|^2}\right) \simeq -e^{-i\phi}\frac{e^{i\pi R}}{2\pi R} \tag{5.37}$$

Here the subscript c denote that the previous expression holds at the critical point.
Therefore point the algebraic decay with the distance of the critical anomalous correlation function $\mathbb{F}_c(R)$ is slower than that of the critical correlation function $\mathbb{C}_c(R)$ (see Fig. 5.5).

5.2 Entanglement entropy

The word entanglement was first introduced by Scröedinger [33] to describe some global states of compound systems that cannot be written as the product of states of the subsystems. Basically, the concept of separability fixes the criteria to establish whether a state is entangled or not [19].
In recent years, entanglement measures have been used to characterize the properties of a quantum many-body system [24, 3]. The thermodynamic entropy, being an extensive e quantity, obeys a volume law, and one could think that also the entanglement entropy of a local quantum-many body system has an extensive character. However, for ground states of systems with short-range interactions one typically finds an area law in gapped regions [11]. This means that if one selects a region, the scaling of the entropy is linear in the boundary area of the region.
The emergence of an area law for the entanglement entropy provides support for the intuition that short ranged interactions require that quantum correlations between a distinguished region and its exterior are established via its boundary surface.
In this chapter we will analyze the behavior of the critical point with respect to the complex parameters of the complex Kitaev Hamiltonian trough the study of the entanglement entropy. Indeed, the quantum phase transitions are governed by quantum fluctuations at zero temperature [11], and therefore we expect to observe signatures of criticality on the level of entanglement. In addition, it turns out that the entanglement spectrum is also an indicator of topological order [35].
In general, the reduced density matrix of a fermionic quadratic model can be obtained in different ways; one of them is via correlation functions as discussed by Peschel and Eisler in [31]. This section aims to extend this method to the complex case where the correlation functions are not generally real and the standard formulas cannot be applied. At the end of the section, this general method is applied to the complex Kitaev model. Moreover, we discuss the dependence of the critical point with respect to the complex Hamiltonian parameters by analyzing the degeneracy structure of the eigenvalues of the reduced density matrix and the scaling properties of the entanglement entropy with the subsystem size.

5.2.1 Entanglement entropy for complex operators from correlation functions

Suppose to divide a one-dimensional chain of length N in two subsystems A and B containing l and $N-l$ sites respectively. The density matrix of the total system is defined as

$$\rho = |GS\rangle\langle GS| \tag{5.38}$$

The reduced density matrix ρ_A of the subsystem A can be obtained by tracing out the degrees of freedom of B from the total ρ

$$\rho_A(l) = \mathrm{Tr}_B \rho \tag{5.39}$$

The subsystem A is in general in a mixed state defined by ρ_A.
From the Wick theorem, it can be demonstrated that, for a system of non-interacting electrons,

the reduced density matrix ρ_A can be written as an exponential of a free fermionic operator [13]

$$\rho_A = \frac{e^{-\mathcal{H}_E}}{Z} \tag{5.40}$$

where

$$\mathcal{H}_E = \sum_{i,j=1}^{l} [c_i^\dagger D_{ij} c_j + \frac{1}{2}(c_i^\dagger E_{ij} c_j^\dagger + \text{h.c.})] \tag{5.41}$$

Here $\mathcal{H}_E$ is the entanglement Hamiltonian whose eigenvalues can be determined from the correlation function $\mathbb{C}_{ij}$ and $\mathbb{F}_{ij}$ of the subsystem A (for which $1 \leq i, j \leq l$).
Indeed, it is possible to derive some equations of these correlation functions in terms of the eigenvalues of the entanglement Hamiltonian which can be therefore calculated explicitly thanks to the already known values of the correlators (see Chapter 2 and equations (5.6) and (5.7)).
In general, the entanglement Hamiltonian $\mathcal{H}_E$ is different form the original Hamiltonian H of the system. Nevertheless, it's still quadratic in the fermionic operators and therefore it can be diagonalized through the method introduced in Section 2.1. Namely

$$\begin{pmatrix} \chi \\ (\chi^\dagger)^T \end{pmatrix} = U^{-1} \begin{pmatrix} c \\ (c^\dagger)^T \end{pmatrix} \tag{5.42}$$

$$U^{-1} = \begin{pmatrix} \vec{g}_1^T & \vec{h}_1^T \\ \vdots & \vdots \\ \vec{g}_N^T & \vec{h}_N^T \\ \vec{h}_1^{*T} & \vec{g}_1^{*T} \\ \vdots & \vdots \\ \vec{h}_N^{*T} & \vec{g}_N^{*T} \end{pmatrix} \tag{5.43}$$

where now U^{-1} is a $2l \times 2l$ unitary matrix. In this basis $\mathcal{H}_E$ takes the diagonal form

$$\mathcal{H}_E = \sum_{k=1}^{l} \epsilon_k \chi_k^\dagger \chi_k \tag{5.44}$$

Then we have $\rho_A = \bigotimes_k \rho_k$ where

$$\rho_k = \frac{e^{-\epsilon_k \chi_k^\dagger \chi_k}}{1 + e^{-\epsilon_k}} \tag{5.45}$$

In matrix form we can write

$$\rho_k = \begin{pmatrix} (1+e^{\epsilon_k})^{-1} & 0 \\ 0 & (1+e^{-\epsilon_k})^{-1} \end{pmatrix} \tag{5.46}$$

Noting that $(1+e^{\epsilon_k})^{-1} + (1+e^{-\epsilon_k})^{-1} = 1$ one has

$$\text{Tr}\left[\rho \chi_k^\dagger \chi_{k'}\right] = (1+e^{\epsilon_k})^{-1} \delta_{k,k'} \tag{5.47}$$

$$\text{Tr}\left[\rho \chi_k \chi_{k'}^\dagger\right] = (1+e^{-\epsilon_k})^{-1} \delta_{k,k'} \tag{5.48}$$

Thus, inverting (5.42) the correlation functions can be written as

$$\mathbb{C}_{ij} = \mathrm{Tr}[\rho c_i^\dagger c_j] = \sum_k (1+e^{\epsilon_k})^{-1} g_{ki} g_{kj}^* + \sum_k (1+e^{-\epsilon_k})^{-1} h_{ki}^* h_{kj} \tag{5.49}$$

$$\mathbb{F}_{ij} = \mathrm{Tr}[\rho c_i^\dagger c_j^\dagger] = \sum_k (1+e^{\epsilon_k})^{-1} g_{ki} h_{kj}^* + \sum_k (1+e^{-\epsilon_k})^{-1} h_{ki}^* g_{kj} \tag{5.50}$$

Using the relation $(1+e^{\epsilon_k})^{-1} - (1+e^{-\epsilon_k})^{-1} = -\tanh\left(\frac{\epsilon_k}{2}\right)$ we obtain

$$\mathbb{C}_{ij} = \frac{\delta_{ij}}{2} + \frac{1}{2}\sum_k \left[-\tanh\left(\frac{\epsilon_k}{2}\right)\right](g_{ki}g_{kj}^* - h_{ki}^* h_{kj}) \tag{5.51}$$

$$\mathbb{F}_{ij} = \frac{1}{2}\sum_k \left[-\tanh\left(\frac{\epsilon_k}{2}\right)\right](g_{ki}h_{kj}^* - h_{ki}^* g_{kj}) \tag{5.52}$$

where we used the relations (2.14) and (2.15).
Using (2.12) and (2.13), in matrix notation we have

$$\begin{cases} \left(\mathbb{C} - \frac{\mathbb{1}}{2}\right)\vec{g}_k + \mathbb{F}\vec{h}_k = -\frac{1}{2}\tanh\left(\frac{\epsilon_k}{2}\right)\vec{g}_k \\ -\left(\mathbb{C} - \frac{\mathbb{1}}{2}\right)^*\vec{h}_k - \mathbb{F}^*\vec{g}_k = -\frac{1}{2}\tanh\left(\frac{\epsilon_k}{2}\right)\vec{h}_k \end{cases} \tag{5.53}$$

The last system coincides with the LSM complex equations (2.31) if $A^* = \mathbb{C} - \frac{\mathbb{1}}{2}$, $B^* = \mathbb{F}$ and $\Lambda_k = -\frac{1}{2}\tanh\left(\frac{\epsilon_k}{2}\right)$. Then, repeating the same steps of section 2.2, the equations in (5.53) can be decoupled. Using (2.44) we obtain

$$\begin{aligned} &\begin{pmatrix} \mathbb{C}_R - \frac{\mathbb{1}}{2} - \mathbb{F}_R & -\mathbb{C}_I - \mathbb{F}_I \\ \mathbb{C}_I - \mathbb{F}_I & \mathbb{C}_R - \frac{\mathbb{1}}{2} + \mathbb{F}_R \end{pmatrix}\begin{pmatrix} \mathbb{C}_R - \frac{\mathbb{1}}{2} + \mathbb{F}_R & -\mathbb{C}_I + \mathbb{F}_I \\ \mathbb{C}_I + \mathbb{F}_I & \mathbb{C}_R - \frac{\mathbb{1}}{2} - \mathbb{F}_R \end{pmatrix}\begin{pmatrix} z_R \\ z_I \end{pmatrix} \\ &= \mathbb{T}\begin{pmatrix} z_R \\ z_I \end{pmatrix} = \frac{1}{4}\tanh^2\left(\frac{\epsilon_k}{2}\right)\begin{pmatrix} z_R \\ z_I \end{pmatrix} \end{aligned} \tag{5.54}$$

where

$$\mathbb{T} = \begin{pmatrix} \mathbb{C}_R - \frac{\mathbb{1}}{2} - \mathbb{F}_R & -\mathbb{C}_I - \mathbb{F}_I \\ \mathbb{C}_I - \mathbb{F}_I & \mathbb{C}_R - \frac{\mathbb{1}}{2} + \mathbb{F}_R \end{pmatrix}\begin{pmatrix} \mathbb{C}_R - \frac{\mathbb{1}}{2} + \mathbb{F}_R & -\mathbb{C}_I + \mathbb{F}_I \\ \mathbb{C}_I + \mathbb{F}_I & \mathbb{C}_R - \frac{\mathbb{1}}{2} - \mathbb{F}_R \end{pmatrix} \tag{5.55}$$

and, as usual, $z = g + h^* = z_R + iz_I$.
If $\mathbb{C}$ and $\mathbb{F}$ are real matrices, taking into account that $\mathbb{C}_I = \mathbb{F}_I = z_I = 0$, equation (5.54) becomes

$$T\vec{\phi}_k = \frac{1}{4}\tanh^2\left(\frac{\epsilon_k}{2}\right)\vec{\phi}_k \tag{5.56}$$

where $T \equiv (\mathbb{C} - \frac{\mathbb{1}}{2} - \mathbb{F})(\mathbb{C} - \frac{\mathbb{1}}{2} + \mathbb{F})$ and $\vec{\phi}_k = \vec{g}_k + \vec{h}_k$. This is exactly the formula obtained by Peschel and Eisler in [31]. If ξ_k are the eigenvalues of $\mathbb{T}$, the eigenvalues of $\mathcal{H}_E$ are

$$\epsilon_k = 2\mathrm{arctanh}(2\sqrt{\xi_k}) \tag{5.57}$$

Therefore from the already known correlation functions, the eigenvalues of the entanglement Hamiltonian can be easily calculated using (5.57). The von Neumann entropy S_{vN} is defined as

$$S_{vN}(l) = -\mathrm{Tr}_A \rho_A \log_2 \rho_A \tag{5.58}$$

Using the additivity of the von Neumann entropy, which holds in the case of a independent states, we obtain

$$S_{vN}(l) = -\sum_{k=1}^{l} \mathrm{Tr}\rho_k \log_2 \rho_k \tag{5.59}$$

In matrix form we can write

$$\rho_k \log_2 \rho_k = \begin{pmatrix} (1+e^{\epsilon_k})^{-1} \log_2 (1+e^{\epsilon_k})^{-1} & 0 \\ 0 & (1+e^{-\epsilon_k})^{-1} \log_2 (1+e^{-\epsilon_k})^{-1} \end{pmatrix} \tag{5.60}$$

Therefore the von Neumann entropy takes the form

$$S_{vN(l)} = \sum_{k=1}^{l} \left[(1+e^{\epsilon_k})^{-1} \log_2 (1+e^{\epsilon_k}) + (1+e^{-\epsilon_k})^{-1} \log_2 (1+e^{-\epsilon_k}) \right] \tag{5.61}$$

As previously explained, the entanglement entropy generally $S_{vN}(l)$ obeys an area law, meaning that, for one-dimensional systems, the entropy saturates to a constant [11].
At the critical point instead, for one-dimensional systems with local Hamiltonian and periodic boundary conditions, the entropy no longer obeys an area law. One finds [9]

$$S_{vN}(l) = \frac{c}{3} \log_2 \left[\frac{N}{2} \sin \left(\frac{\pi l}{N} \right) \right] + a \tag{5.62}$$

where c is the central charge of the underlying conformal field theory and a is a nonuniversal constant.

5.2.2 Entanglement entropy for the complex Kitaev model

In the following, the previous analysis is applied to the complex Kitaev model. Fig. 5.6 shows the entanglement entropy as a function of the size l of the subsystem A for the real case and different values of μ. At the critical point, as expected, the entropy scale as (5.62); out of the critical point instead, it saturates to a constant.
The eigenvalues of the reduced density matrix ρ_A and the entanglement entropy don't depend on ϕ.
In fact, if $\Delta \to |\Delta| e^{i\phi}$ both $\mathbb{F}$ and B acquire a phase $e^{i\phi}$ and so, since the eigenvalues Λ_k of the standard LSM procedure don't depend on ϕ, neither do the entanglement Hamiltonian eigenvalues.
On the other hand, if θ is different from zero and $x = \pm 1$ the entanglement Hamiltonian eigenvalues are equal to those of the real case with $t \to |t| \cos\theta$ as can be easily seen from the explicit structure of the ground state (see Chapter 4.3.1 and Fig. 5.7). The graph 5.8 represents the largest four eigenvalues λ_i of the reduced density matrix ρ_A as a function of μ for different values of θ as performed in [36]. The entanglement spectrum is clearly distinguishable in the two phases, especially since the non-trivial phase has a degeneracy structure as do all symmetry protected topological phases [35]. In particular, the degeneracy of the eigenvalues in the topological phase is even. Indeed, in this case, it can be seen that one eigenvalue of the entanglement Hamiltonian is zero.

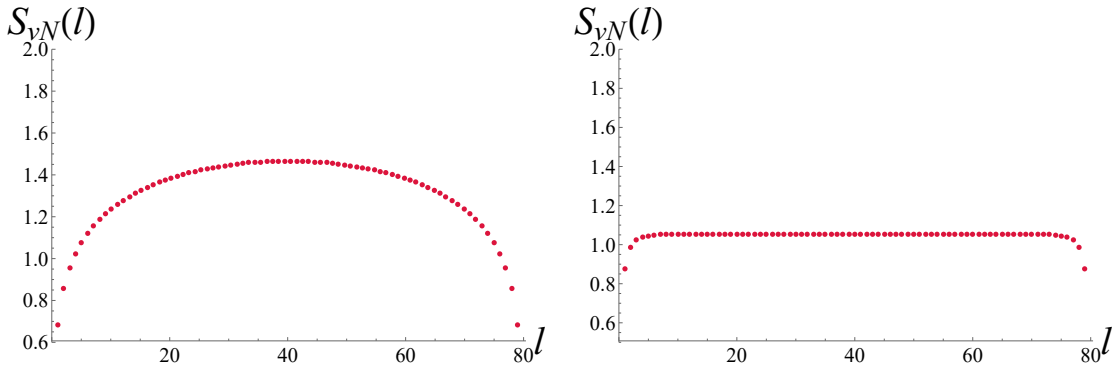

(a) $\mu = 2$ **(b)** $\mu = 1.5$

Figure 5.6: Entanglement entropy $S_{vN}(l)$ for $N = 80, x = 1, |t| = |\Delta| = 1, \theta = 0, \phi = 0$ and different values of μ. At the critical point the central charge is $c = \frac{1}{2}$ as expected from the general theory of the XY-Ising model [12].

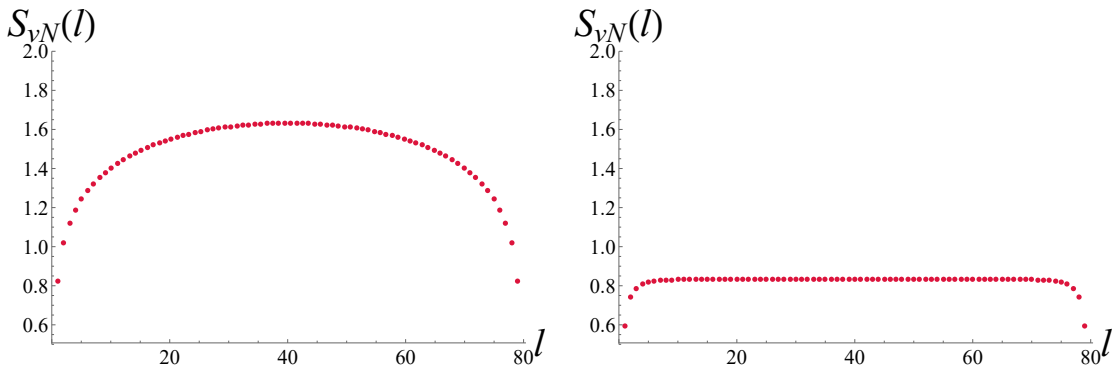

(a) $\mu = 1$ **(b)** $\mu = 1.5$

Figure 5.7: Entanglement entropy $S_{vN}(l)$ for $N = 80, x = 1, |t| = |\Delta| = 1, \theta = \frac{\pi}{3}, \phi = 0$ and different values of μ.

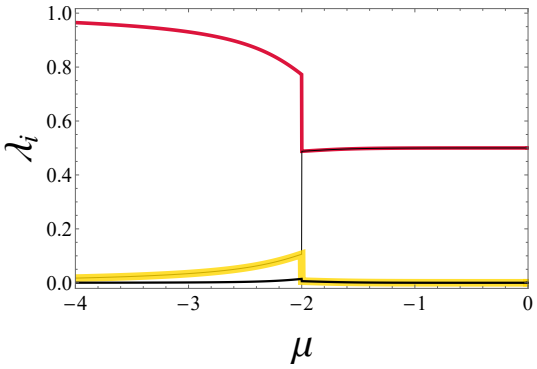

(a) $\theta = 0$

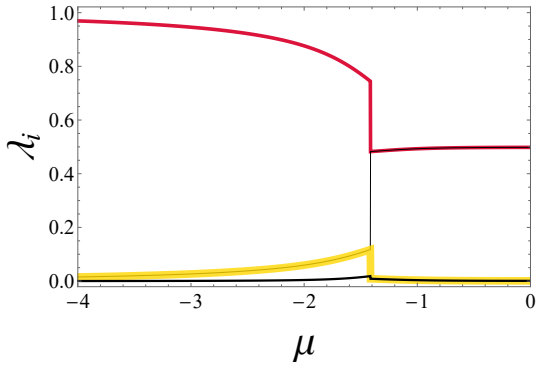

(b) $\theta = \frac{\pi}{4}$

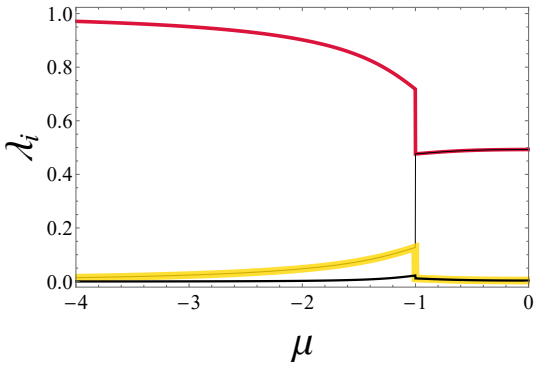

(c) $\theta = \frac{\pi}{3}$

Figure 5.8: Plot of the largest four eigenvalues λ_i of the reduced density matrix ρ_A as a function of μ for $N = 20, l = 10, x = 1, |t| = |\Delta| = 1$ and different values of θ. Each line has a different color (red, yellow, black, bold black) and represents one of the four eigenvalues. Wee see that the transition is at the point $\mu = 2|t| \cos\theta$.

Conclusion and outlooks

In this thesis we obtained the wavefunctions and the spectrum of the complex Kitaev model both analytically and numerically. In an attempt to do this, we have discussed two methods to diagonalize a complex quadratic Hamiltonian for generic boundary conditions. In particular, we extended the LSM method to the fully complex case to diagonalize the complex Kitaev model where both the hopping parameter and the superconductive gap are complex. We solved analytically the LSM equations by exploiting two methods: the perturbative and the ansatz approach. Within the perturbative approach, we derived some analytical solutions for the real case where $t = \Delta$ and for both $x = 0$ and $x \neq 0$. However, for $x \neq 0$ we obtained only an approximate formula for the eigenvalues which is valid in the limit where μ and x are small parameters. Within the ansatz approach we found simpler expressions and we solved also the case $t \neq \Delta, \mu = 0$ and the simpler non-trivial complex one. In this way, we showed that the underlying physics of the model for $t \neq \Delta$ is the same as the case $t = \Delta$. In the topological region, for OBCs, we found that, in the thermodynamic limit, the ground state is doubly degenerate. As expected, in general, this degeneracy is removed for a finite chain length. However, if $x \neq 0$ this degeneracy is lifted in the whole topological region for each value of N. In the fully complex case we derived that the transition point is shifted from $|\mu| = 2|t|$ to $|\mu| = |2t\cos\theta|$. Moreover, the complex phase ϕ of the superconductive gap doesn't affect the spectrum. However, the wavefunctions and in particular the ground state depend on ϕ.
Then, we have obtained some relative simple analytical hyperbolic expressions of the Majorana edge states for the real hopping case and we showed that they survive even when $x \neq 0$ ($x \neq 1$). These eigenstates become more peaked at the edges of the chain as $\mu, x \to 0$ and $t \to \Delta$.
In the last part of this work, we calculated the correlation functions both analytically and numerically for a finite chain and in the thermodynamic limit. As expected, the correlations between the first and the last sites are substantially different from zero in the topological phase. Furthermore, the correlation length diverges at the critical point where the correlation functions have a power-law decay.
The entanglement spectrum confirms our previous results. In particular, we recovered that the critical point depends on the complex hopping phase and that at the critical point the entropy no longer obeys an area law. Besides, the topological phase has the expected degenerate structure.

A possible further study can investigate the role of the complex hopping phase on the Majorana edge states. In fact, in this case, the LSM coefficients are both complex and the phase cannot be eliminated by a simple redefinition of the Majorana operators. Thus, the Majorana

operators, being simply the real and the imaginary part of the Dirac operators, may mix in a non-trivial way.
Furthermore, it could be interesting to test if, for different domains, as for the SSH model, the number of the edge states increases with the number of the domain walls where these states should be localized.
Finally, we could try to understand how our results obtained for a 1-D chain could be extended to a two-dimensional lattice.

Ringraziamenti

Per prima cosa vorrei ringraziare la prof.ssa Elisa Ercolessi per il suo supporto costante durante questo lavoro di tesi.
Inoltre vorrei ringraziare Davide Vodola per i suoi consigli e la sua disponibilità.
Un grazie speciale va alla mia famiglia e a Valentina che mi sono sempre stati accanto durante questi anni.
Una nota speciale va ai miei compagni di avventura Andrea, Enrico, Marco e Giovanni (e anche Riccardo e Vincenzo) per le belle serate passate insieme.
Infine grazie a Federico, Alessandro, e e Alessandro, miei compagni di studio e non solo.

Bibliography

[1] M Abramovitz and IA Stegun. Handbook of mathematical functions, applied mathematics series 55. *Washington, D. C.: NBS*, page 882, 1964.

[2] Jason Alicea, Yuval Oreg, Gil Refael, Felix Von Oppen, and Matthew PA Fisher. Non-abelian statistics and topological quantum information processing in 1d wire networks. *Nature Physics*, 7(5):412, 2011.

[3] Luigi Amico, Rosario Fazio, Andreas Osterloh, and Vlatko Vedral. Entanglement in many-body systems. *Reviews of modern physics*, 80(2):517, 2008.

[4] János K Asbóth, László Oroszlány, and András Pályi. A short course on topological insulators. *Lecture notes in physics*, 919, 2016.

[5] Andrei Bernevig and Titus Neupert. Topological superconductors and category theory. *Lecture Notes of the Les Houches Summer School: Topological Aspects of Condensed Matter Physics*, pages 63–121, 2017.

[6] B Andrei Bernevig and Taylor L Hughes. *Topological insulators and topological superconductors*. Princeton university press, 2013.

[7] Michael Victor Berry. Quantal phase factors accompanying adiabatic changes. *Proceedings of the Royal Society of London. A. Mathematical and Physical Sciences*, 392(1802):45–57, 1984.

[8] James R Bunch, Christopher P Nielsen, and Danny C Sorensen. Rank-one modification of the symmetric eigenproblem. *Numerische Mathematik*, 31(1):31–48, 1978.

[9] Pasquale Calabrese and John Cardy. Entanglement entropy and quantum field theory. *Journal of Statistical Mechanics: Theory and Experiment*, 2004(06):P06002, 2004.

[10] Xie Chen, Zheng-Cheng Gu, Zheng-Xin Liu, and Xiao-Gang Wen. Symmetry protected topological orders and the group cohomology of their symmetry group. *Physical Review B*, 87(15):155114, 2013.

[11] Jens Eisert, Marcus Cramer, and Martin B Plenio. Colloquium: Area laws for the entanglement entropy. *Reviews of Modern Physics*, 82(1):277, 2010.

[12] Fabio Franchini. *An introduction to integrable techniques for one-dimensional quantum systems*, volume 940. Springer, 2017.

[13] Michel Gaudin. Une démonstration simplifiée du théoreme de wick en mécanique statistique. *Nuclear Physics*, 15:89–91, 1960.

[14] Gene H Golub. Some modified matrix eigenvalue problems. *Siam Review*, 15(2):318–334, 1973.

[15] Robert M Gray et al. Toeplitz and circulant matrices: A review. *Foundations and Trends® in Communications and Information Theory*, 2(3):155–239, 2006.

[16] Zheng-Cheng Gu and Xiao-Gang Wen. Symmetry-protected topological orders for interacting fermions: Fermionic topological nonlinear σ models and a special group supercohomology theory. *Physical Review B*, 90(11):115141, 2014.

[17] F Duncan M Haldane. Continuum dynamics of the 1-d heisenberg antiferromagnet: Identification with the o (3) nonlinear sigma model. *Physics Letters A*, 93(9):464–468, 1983.

[18] M Zahid Hasan and Charles L Kane. Colloquium: topological insulators. *Reviews of modern physics*, 82(4):3045, 2010.

[19] Ryszard Horodecki, Paweł Horodecki, Michał Horodecki, and Karol Horodecki. Quantum entanglement. *Reviews of modern physics*, 81(2):865, 2009.

[20] Charles L Kane. Topological band theory and the z2 invariant. In *Contemporary Concepts of Condensed Matter Science*, volume 6, pages 3–34. Elsevier, 2013.

[21] A Yu Kitaev. Unpaired majorana fermions in quantum wires. *Physics-Uspekhi*, 44(10S):131, 2001.

[22] Alexei Kitaev. Periodic table for topological insulators and superconductors. In *AIP conference proceedings*, volume 1134, pages 22–30. AIP, 2009.

[23] John Michael Kosterlitz and David James Thouless. Ordering, metastability and phase transitions in two-dimensional systems. *Journal of Physics C: Solid State Physics*, 6(7):1181, 1973.

[24] José Ignacio Latorre, Enrique Rico, and Guifré Vidal. Ground state entanglement in quantum spin chains. *arXiv preprint quant-ph/0304098*, 2003.

[25] Martin Leijnse and Karsten Flensberg. Introduction to topological superconductivity and majorana fermions. *Semiconductor Science and Technology*, 27(12):124003, 2012.

[26] Elliott Lieb, Theodore Schultz, and Daniel Mattis. Two soluble models of an antiferromagnetic chain. *Annals of Physics*, 16(3):407–466, 1961.

[27] Andreas WW Ludwig. Topological phases: classification of topological insulators and superconductors of non-interacting fermions, and beyond. *Physica Scripta*, 2016(T168):014001, 2015.

[28] Michael A Nielsen. The fermionic canonical commutation relations and the jordan-wigner transform. *School of Physical Sciences The University of Queensland*, 2005.

[29] Silvia Noschese, Lionello Pasquini, and Lothar Reichel. Tridiagonal toeplitz matrices: properties and novel applications. *Numerical linear algebra with applications*, 20(2):302–326, 2013.

[30] HyungSeon Oh and Zhe Hu. Multiple-rank modification of symmetric eigenvalue problem. *MethodsX*, 5:103–117, 2018.

[31] Ingo Peschel and Viktor Eisler. Reduced density matrices and entanglement entropy in free lattice models. *Journal of physics a: mathematical and theoretical*, 42(50):504003, 2009.

[32] Andreas P Schnyder, Shinsei Ryu, Akira Furusaki, and Andreas WW Ludwig. Classification of topological insulators and superconductors in three spatial dimensions. *Physical Review B*, 78(19):195125, 2008.

[33] E Schrödinger. Mathematical proceedings of the cambridge philosophical society. In *Mathematical Proceedings of the Cambridge Philosophical Society*, volume 31, pages 555–563, 1935.

[34] W_P Su, JR Schrieffer, and Ao J Heeger. Solitons in polyacetylene. *Physical review letters*, 42(25):1698, 1979.

[35] Ari M Turner, Frank Pollmann, and Erez Berg. Topological phases of one-dimensional fermions: An entanglement point of view. *Physical review b*, 83(7):075102, 2011.

[36] Evert PL Van Nieuwenburg, Ye-Hua Liu, and Sebastian D Huber. Learning phase transitions by confusion. *Nature Physics*, 13(5):435, 2017.

[37] Oscar Viyuela, Davide Vodola, Guido Pupillo, and Miguel Angel Martin-Delgado. Topological massive dirac edge modes and long-range superconducting hamiltonians. *Physical Review B*, 94(12):125121, 2016.

[38] Xiao-Gang Wen. Topological orders in rigid states. *International Journal of Modern Physics B*, 4(02):239–271, 1990.

[39] Edward L Wolf, Gerald B Arnold, Michael A Gurvitch, and John F Zasadzinski. *Josephson Junctions: History, Devices, and Applications*. Pan Stanford, 2017.

[40] Bei Zeng, Xie Chen, Duan-Lu Zhou, and Xiao-Gang Wen. Quantum information meets quantum matter. *arXiv preprint arXiv:1508.02595*, 2015.